A Project Report on

Optimization Based Design and Analysis of Quad-band Inverted T-shape Slotted Rectangular Microstrip Patch Antenna

submitted by

SABHYA (ROLL NO. 2004327504)

under the guidance of

DR. MAHENDRA KUMAR, ASSOCIATE PROFESSOR

DR. ATUL KUMAR DWIVEDI, ASSISTANT PROFESSOR

in partial fulfilment of the requirements

for the award of the degree of

BACHELOR OF TECHNOLOGY

DEPARTMENT OF ELECTRONICS AND COMMUNICATION ENGINEERING

BUNDELKHAND INSTITUTE OF ENGINEERING AND TECHNOLOGY, JHANSI, INDIA

2022-2023

Declaration

I hereby declare that the work presented in this report entitled **Optimization Based Design and Analysis of Quad-band Inverted T-shape Slotted Rectangular Microstrip Patch Antenna** for M.Tech. Degree at Department of Electronics and Communication Engineering, Bundelkhand Institute of Engineering and Technology, Jhansi in academic session 2021-2022, is my own work. Information taken from other sources is appropriately acknowledged.

Kajal Verma	**Shalini Singh**	**Manisha Yadav**
Roll no.1604331021	Roll no.1704331910	Roll no.1604331024

Certificate

This is to certify that the thesis entitled **Optimization Based Design and Analysis of Quad-band Inverted T-shape Slotted Rectangular Microstrip Patch Antenna** submitted by **Sabhya** for the award of the degree of M. Tech, is carried out by him/her under my supervision.

Dr. Atul Kumar Dwivedi	**Dr. Mahendra Kumar**
Assistant Professor	Associate Professor

Verification

This is to verify that the project entitled " **Optimization Based Design and Analysis of Quad-band Inverted T-shape Slotted Rectangular Microstrip Patch Antenna** " submitted.

Prof. Deepak Nagaria
Head
Department of ECE, BIET Jhansi

DEDICATION

To my beloved Parents and almighty

Program Outcomes(POs)

S. N.	**Program outcomes** After completing this project students will be able to
PO1	**Engineering Knowledge** Apply the knowledge of mathematics, science, engineering fundamentals, and an engineering specialization to the solution of complex engineering problems.
PO2	Apply the knowledge of electronics in order to find the most efficient sensors and suitable microcontroller.
PO3	Analyse the inputs and outputs for reaching the most accurate results.
PO4	Evaluate developed system for number of patients by testing it several times.
PO5	Design connections diagram of the system and creating a path of communication between the device and mobile phone through WIFI.
PO6	**Engineering Knowledge** Apply the knowledge of mathematics, science, engineering fundamentals, and an engineering specialization to the solution of complex engineering problems.
PO7	Apply the knowledge of electronics in order to find the most efficient sensors and suitable microcontroller.
PO8	Analyse the inputs and outputs for reaching the most accurate results.
PO09	Evaluate developed system for number of patients by testing it several times.
PO10	Design connections diagram of the system and creating a path of communication between the device and mobile phone through WIFI.
PO11	Evaluate developed system for number of patients by testing it several times.
PO12	Design connections diagram of the system and creating a path of communication between the device and mobile phone through WIFI.

Project Outcomes(Ps)

S. N.	**Project outcomes** After completing this project students will be able to	**Bloom's knowledge level**
P1	Interface various sensors with ESP8266	KL3
P2	Apply the knowledge of electronics in order to find the most efficient sensors and suitable microcontroller.	KL3
P3	Analyse the inputs and outputs for reaching the most accurate results.	KL4
P4	Evaluate developed system for number of patients by testing it several times.	KL5
P5	Design connections diagram of the system and creating a path of communication between the device and mobile phone through WIFI.	KL6

KL: Bloom's knowledge level, KL1: remember, KL2: Understand, KL3: Apply, KL4: Analyse, KL5: Evaluate, KL6: Create/Design

Mapping of project outcomes with Program Outcomes (POs)

S. N.	**PO1**	**PO2**	**PO3**	**PO4**	**PO5**	**PO6**	**PO7**	**PO8**	**PO9**	**PO10**	**PO11**	**PO12**
Mapping	3	3	3	3	2	3	3	3	3	3	3	3

Mapping rules (Rubrics)

1: poor 2: medium 3: best

Acknowledgment

I would like to express my deep sense of gratitude to my supervisors and guides Dr. Mahendra Kumar and Dr. Atul Kumar Dwivedi, Department of Communication Engineering, BIET, Jhansi, for their constant guidance and motivation during the project work from last one year. I really appreciate and value their guidance and constant motivation from the beginning of the project. Without their guidance and persistent help this thesis would not have been possible. I am also indebted to Professor Deepak Nagaria, Head Department of Electronics and Communications Engineering for his encouraging co-operation and continued interest in shaping this project. I express my sincere gratitude to Prof. P. M. Pandey, Director, BIET, Jhansi, who has been instrumental in providing an ideal environment for wholesome individual development and appreciating talents in both academic and extracurricular activities. I take immense pleasure to thank Prof Abhay Verma, Dean Academics, BIET, Jhansi, for his valuable and constant feedback, focused instructions, motivated suggestions, and encouragement. I extend my sincere thanks to all faculties of the Department of Electronics and communication engineering, BIET, Jhansi, for their focused guidance and encouragement. I would like to thank my parents and friends and all those people who have supported me directly or indirectly to complete this project work.

Sabhya

Roll no.2004327504

ABSTRACT

KEYWORDS: IE3D, MATLAB, Curve Fitting, Fragmentary Bandwidth, Return Loss, Inverted T-Shaped Slot, Microstrip patch Antenna.

This work contains design proposals for three antennas obtained by applying three completely different strategies of optimization. In order to create miniature antennas that perform better than traditional antennas, all three use the idea of slotting across the patch and altering the slot dimensions. This study also compares the analysis of the initially designed Inverted T-shape slotted rectangular microstrip patch antenna (RMSPA) and the same Inverted T-shape slotted RMSPA designed by strategic optimization strategy 1, strategy 2, and strategy 3 using IE3D. Additionally, the same initial antenna has also been designed using MATLAB by formulating code in order to perform PSO optimization and comparing it to the initial antenna and strategically optimized antennas. The suggested slotted RMSPAs were experimentally tested to verify the essential properties of the design, which include multiple-band operation, a high bandwidth percentage, and low return loss, and a comparative analysis is also performed with the results of the same antenna simulated over IE3D.

Primarily, a regular radiating rectangle shaped- MSPA features inverted T-shaped slots in its design. which has obtained Quad-bands and the same has been strategically optimized in strategy 1, keeping some dimensional parameters as variables. These variables are varied to a certain range in order to bring out the strategic optimization (strategy 1) utilizing IE3D Software to get the resonant frequency data and bandwidth outcomes. Then, utilizing the same outcomes the equivalent model for the antenna is obtained by curve fitting using the MATLAB curve fitting tool. This tool establishes the relationship of the selected parameter with respect to bandwidth and return loss against each parameter value from the prescribed range. The strategic T-shape of the slot has been finalized after a number of iterative designs simulated in strategic optimization 1, keeping bandwidth and return loss as selecting criteria. The selected strategy 1 antenna has

attained Triple band outcomes with the bandwidth increment. Thus, the finalized triple-band antenna has been practically realized and analyzed. This antenna has the ability to be used for WiMAX applications since it resonates in the S-band.

The second suggestion is for a Triple-band microstrip patch slotted with an inverted T-shape, which uses optimization strategy 2 to propose a self-similar iterative design. Combinations of the selected best values of the variables are made and the antennas are delineated. Triple band performance is achieved with the strategy2 antenna. It can resonate at three distinct frequencies between 1.8 and 5.8 GHz, making it suitable for a wide range of applications like UMTS (1.92–2.17 GHz), DCS (1.7-1.8GHz), PCS (1.85-1.99GHz), ISM band (2.4 - 2.485GHz), WLAN bands and WiMAX, etc.

The third proposal is for a UWB "T" slotted patch antenna, which was likewise constructed using optimization approach 3. It is designed by moving in the range of all four selected variable parameters for achieving the best value and fixing it. Again tune in the range of the second variable to achieve the best and similarly by fixing the variable's value at best for the other two parameters, attained the final antenna with increased bandwidth % up to 100.85 % Also, by curve fitting the relationship of the variable parameters individually with the bandwidth % and return loss is represented.

In the fourth scheme, the initial design has been implemented in the ".m" file over MATLAB which has been simulated to obtain the S(1,1), RL, VSWR, and Gain. Thereafter the PSO is applied by formulating the objective function to vary the feed location to best match the Rf to the Design frequency (fr) as well as some dimensional parameters of the Slot and feed strip are tuned to get the best value in order to obtain the increased BW % while maintaining the good RL and Rf matching.

The Zealand IE3D software is used for all simulations. All of them are implemented on the $\epsilon_r = 4.4$ FR4 substrate, which is easily available and inexpensive. Simulations are used to examine antenna properties such as bandwidth percentage, return loss, VSWR, radiation pattern, and gain. MATLAB was also utilized to generate an equivalent model to represent the proposed antenna by curve fitting and for PSO and hybrid PSO optimization.

TABLE OF CONTENTS

Table of Contents (continued) **Page**

LIST OF TABLES

LIST OF FIGURES

Major contributions

The main objective of this project is to design optimized Inverted "T" shaped slotted rectangular Microstrip patch antennas. The main contributions of the work can be listed as

1 Initial Inverted "T" shaped slotted rectangular Microstrip patch antenna have been designed utilizing IE3D using parent design equations 3.3 to 3.8 for dimensional specifications.

2 Initial Inverted "T" shaped slotted rectangular Microstrip patch antenna have been optimized using three strategic optimization techniques.

3 In addition to this, the same initial antenna have been designed using a particle swarm optimization (PSO) algorithm and the results are analyzed as well as compared.

4 Also, the relationship equations to represent antennas have been carried out by curve fitting.

5 A final optimized inverted "T" shaped slotted rectangular Microstrip patch antenna with increased fragmentary bandwidth and good return loss have been proposed and experimentally verified by fabricating also, the PSO optimized antenna is obtained, designed, simulated and compared with the initial antenna.

ABBREVIATIONS

AD	Antenna Design
BW%	bandwidth percentage
FBW	Fragmentary bandwidth
USRMSPA	Unsoltted Rectangular Micro strip patch antenna
RMSPA	Rectangular Micro strip patch antenna
MSPA	Micro strip patch antenna
MSAs	Micro strip antennas
WCS	Wireless communication systems
GA	Genetic Algorithm
PSO	particle swarm optimization
RL	Return Loss
VSWR	Voltage standing wave ratio
UWB	Utra wide band
UHF	Ultra high frequency
HPBW	Half power beam width
RP	Radiation Pattern
RFID	Radio-Frequency identification
MMICs	Monolithic microwave integrated circuit
VNA	Vctor network analyser
WLAN	Wireless local area network
GHz	Giga Hertz
IE3D	Integral Equation in 3Dimension
PCS	Personal Computing Systems
dB	Decibel

NOTATION

English Symbols

R_f	Resonant frequency
f_r	Design frequency
c	Velocity of EM waves in free space
E	Electric Field
H	Magnetic field
L	Absolute length of the patch
ΔL	Extension length
L_{gnd}	Length of ground plane
W_{gnd}	Width of ground plane
W	Width of the patch
S	Scattering Parameter
P_{rad}	Power radiated
P_s	Power supplied
P_a	Input power to antenna
dBi	Decibel with respect to isotropic
h	Thickness of the substrate layer
R_f	Resonant frequency
f_r	Design frequency
f_h	Higher cutoff frequency
f_l	Lower cutoff frequency
f_c	Center frequency
A_e	Ae effective apperture

Greek Symbols

Γ	Reflection coefficient
λ	Wavelength
ϵ_r	Dielectric constant of the substrate
ϵ_{eff}	Effective dielectric constant
μ_0	Permeability of free space
θ	Elevation angle
Φ	Azimuthal angle
η_{ant}	Antenna efficiency
η_{rad}	Radiation efficiency

CHAPTER 1

INTRODUCTION

1.1 Back Ground and Motivation

Antennas have a long history dating back to James Clerk Maxwell, who united the ideas of electricity and magnetism and eloquently described their relationships through a set of complex equations known as Maxwell's equations, which were originally published in 1873. The very first wireless electromagnetic system was presented by Professor Heinrich Rudolph Hertzin in 1886. Guglielmo Marconi was the first to establish a system transmitting a signal across a long distance in 1901[1].

One of the most vital elements of technologically advanced wireless communication systems (WCS) is the antenna. Microstrip patch antennas (MSPAs) fit in perfectly because they have proven to be indispensable in a variety of fields, including satellite communication, aircraft signaling systems, Synthetic Aperture Radar (SAR), WCS, and MMIC design[2]. Munson and Howell constructed workable antennas in the 1970s[3] after the microstrip antenna (MSA) was first emphasized in 1953[1]. It is proven to have various benefits, including small size (tiny length and width), affordable production, lightweight, simple fabrication, and robustness, come with its simple 2-D shape. Due to the fact that the antenna size is proportional to the wavelength at the resonant frequency, they are widely utilized at UHF and higher frequencies[4].

A microstrip patch is made up of a radiating patch of any planar geometry (such as a circle, square, trapezoidal, ellipse, ring, or rectangle) on the front side of a dielectric material substrate and on the opposite(back) side to the substrate, a ground plane is created and a feeding component is also provided on the ground side or at the edge[5]. The 1980s saw the creation of the first numerical method for analyzing microstrip antennas, called the Method of Moments (MoM)[6][7][8]. A rectangular patch is the most typical microstrip antenna. Also, due to the fringing fields in between the patch's boundary and the ground plane, MSA radiates significantly. [9]

The microstrip patch antenna's main shortcoming is its intrinsically narrow impedance bandwidth. In recent years, a lot of work has gone into developing bandwidth augmentation strategies[10]. These strategies include using a thick substrate with a low dielectric constant (usually less than 2.5), as well as various patch forms and a slotted patch. microstrip line feed is chosen because it is easy to produce, easy to match by manipulating the inset location, and relatively easy to model[1][3].

with MSA's drawbacks comes the need to improve FBW, which is also accomplished by utilizing various Nature- encouraged algorithms for optimization. These algorithms have been developed based on the natural behavior of specific animal species found in nature like fish schools or bird flocks[11] and have grown to be the foundation of optimization research providing many benefits, including fewer switching parameters, stronger search capabilities, and a lack of adjustment based on problems, therefore, Researchers have been attracted to these methods for the past three decades to answer various domain challenges for practical applications, like power systems[12], training of artificial neural networks[13][14], MIMO applications in 5G communications[15], satellite communication[16], Arrays of antenna[17], RFID[18], etc. Genetic algorithms[19] formed the foundation of optimization algorithms followed by the DE (differential evolution)algorithm, naked mole-rat (NMR) algorithms, and Hybrid of both DE and NMR algorithms[20], Particle Swarm Optimization (PSO)[21][22][23], the classical Inertia Weight PSO (IWPSO) and the Constriction Factor PSO (CFPSO)[19], machine learning algorithms[24], Hybrid algorithm[25], Salp Swarm algorithm (SSA)[15], Binary Salp Swarm Algorithm (BSSA)[16], Artificial bee colony (ABC)[26], hybrid ABC and DE (H–ABCDE)[27], Ant Colony Optimization[19], Wind Driven Optimization (WDO)[28], Cuckoo search are the most recent algorithms[17] to be employed in optimization research, and they are being applied in practically all study fields.

Furthermore, these algorithms have the extra benefits of quicker convergence, lower likelihood of local optima stagnation is extremely difficult, and have significantly outperformed their rivals[20]. The great interest in using the PSO technique to improve antenna designs is evident given the variety of real-world issues that PSO, an evolutionary algorithm, can resolve. Swarm intelligence is incorporated into the design process and is modeled by basic Newtonian mechanics to support various optimizations in PSO[13]. The antenna's performance metrics, such as its gain, directivity, radiation pattern, FBW enhancement[29][30], Feed positioning, and antenna efficiency, are estimated and enhanced at its resonant frequencies using the particle swarm optimization (PSO) technique[31].

1.2 Prefatory Concepts

An antenna is a bi-directional transducer that converts electrical signals to electromagnetic waves. Antennas are used to transmit and/or receive electromagnetic waves from one point to another. Antennas find their applications in the field of communication (particularly long-range radio wave communication). All thanks to "Maxwell's Equations" which gave us the idea about the relationship which exists between electric field and magnetic field.

It is quite interesting to know that antenna has come a long way till date since the day we started using it. It can be broadly categorized on the basis of its size and shape [1]. Some of them include a wire antenna, loop antenna, horn Antenna, patch Antenna, helical antenna, parabolic antenna, and so on.

With the advent of new technologies and the requirement of the present world we are developing new antennas which are small in size but equally capable / but no less in any aspect than a big size antenna. Long-range communication like mobile communication requires an antenna but we are bound to miniaturize the size because we are moving towards a world where we not only use but also like to wear technologies. To make gadgets like phones, digital watches, etc portable we have to continuously work on designing compact antennas. The immense use of compact size antennas does not straight away rule out the applications of large-sized antennas. For example: To detect the signals coming from outer space, or in satellite communication, we still require big-sized antennas.

On the basis of obtained band characteristics antennas are classified as narrow bandwidth, wide bandwidth, and ultra-Wide Bandwidth.

Narrow Bandwidth Antennas are those that have an operational frequency bandwidth that is coherent with the frequency channel or design frequency. These possess a Fragmentary bandwidth of less than 50 %. These antennas can be used for a variety of purposes, including RFID, and they cover short-range communication.

Wide Bandwidth Antennas have operating frequency bandwidth greater than the passband frequency of the channel are called wide bandwidth antennas. Such antennas cover long-range communication and have applications like video conferencing.

Ultra-wide Bandwidth Antennas [32] are antennas whose operating frequency is very high (in GHz) and are designed for the transmission and reception of electromagnetic energy for a short period of time.

1.2.1 Bandwidth

The range of frequency within which our required objective of antenna design is fulfilled is what we call bandwidth. To be more precise, we can state that the frequency range at which our antenna demonstrates the appropriate properties is its bandwidth.

$$BW_p = \frac{f_h - f_l}{f_c} * 100\% \tag{1.1}$$

Broadband by the ratio :

$$BW_b = \frac{f_h}{f_l} \tag{1.2}$$

where, f_c is Center frequency,f_l is Higher Cut-off frequency and f_h is lower Cut-off frequency

1.2.2 Return loss

It is the power lost in the signal that is sent back by a break in an optical fiber or discontinuity in the transmission line. Decibels are typically used to express this. Alternatively, put if the load received all of the power, the return loss would therefore be limitless. In contrast, if there is a short circuit or open circuit termination, Afterwards, all of the power will be restored and no return loss will occur.

Typically, the return loss is determined as follows:

$$R = 10\log_{10}(\frac{Pi}{Pr}) \tag{1.3}$$

where P_i is the forward power and P_r is the reflected power when reflection coefficient (Γ) = $\sqrt{\frac{P_r}{P_i}}$, P_r is reflected power and P_i is forward power. Thus,

$$R(dB) = -20\log_{10}(\Gamma) \tag{1.4}$$

when utilizing a vector network analyzer to measure a network's properties. The return loss is a crucial characteristic as a result.

1.2.3 Voltage standing wave ratio

According to the voltage standing wave ratio (VSWR) definition, the VSWR is determined by dividing the line's maximum voltage by its minimum voltage. The sum of the voltage components from the forward power and the reflected power causes the voltage variations.

$$VSWR = \frac{Vmax}{Vmin} \tag{1.5}$$

VSWR stated in terms of the voltages for the forward and reflected waves.

$$VSWR = \frac{Vfwd + Vref}{Vfwd - Vref} \tag{1.6}$$

VSWR as a function of the reflection coefficient.

$$VSWR = \frac{(1 + |\Gamma|)}{(1 - |\Gamma|)} \tag{1.7}$$

where, Γ = reflection coefficient, the reflection coefficient, Γ is defined as the ratio of the reflected current or voltage vector to the forward current or voltage.

1.2.4 Input Impedance

For maximum power transfer in an antenna, we need to keep the VSWR (voltage standing wave ratio) as low as possible, which can only be done when we achieve impedance matching. For this purpose, we need to take input impedance carefully into account. It is the total sum of resistance and reactance at the input terminal.

1.2.5 Resonant frequency

The resonant frequency is the frequency at which the patch receives the most power, i.e., when the feedline and patch's impedances are most closely matched. Additionally, it is the point at which the impedance is solely resistive and inductive reactance equals capacitive reactance[33].

1.2.6 Radiation Pattern

The radiation pattern is the pictorial representation of antenna radiation. When the antenna radiates, then radiation lobes are created, which consist of some prominent lobes called the main lobe or major lobe, and various side lobes or minor lobes. These lobes account for the directivity of the antenna as to which direction the antenna radiates the most[33].

1.2.7 Half Power Beam width

Half Power Beam width (HPBW) is evaluated by the angular width of the major lobes at $\log \frac{1}{\sqrt{2}}$ points (or $-3db$ points)[1].

1.2.8 Polarization

When an antenna radiates electromagnetic waves, an electric field is induced, and the orientation of such an induced electric field is called polarization in the antenna. There can be broadly three kinds of polarization, namely, linear, circular, and elliptical[33].

1.2.9 Gain

“The ratio of radiation intensity in one direction to that which would be obtained if the antenna were to broadcast its power isotopically.”[1]
it is given as

$$G = \frac{U(\theta, \phi)}{U_a} = \frac{4\phi U(\theta, \phi)}{P_a} \tag{1.8}$$

where P_a is the input power to the antenna. An antenna’s efficiency determines its gain. (Gain = Directivity X radiation efficiency)[34] The gain of an antenna can also be expressed in terms of its effective apertureA_e and wavelength.
This is,

$$G = \frac{4\pi}{\lambda^2} A_e \tag{1.9}$$

1.2.10 Directivity

The maximum gain in a specific or intended direction is referenced as directivity.

1.2.11 Efficiency

"The proportion of an antenna’s radiated power to its input power is known as antenna efficiency." Antenna efficiency (η_{ant}) and Radiation efficiency (η_{rad}) are both calculated in percentage terms (%).
Below is a mathematical expression for antenna efficiency.

$$\eta_{ant} = \frac{P_{rad}}{P_{input}} \tag{1.10}$$

where, η_{ant} is antenna efficiency, P_{rad} is the power radiated, P_{input} is the input power.

1.3 Micro strip patch antennas

With technological advancement, antenna portability and Miniaturization has become crucial feature of antenna design, resulting in the development of very small-sized antennas having dimensions in mm. One such kind of antenna is a microstrip patch antenna. With the requirements of portable and wearable technologies in mobile communications, the microstrip antenna has amassed a lot of popularity[2].

The MSPA's comes with various Preeminence perfectly matching the requirements of the advanced WCS like their ability to adapt to any surface, the planar configuration with a low profile, low volume and is lightweight[35]. Not only that, but they also possess a compact size due to low volume and can facilitate both linear as well as circular polarization. As they use PCB technology that allows for mass production[36], resulting in a lower cost or less expensive method of creation. Their scattering cross-section is low with multiple frequencies of operability. It requires no cavity backing and the simplicity of mounting on missiles and other space-critical equipment makes them heroes in the new era. It's a lot easier to integrate with other monolithic integrated circuits if the same substrate is used. Concurrent fabrication of feed lines and matching networks are also possible. They can be created with a variety of geometrical shapes and dimensions[37]. Four main categories can be used to classify all microstrip antennas are given in Figure 1.1

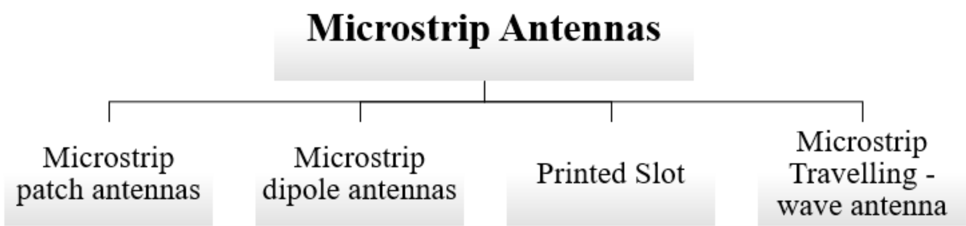

Fig. 1.1: Basic Categories of MSAs

The Microstrip patch antenna is used for narrow-band microwave wireless links.

There exist several layers in the microstrip patch antenna. One among the many layers, the base of an antenna is made up of dielectric substrate who's on the front side lies the patch which radiates electromagnetic waves attached along with a metallic patch known as a feed line which is grounded on the other side as reflected in figure 1.2 Photolithography technique i.e., the process which is taken into account to print the feed lines and the patch of an antenna is used to print on the dielectric substrate.

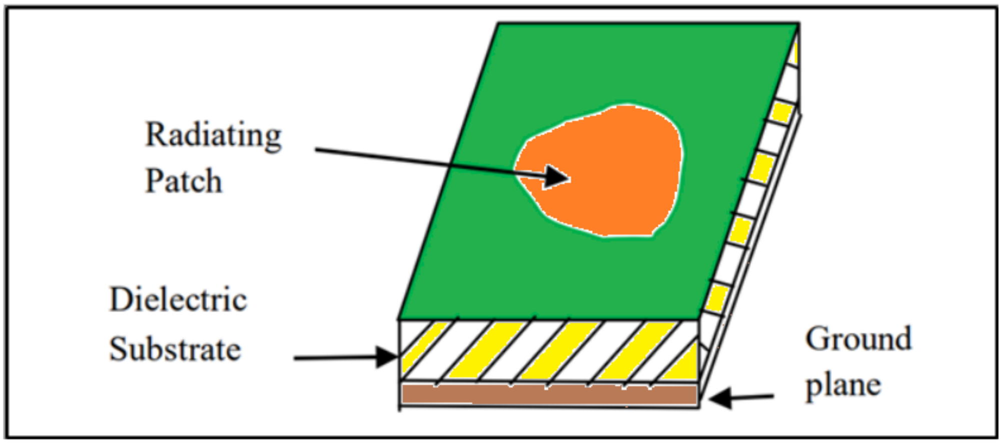

Fig. 1.2: Microstrip antenna configuration

Additionally, the patch can be of various shapes and sizes as per the requirement of antenna design. For various shapes of patches see fig 1.3 [10]

MSPAs can be designed by taking a rectangular patch and FR-4 substrate with a worthwhile thickness whose dielectric constant lies in the range of 3.8. to 4.8 which is considered to be as low in value to reap the desired gain of the antenna leading to a substantially good performance refer figure 1.4.

As the microstrip patch antenna is a resonant antenna, thereby feedlines become perhaps the most important aspect of an antenna as it allows it to drive on the desired frequency. We have several methods by which antenna can be fed. Most admired feeding techniques [33] are microstrip feedline, Aperture Coupling, Proximity Coupling, Coaxial Probe, and coplanar waveguide (CPW) feeding. Among the list, we choose that method with which we can derive maximum power transfer and minimum input loss.

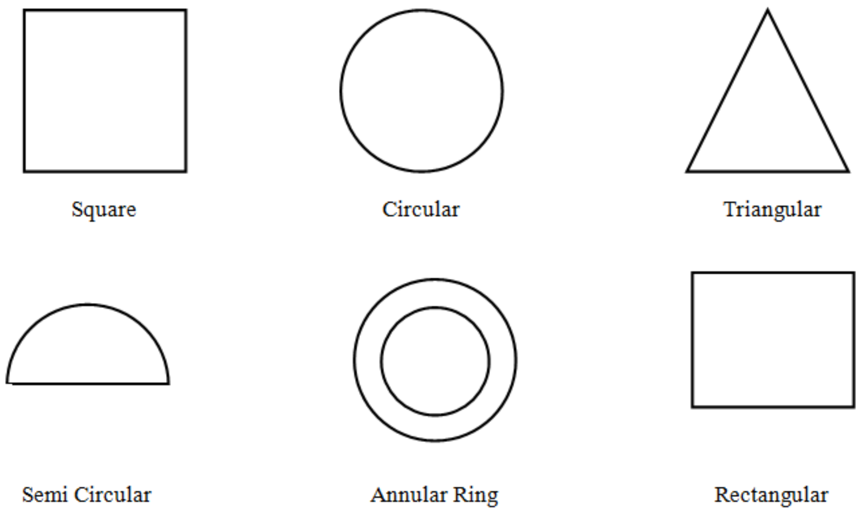

Fig. 1.3: Various patch Shapes

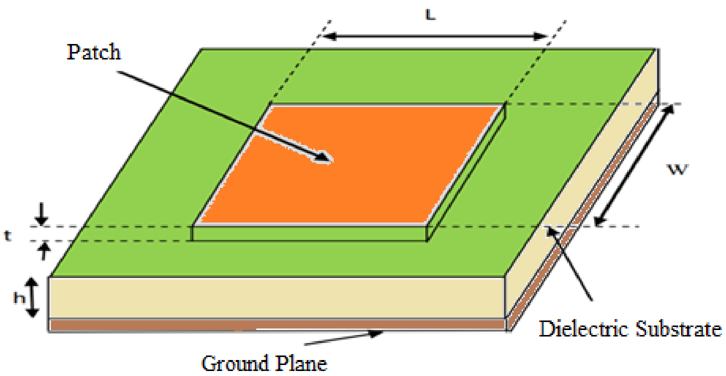

Fig. 1.4: Structure of RMSPA

1.3.1 Microstrip feedline

A microstrip feedline is a narrow conducting strip that is minuscule in terms of width as compared to that of the patch. The feed-line has the advantage that it can be easily constructed by just etching along with the patch of the antenna, giving rise to the planar structure. The feed locale can be maneuvered easily leading to flawless impedance matching[33].

1.3.2 Aperture Coupling

The aperture technique for antenna feed is used when the antenna consists of two substrates (i.e., lower and upper substrate), provided that the ground plane is between the substrates and a microstrip feedline is underneath the lower substrate[38].

1.3.3 Proximity Coupling

Unlike the aperture technique for antenna feed, the ground plane lies underneath the two substrates. In proximity coupling the spurious radiation is low. Although this technique is easy to design, we encounter a lot of complications with the fabrication[33] [38].

1.3.4 Coaxial Probe

In the coaxial probe technique for antenna feed, the coaxial probe's inner conductor is attached to a patch, allowing the element to radiate while the outside conductor makes contact with the ground plane. Since the intended location of the feed inside the patch can be easily matched to the input impedance, this technique is more extensively used. However, the construction of the antenna is a complicated job[38].

1.3.5 Coplanar Waveguide (CPW) feeding

The coplanar waveguide technique for antenna feed has a simple configuration in which there is no need for coupling via holes[39].

1.4 Outline

Parameters for testing the system were discussed in this chapter, and the remaining portion of this work is undermentioned. The literature review is presented in the report's following chapter that is, Chapter 2. This chapter discusses the reviewed research publications that are pertinent to this project. Problem identification is described, and then the project's main goals are discussed. The recommended methodologies are described in Chapter 3 up to Chapter 5 of the study. These chapters present block diagrams and descriptions of the proposed methodologies with the components used to prepare the systems. Chapter 6 gives a detailed explanation of the PSO algorithm and its application to the proposed design. The completed project is depicted and discussed in chapter 7, i.e., results and discussion. Conclusions of complete work are outlined in chapter 8.

CHAPTER 2

Literature Review

It is a vital step before starting any project since it informs the reader about the author's personal involvement in recent developments in a certain area of research. There are other motivations as well, such as identifying issues that need to be addressed, coming up with solutions to those problems, and so on. Identifying the research methodologies that were employed to examine the provided solutions. Creating a framework for launching new research projects Identifying research gaps in the current state-of-the-art and identifying a unified body of work in the field.

2.1 Summary of Related Literature

Shi-Chang Gao, et al [2002] presented a Microstrip antenna with an H-shaped coupling aperture for a wider band. The input impedance parametric work is presented via the finite-difference time-domain approach. The impedance 2 bandwidth of the antennas is 21.7%. The front-to-back ratio and cross polarisation of the antenna RP were both about 22 dB and about 23 dB, respectively[40]

Chourasia et al [2004] described various microstrip patch antennas including Triangular, I shape, rectangular, pentagonal, and circular shapes made with the substrate material and functioning at 1.5 GHz. By Using Computer Simulation Technology's (CST) Microwave Studio, she created circuits. Return loss, efficiency, and directivity are only a few of the parameters that are simulated, examined, and contrasted. She concluded from the findings that triangular microstrip patch antennas deliver the best outcomes with good return loss and efficiency trade-offs for downsizing at 1.5 GHz, which has broad applications in military telemetry, GPS, mobile phones, and amateur radio[10].

Jin et al [2005] introduced a brand-new evolutionary optimization technique for designing wide- and multiband patch antennas. In the study, he looked at two things:

First, he tested the parallel PSO/FDTD method using the design of rectangular patch antennas. Then, E-shaped patch antennas are designed using the optimizer. He noticed that by utilizing several fitness functions, the optimization produced dual-frequency and wideband antennas with the needed performance [22].

Jin et al [2008] gave three examples to show how PSO can be used to solve a wide range of practical issues. These examples fall under the optimizations of return loss and radiation pattern, but because the fitness function may be defined in a variety of ways, PSO is also able to take into account additional design needs. He noted that because antenna optimizations are typically highly nonlinear and multimodal, PSO is particularly well suited for them as a stochastic global optimizer. Each example presented the simulation and measurement results of PSO-optimized antennas in order to demonstrate the power of PSO to provide a usable and workable design[41]

Kushwaha et al [2012] A novel compact microstrip antenna for enhancing gain and bandwidth has been designed and simulated successfully. Simulation results of a wide band microstrip patch antenna covering 1.73 GHz to 2.23 GHz frequencies have been present. With the use of a 50-ohm microstrip line feed, the proposed microstrip patch antenna achieves an impedance bandwidth of 25% at -10 dB return loss. Good antenna performance and impedance matching can be realized by adjusting the length and width of the microstrip line. It is also observed that the bandwidth increases with the increase in the length of the offset present in the middle of the feed line. It can be concluded from the results that the designed antenna has satisfactory performance and hence can be used for indoor wireless applications[42].

Sharma et al [2012] proposed an application-specific small-size microstrip antenna for WLAN using the feeding techniques of probe feed and aperture feed. She came to the conclusion that an aperture coupled feed microstrip antenna gives a bandwidth of almost 24% with 1.04 VSWR and an uneven slot in the patch provides a bandwidth of 16.4 % with 6 dB gain and near to about 1.06 VSWR. and hence, provided improvement in the impedance bandwidth and good matching by making slots on the patch and using the aperture coupled feed feeding method[43].

Rajput et al [2014] designed an I shape antenna and illustrated the Particle Swarm

Optimization (PSO)-based optimization with Curve Fitting maintaining Fr fix near 2.4 GHz. Data for creating the PSO program in MATLAB is gathered by tweaking various antenna characteristics. The PSO optimized antenna's performance is contrasted with that of the initial antenna. The findings show that PSO-optimized antennas have resonance near 2.414 GHz and substantially increase fractional bandwidth near to 25% than that of the original antenna[29].

Raithatha et al [2015] presented a microstrip patch antenna to learn about its feeding methods, shapes of the patch, and different parameters that reveal the output characteristics of the antenna, such as VSWR, Gain, Bandwidth, Return loss, Directivity, etc. He also mentioned the most recent advancements in microstrip patch antennas (MSTPA), the significance of the patch's shape and size, and the implications of the substrate in obtaining the appropriate output parameters[44].

Sidhu et al [2016] suggested a rectangular microstrip patch antenna (RMPA) with a circular slot suitable for S-band and X-band applications. He has performed comparative observations between the proposed antenna's various feed positions and its slotted architecture using traditional RMPA which resulted in the geometry of the RMPA's second iteration that displays a dual band with frequency swept to the lower side compared to traditional RMPA that is 46% smaller in size, and the third iteration of the RMPA's shape, which displayed a further frequency shift to the lower side and size reduced to 48% [45].

Zhang et al[2017] suggested the AVDABC adaptive variable differential approach as an ABC paradigm. Additionally, the selected choice variables could undergo modification based on various search formulas. He has shown the effectiveness of AVDABC On a Yagi-Uda antenna design and a sparse non-uniform antenna array design. Even when utilizing a small colony size, the algorithm achieves a respectable level of performance and demonstrates strong robustness and efficiency. In his review, he explained that multi-objective optimization problems can be used to model antenna design challenges, if more research is done, AVDABC might be expanded to address these issues [26].

Anum et al. [2018] discovered that adding slots to the patch and feed line, altering the substrate's height, maximizing the placement of the feed line, and changing the patch's form all help to increase bandwidth in the ultra-wideband (UWB) range. Utilizing a partial ground plane lowers the antenna's quality factor, increasing its bandwidth. He curved slots and patches to offer greater impedance matching and excite higher-order modes. His proposed antenna produced simulated results with a yield impedance bandwidth of 9.1(2-11.1) GHz, a 121 % bandwidth improvement over the traditional antenna, and a 32 % improvement over the feedline antenna[46].

Kumar et al. [2018]proposed a three-stage band notching process using circular, truncated, and T-shaped slots in the framework. The design of a planar rectangular microstrip patch antenna with a full ground plane was the initial stage, and two circular truncations were added to the radiating patch and the partial ground plane in the second stage to increase the structure's bandwidth. Also, on the right side of the radiating patch, one rotating T-shaped slot was added in the third stage, and at 4.6 GHz it reached the greatest return loss of roughly-45.5 dB. The structure's highest gain, of 5.478 dB at 9 GHz, is the result of a piecewise constant gain over the full UWB.[47]

Fernandes et al [2019] designed and optimized a dual-band patch antenna and simulated it, and his results showed an improved gain of 7.54 dBi and 6.8 dBi at 2.4 GHz and 5.8 GHz, respectively. He suggested that an FSS, dual-band, be used as a reflector plane for this objective. He also achieved a bandwidth of 7% at the central frequency of 2.4 GHz, while a bandwidth of 1.07 GHz (18.8% fractional bandwidth) was achieved at the frequency of 5.8 GHz[48].

Verma et al [2019] used manual (traditional) optimization and particle swarm optimization (PSO) with curve fitting to optimize and conduct comparative analysis for a rectangular microstrip patch antenna loaded with a "T"-shaped slot. He achieved the fragmentary bandwidth enhancement in his antenna to 16.86% by applying PSO using equations by curve fitting and a fixed resonant frequency near to 2.45 GHz, i.e., at 2.477 GHz. He also obtained an efficiency of 99.99% and a 3.432 dB gain with his final design[30].

Rajan s et al [2019] created a microstrip patch antenna for 77.32GHzthrough simulation. He also suggested that a microstrip patch antenna is one of the study fields that has seen quick growth and They have a wide range of potential uses because of their low weight, small size, and simplicity of manufacture. Additionally, he predicted antennas with small dimensions, good radiation pattern performances, and applications in a variety of communication devices[49].

Verma et al [2019] worked on a T-shape patch antenna that was fed directly by a 50-microstrip line and loaded with a rectangular slot using the IE3D simulation program, he improved it by changing each of its four parameters while holding the other three constants in order to increase its bandwidth at a frequency of 2.45 GHz. In the frequency range of 1.682-3.988 GHz, he enhanced the impedance bandwidth of the optimized antenna from 40.05 to 81.34 %. The optimized antenna has a high return loss of 47.47 dB and resonates at 2.181 GHz. Bluetooth, wireless local area networks (WLAN), and Worldwide Interoperability for Microwave Access (WiMAX) applications can all make use of this frequency spectrum[50].

Sabir et al [2020] presented a small, T-shaped fractal patch antenna for X-band applications at Rf = 9.0 GHz. To increase effectiveness and improve antenna parameters including RL, VSWR, FBW, directivity, etc., iterations up to the third order have been carried out and developed the antenna for a number of X-band (8 GHz to 12 GHz) applications, including radar, terrestrial networking, space communications, etc. [51]

Maurya et al [2020] proposed a brand-new asymmetrical feed circularly polarised hexagon ring microstrip patch antenna (HRMSA) for use in S, C, and X bands. He added a slot with a semi-arc form to the ground plane, and a 25-degree tilt has been applied to the hexagonal ring along with the microstrip-line feed. It led to the creation of an impedance bandwidth of 134% for the UWB frequency range with an average gain of 4.15 dBi[52].

Mazen et al [2021] built an antenna on the Rogers RT5880 substrate's top to facilitate multi-band operation and etched a slot in the patch's surface with a rectangle and a circle to support multi-band frequency capabilities for mid-band 5G applications having dimensions (94 × 76 × 3.18 mm3). He designed and fabricated two antennas covering multi-band microstrip patch antennas. $Antenna_1$ supports tri-band frequencies at 6.45 GHz for C-band, 3.86 GHz for WLAN, and 2.53 GHz for WiMAX, which has the capability to be used for 5G services. $Antenna_2$ has dual-band capabilities for C-band

and X-band at 6.92/ 7.707 GHz, which is serving for C-band and has a peak under -45 dB appropriate for mid-band 5G applications[53].

2.2 Problem Identification

The MSAs are the unsung heroes of modern wireless communication systems because of their many advantages, such as their lightweight and compact size. However, one of the most significant challenges in the design of a microstrip antenna with a wider bandwidth, as the limited bandwidth is its major shortcoming, as well as the resonant frequency matching with design frequency is an important factor. This is because these antennas are narrow band antennas. Despite the fact that a lot of research has already been done, there is still scope for enhancing their efficiency, gain, and bandwidth while also making them more compact. Therefore, the Antenna design problem consists in finding an implementable Microstrip patch antenna design whose profile is low, whose fragmentary bandwidth is wider, and whose resonating frequency also best approximates the specified ideal design frequency, which is given as the desired design specifications or constraints.

2.3 Objectives

Based on the problems identified from the literature review following objectives are framed.

1. To Convert the desired Antenna design constraints into precise specifications of the type of antenna, size, the shape of a patch, shape of slot, type of substrate material, dielectric constant, type of feed, return loss criterion, band characteristics, and frequency range.

2. To carry out the parametric calculations to obtain basic dimensions using design equations.

3. To realize the Antenna using the digital simulation technology most suitable for the considered application. This step depends on the technology or software used to build the Antenna with ease and perfection.

4. To optimize the designed antenna for enhancing the FBW which is usually done with computer software that implements sophisticated numerical optimization routines. In addition, these design packages usually have a convenient graphical user interface to aid in the conversion of specs needed in objective 1. With such software, an Antenna design can be carried out quickly so that many designs can be tried in the process of getting the best Antenna.

5. For objective 4 global optimizations (GA, PSO, ABC, etc.) and some strategic techniques are chosen to be applied.

2.4 Major Techniques/Tools used

2.4.1 Zeland software IE3D

IE3D is a full-wave electromagnetic simulation and optimization tool for 3D and planar Antennas, microwave circuits, RFIDs, MMICs, digital circuits, and high-speed printed circuit boards (PCB). Ie3d has seen widespread applications in the design of patch antennas, microwave circuits, wire antennas, and other RF/wireless antennas. It was formally introduced in 1993 for the first time (IEEE IMS 1993) thereafter it was adopted for industrial usage Since then, it has seen significant improvements.

Application Program of IE3D used :

MGRID: This is the standard layout editor for building geometrical structures. A user can construct and alter a structure using polygons and vertices. Layout editing, s-parameters display and post-processing, current distribution visualization, near-field, and far-field post-processing, and modeling are all included in this. In addition, Fast EM Design Kit is also included for real-time full-wave EM tuning and optimization. The complete procedure to obtain the simulation results does contain the next mentioned steps as follows:

Start the design by setting up the basic requirements of layers like Dielectric constant, thickness, and loss tangent, and set the z-axis at zero for the ground plane. Thereafter, get into the Polygon-based layout editing on MGRID or IE3D EM Design System followed by drawing polygons from GDSII, DXF, GERBER or ACIS Build 3D features such as vias, thickness traces, and wire bonds. Then the ports have to be defined in the structure to carry out further operations. The EM simulations are performed over the structure on MGRID and Real-time full-wave EM tuning and operations are obtained.

2.4.2 MATLAB

MATLAB is a mathematical program for engineers. Unlike other related applications like Mathematica, MATLAB focuses on numerical computation over algebraic analysis. This makes it far better suited to data manipulation than others.
It is a high-performance language for technical computing that combines computation, visualization, and programming in an easy-to-use environment where problems and solutions are expressed in easily understandable mathematically related notations. It is used for Wireless Communications, Robotics, Deep Learning, Mechatronics, Signal Processing, Test and Measurement, Power Electronics Control Design, Embedded Systems, Image Processing, Computer Vision, Control Systems, Machine Learning, Internet of Things, Math and computation, Algorithm development, Antenna designing, Data acquisition, Scientific and engineering graphics, Modeling, simulation, and prototyping, Data analysis, exploration, and visualization, etc.

MATLAB facilitates a bunch of additional application-specific toolboxes. They give you the ability to understand and use sophisticated technologies. Toolboxes are collections of MATLAB functions that allow you to expand the MATLAB platform to solve particular types of problems. Toolboxes for signal analysis, antenna design, curve fitting, antenna array design, image segmentation, PCB Antenna designer, neural networks, fuzzy logic, simulation, and many other disciplines are offered as add-ons.
Additionally, it makes optimization techniques rely on pseudo-random search algorithms easier to use, like Particle Swarm Optimization (PSO), Hybrid PSO, Genetic Algorithms, Artificial Neural Networks, and Bees Algorithms, etc.

The MATLAB System comes mainly with Desktop Tools and Development Environment. These are the tools and resources that assist you in utilizing and improving your productivity with Algorithms and scripts. These also include the MATLAB desktop and Command Window, an editor and debugger, a code analyzer, workspaces, folders, and browsers for accessing help.

MATLAB language is a high-level matrix/array programming language that comes with the capabilities such as functions, control flow statements, input/output, data structures, and problem-oriented programming.

MATLAB Graphics comprises a variety of options for visualizing vectors and matrices as graphs, as well as editing and printing them. It contains high-level visualization tools, animation, image processing, and presentation graphics functions in two and three dimensions. It also includes low-level utilities for extensively customizing the appearance of visuals and creating complete GUIs (graphical user interfaces) for our MATLAB projects.
MATLAB also facilitates external language Interfaces; this can be done with MATLAB's Engine APIs. It also allows you to run MATLAB commands from within your programming language without having to open a MATLAB desktop session. The following are some of the APIs are C/C++, Java, FORTRAN, Python, components, and applications including many programs written in languages such as Visual C# ® .N and Visual Basic® .NET
It offers functions for dynamically connecting MATLAB routines, calling MATLAB as a computational engine, and reading and writing MAT files.

2.4.3 Vector Network Analyser

Vector network analyzers are also called gain-phase meters or automatic network analyzers. Vector network analyzers are a part of test instrumentation generally for testing microwave components in radio frequency design laboratories. It carefully analyses the performance and operation of all types of RF networks. VNAs provides significantly more information than scalar network analyzer but are also quite expensive. It gives input to the RF network and checks the output response. It has multi-frequency operability, to be precise, it can be used for all microwave and RF frequencies. VNA can measure more parameters as compared to the scalar network analyzer about the device under it examines the phase as well as the amplitude response, henceforth called a gain-phase meter or an automatic network analyser[54].

CHAPTER 3

Antenna Design using Proposed Optimization Technique-I

3.1 Overview

In this chapter, a triple-narrowband inverted T-slotted rectangular microstrip patch antenna is designed and analyzed, as well as its optimization, employing strategy 1 to enhance the antenna's fragmentary bandwidth while maintaining a decent return loss. The design consists of an inverted T-shape slot that constitutes the base on which a rectangular microstrip patch is implemented. The patch is mounted on an FR4 substrate with a dielectric constant of 4.4. The simplicity of use, accessibility, and affordability of FR4 as a substrate were the main factors in the choice. Beneath the substrate, ground exits, and over the substrate the combination of rectangular patches and slots of an inverted T-shape lies. The initial antenna is designed to obtain narrow-band characteristics. Since an antenna's impedance bandwidth must be below 50% in order to be classified as a narrow band, it reflects a narrow band.

condition to be satisfied for an antenna to fall under narrow-band characteristics

$$FBW(impedancebandwidth) = \frac{(f_{ub} - f_{lb})}{f_c} 100 < 50\% \tag{3.1}$$

f_{ub} is the upper bound frequency of the band/The higher cutoff frequency.
$f_l b$ is the lower bound frequency of the band/The lower cut-off frequency.

$$f_c = \frac{(f_{ub} + f_{lb})}{2} \tag{3.2}$$

where f_c is the central resonance frequency.

Note: Fractional bandwidth ranges from 0 to 2 and is frequently expressed as a percentage (between 0% and 200%). The greater the percentage, the broader the bandwidth.

The upcoming explanations will show the initial antenna's fragmentary bandwidth attained is 29.26% which clearly reflects the antenna is a narrow band antenna. A brief review of the upsides and downsides of narrow-band is addressed before moving on to the design specifications, simulation outcomes, and conclusions reached from them. Narrowband antenna devices are more expensive to install and have a larger size than wide band modules. As Narrow Band antennas possess very small bandwidth and gain is also not decent hence, the data communication speed is accompanied by latency. Though these shortcomings are covered up and balanced in its advantages, as it's quite useful for ensuring long-range communications stability. Carrier purity is also relatively high in the related transmission spectrum. Also, the transmission energy can be focused on a smaller section of the spectrum in narrowband devices. As a result, these have better channel-to-channel isolation. One of the most significant benefits of having a narrower signal bandwidth is that the chance of signal overlap with interfering signals is reduced but at the same time the applications for the usage become confined. Thus, the slotting is performed on USRMSPA and the strategic optimization technique (strategy 1) has been carried out for the initial inverted T-shape slotted RMSPA, in this chapter for the broadening of the bandwidth and to obtain more numbers of the band as well as for a better return loss.

3.2 Basic Design Procedure Antenna

This section of the chapter thoroughly explains the antenna design, as well as the technique for obtaining the design and the simulation outcomes.

Design parameters

The proposed design is initially carried out over dielectric material glass epoxy (FR4) substrate possessing the dielectric constant 4.4 at 2.45 GHz design frequency. The Fr4 is chosen since it is less expensive and more readily available also, it comes with a flexibility of smaller thickness at higher frequencies. The thickness that is taken is 1.6mm. To decide the geometric parameters including the ground plane dimensions, the antenna geometry design equations are utilized. The equations for the dimensional calculations are below:

$$w = \frac{c}{2f_r}\sqrt{\frac{2}{\epsilon_r + 1}} \tag{3.3}$$

where, f_r is the predetermined frequency (design frequency) in GHz,ϵ_r is the "dielectric constant" of the substrate, The speed of light in a vacuum is $c = 3\text{x}10^8$ m/s denoted as "c" here, and W is the patch's width.

The substrate material's effective dielectric constant (ϵ_{ref}) is assessed using [5][55][56] :

$$\epsilon_{reff} = \frac{(\epsilon_r + 1)}{2} + \frac{(\epsilon_r - 1)}{2}(1 + \frac{12h}{w})^{\frac{(-1)}{2}} \tag{3.4}$$

The radiating patch's extended length (ΔL) is determined by[5][55][56]:

$$\frac{\Delta L}{h} = 0.412\frac{(\epsilon_{reff} + 0.3)(\frac{w}{h} + 0.264)}{(\epsilon_{reff} - 0.258)(\frac{w}{h} + 0.8)} \tag{3.5}$$

The aforementioned value of (ΔL) is utilized to determine the patch's absolute length (L), It is depicted below[5][55][56] :

$$L = \frac{c}{2f_{r\sqrt{\epsilon_{reff}}}} - 2(\Delta L) \tag{3.6}$$

The computed patch has dimensions of 27.69 mm in length(L_p) and 37.26 mm in width (W_p). Eqs.3.7 and 3.8 are used to calculate the ground length (L_{gnd}) and width (W_{gnd}) as follows:

$$L_{gnd} = 6h + L_p \tag{3.7}$$

$$W_{gnd} = 6h + W_p \tag{3.8}$$

According to the preceding equations, ground plane length (L_{gnd}) is 38.43 mm and width (W_{gnd}) is 46.86 mm.

Table 3.1: Salient dimensional parameters of initially designed un-slotted rectangular microstrip patch antenna.

Substrate (glass proxy)	$\epsilon_r = 4.4$
	$h = 1.6$
Rectangular-shape ground plane's dimensions	$L_{gnd} = 38.43mm$
	$W_{gnd} = 46.86mm$
Patch length	L_p=27.69 mm
Patch width	W_p=37.26 mm
Line Feed's length	L2=1.6mm
Line Feed's width	W2=4mm
Feed's coordinate	(-15.245,16.63)

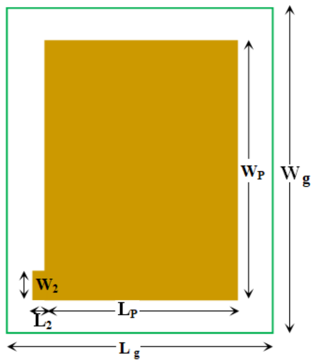

Fig. 3.1: Parametric geometry of the un-slotted rectangular microstrip patch antenna

Initially, the proposed antenna has been designed using the above-mentioned equations; also, the microstrip line length (L_2) is taken as 1.6 mm and the width(W_2) as 4 mm. The geometry of the un-slotted rectangular patch antenna is expressed below in figure 3.1 and parameters are described in table 3.1. The design has been carried out using IE3D software and the simulations are done for the outcomes over the same software.

As per the table 3.1, the substrate taken is FR4(glass epoxy) with a dielectric constant of 4.4 and the substrate thickness of 4.4 mm. This table also reflects the antenna's ground plane dimensions, strip line feed dimensions as well as feed coordinates.

Utilizing the dimensional data in table 3.1 and taking the center coordinate (0.2, 0) of the patch the other coordinates are determined and the antenna is realized over IE3D software and constructed as figure 3.1. The lower corner on the left of the radiating

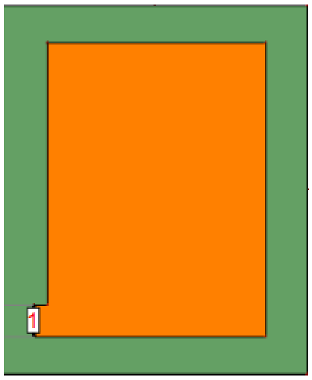

Fig. 3.2: Designed geometry of the un-slotted rectangular microstrip patch antenna over IE3D.

patch has been supplied with the microstrip line feed (50Ω). Figure 3.2 depicts the antenna's design geometry over the IE3D workspace.

The un-slotted antenna has obtained three bands with FBW($<$ -10 dB) of 14.72%,7.82%, and 10.84% resonating at 1.91 GHz,3.7 GHz, and 4.90 GHz providing the return loss of –14.7 dB, –12.60 dB, –28.06 dB respectively.When the feed length is 1.6 mm and the width is 4 mm. These outcomes are generated by simulating the USRMSPA between the meshing frequency range of 1 GHz to 6 GHz for the 1000 points of frequency for the calculation of the result including the s-parameter spectrum. The upper and lower frequency of cutoff of the USRMSPA is 1.78 GHz and 2.07 GHz for band 1, 3.64 GHz, 3.9 GHz for band 2, and 4.61 GHz and 5.14 GHz for band 3, respectively.

The return loss graph of the USRMSPA is represented in Figure 3.3. It is clear from the figure as well as from table 3.2 that the bandwidth obtained is not good. Also, the notch of the return loss falls below -20 dB for two of the bands and the notch is neither coinciding nor near the design frequency. A microstrip antenna's design must precisely coincide with its resonance frequency at the design frequency due to its limited bandwidth. An antenna can operate effectively at the resonance frequencies in the narrowband region.

As a result, using a method that matches the resonance frequency leads to better antenna design, for the same primarily we followed the following steps:

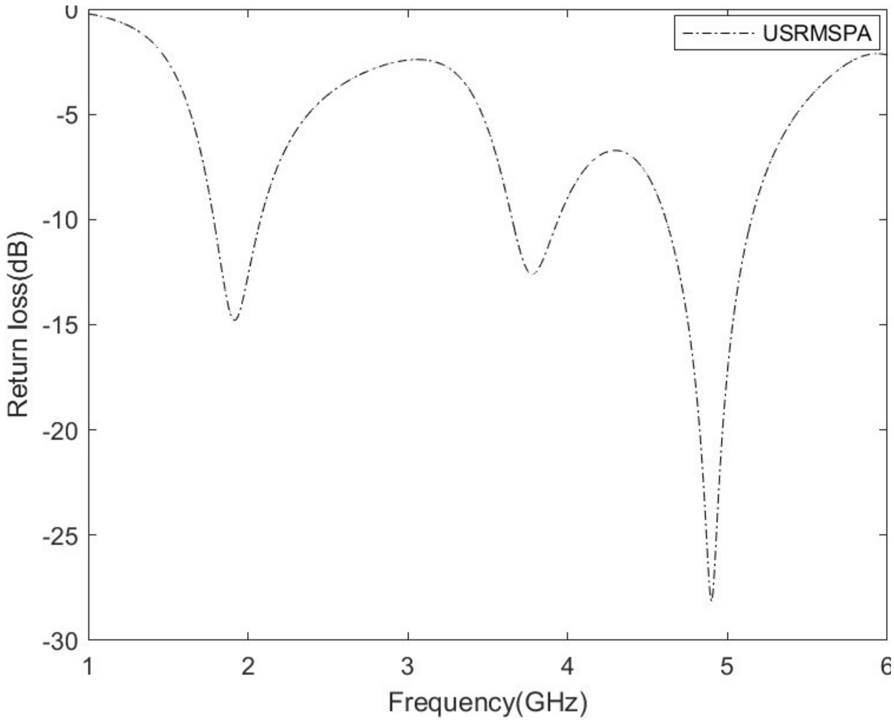

Fig. 3.3: Return loss graph of the un-slotted rectangular microstrip patch antenna.

Table 3.2: S (1,1) parameter outcomes of initially designed USRMSPA.

Antenna	Bands	Lower freq. (GHz)	Higher freq. (GHz)	Bandwidth (%)	Resonant freq. (GHz)	Return loss (dB)
USRMSPA	B1	1.785	2.07	14.73	1.92	-14.78
	B2	3.64	3.94	7.83	3.78	-12.60
	B3	4.6	5.14	10.85	4.90	-28.06

Step-1: Design USRMSPA utilizing selected table 3.1.

Step-2: Slot cut over the rectangular patch as per the desired inverted "T" shape at different positions.

Step-3: Analyze the effectiveness of the suggested patch antenna designed in terms of return loss.

Step-4: When the return loss is less than -20dB, then the proposed patch antenna is optimized otherwise go to Step-2.

The flowchart below (figure 3.4) explains the steps followed to reach the initial inverted T-shape slotted RMSPA where RL stands for the return loss or the return loss obtained from S (1,1) parameter analysis.
By removing the slots as illustrated in Figure 3.5, the initially proposed Inverted T-Slotted rectangular microstrip patch antenna was realized. The suggested antenna's radiating patch has a center coordinate of (0.2, 0), and a microstrip line feed (50Ω) has been supplied at the lower corner on the left side of the radiating patch, with a strip that is 1.6 mm in length (L_2) and 4 mm in width (W_2). The center of the T-shape slot is also shifted on the x-axis by 0.2 as well as it's designed to touch the upper horizontal edge of the patch and accordingly the dimensional coordinates are carried out. The bandwidth and the return loss of the initial inverted 'T'-shape slotted RMSPA can be optimized by making iterative changes in four selected dimensional parameters of the antenna. Out of a total of ten salient dimensional parameters, four are selected as variables. All salient parameters of the initial inverted 'T'-shaped slotted antenna are indicated in Table 3.3. The initial inverted 'T' shape slotted RMSPA has been designed using table 3.3 and simulated using the IE3D(ZLS) software, according to its analysis as results it has provided the maximum bandwidth (below -10 dB) of 29.26 % at resonant frequency 1.85 GHz with the minimum return loss of -27.48 dB provided the line feed with the width of 4mm and length of 1.6 mm.

The initial antenna has been simulated in the range of 1 to 6 GHz for 1000 sample points. After the simulation, the three bands are obtained as shown in the S (1,1) parameter graph or the return loss graph in figure 3.6. Band 1 has obtained the deepest

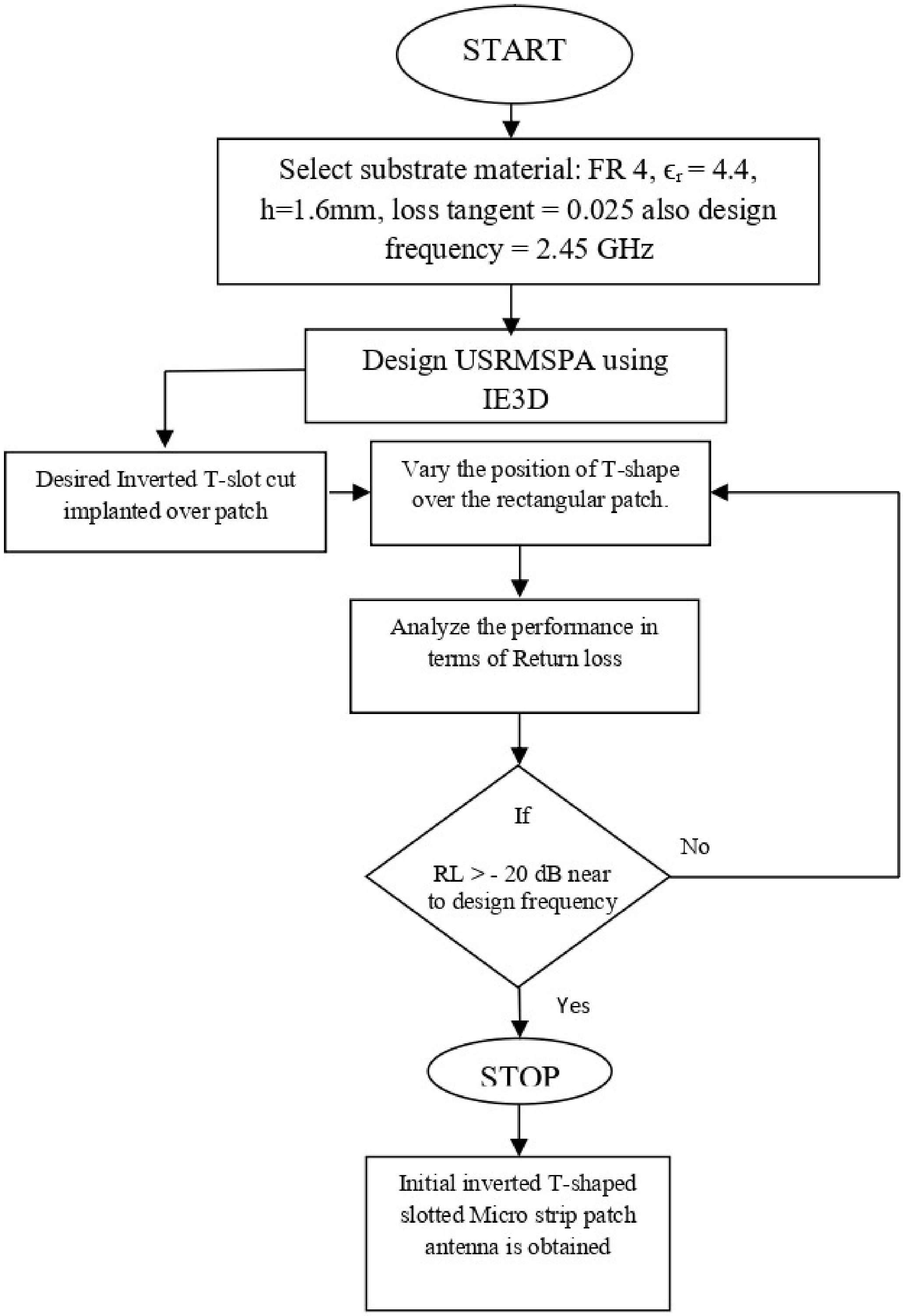

Fig. 3.4: Flow Chart to reach the initial inverted T-shape slotted RMSPA.

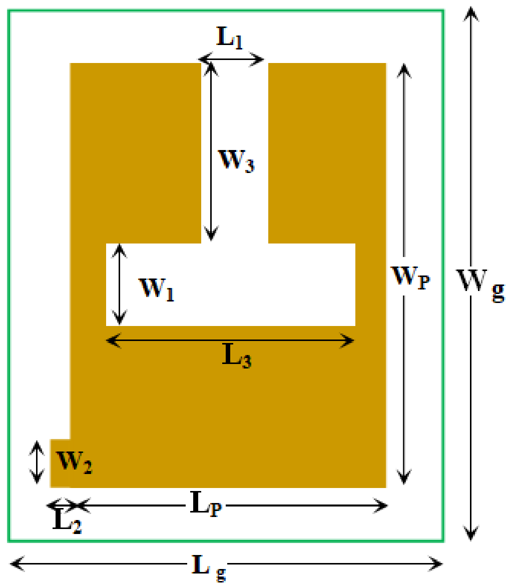

Fig. 3.5: Parametric geometry of the initial inverted T-shaped slotted RMSPA.

Table 3.3: Salient dimensional parameters of initially designed inverted T- shape slotted RMSPA.

Substrate (glass proxy)	$\epsilon_r = 4.4$
	$h = 1.6mm$
Rectangular-shape ground plane's dimensions	$L_{gnd} = 38.43mm$
	$W_{gnd} = 46.86mm$
patch length.	$L_p = 27.69mm$
patch width	$W_p = 37.26mm$
slot parameters	$L_1 = 6mm$, $L_3 = 22mm$
	$W_3 = 16mm$, $W_1 = 7.26mm$
Line Feed's length	$L_2 = 1.6mm$
Line Feed's length	$W_2 = 4mm$
Feed position coordinate	$(-15.245, -16.63)$

notch, providing the minimum return loss of -27.48 dB. The upper and lower cutoff frequencies of band 1 are 1.74 GHz and 2.33 GHz, respectively, resulting in a bandwidth percentage of 29.26%. Band 2 has an upper and lower cutoff frequency of 3.54 GHz and 4.02 GHz, respectively, providing a bandwidth percentage of 12.68% and the return loss for Band 2 is -22.5dB at 3.796 GHz. Band 3 has the upper and lower cutoff frequencies of 4.85GHz and 5.27GHz, respectively, obtaining 8.26% of bandwidth and the return loss is -23.05 dB. The VSWR obtained for the same is shown in figure 3.7 reflecting VSWR to be 1.08816 dB.

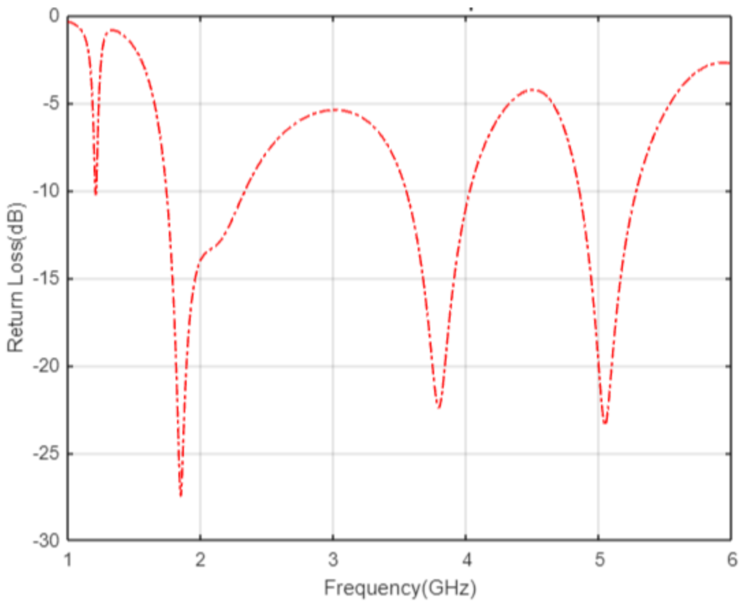

Fig. 3.6: Return loss graph of the initial inverted T-shape slotted RMSPA.

Table 3.4: S(1,1) parameter outcomes of initial inverted "T" shape slotted RMSPA

Antenna	Bands	Lower freq. (GHz)	Higher freq. (GHz)	FBW (%)	Rf (GHz)	RL (dB)
Initial Inverted	B1	1.74	2.34	29.26	1.85	-27.49
T-shaped slotted	B2	3.54	4.02	12.68	3.80	-22.58
RMSPA	B3	4.86	5.27	8.26	5.04	-23.05

Table 3.4 illustrates the simulation outcomes of the antenna. These are noted from the S-parameter graph i.e, S(1,1) parameters. As a result of the initial antenna, we have obtained the triple-band with increased bandwidth % as well as the return loss is also improved for each of the bands but the resonating frequency is still not that near to the design frequency hence there is a need of optimization.

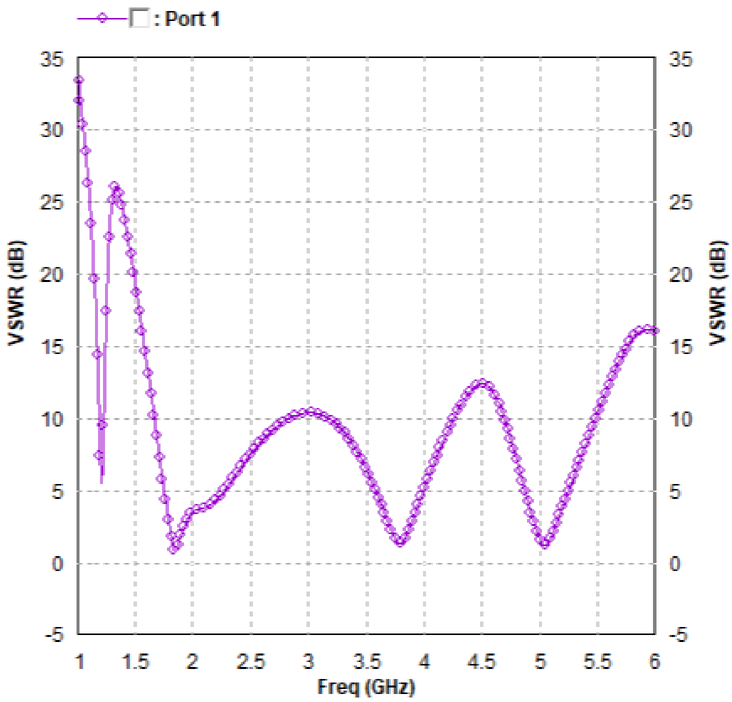

Fig. 3.7: VSWR graph of the initial inverted T- shape slotted RMSPA.

3.3 Optimization Technique - I

Optimization of the initial antenna has been executed by utilizing strategic iteration optimization. In order to do this, some prominent baseline antenna dimension characteristics are used as the variable parameters. Ten parameters make up the basic design, but only four-dimensional parameters are chosen, which are the vertical arm length of the T-shape, the horizontal arm width of the T-shape, line feed length, and line feed width. These are varied in such a way that three of them, including other parameters, are kept constant while one of these is varied to a certain range with a certain step size. This procedure is applied to each variable parameter for Strategic Optimization.

The initial antenna has been optimized by the variation of some of the dimensional parameters which have been selected as variables. The four parameters L_1, L_2, W_1, and W_2 have been selected out of all ten parameters, L_g, W_g, L_p, W_p, L_1, L_2, L_3, W_1, W_2, and W_3.The parameters L_2 and W_2 are the strip line feed parameters (line feed length and width, respectively), and the other two, L_1 and W_1, are the inverted 'T' shaped slot parameters (vertical arm length and horizontal arm width, respectively).

Table 3.5: Variable dimensional parameters range.

Selected parameters	Lower limit(mm)	Upper limit(mm)	Step size (mm)
L_1	1	18	1
L_2	1.4	4	0.1
W_1	2.26	16.26	1
W_2	3	9	0.5

These selected parameters have been varied one after the other. At a time, only one parameter is picked and varied to a certain range (lower bound, upper bound, and step size) as reflected in Table 3.5 by keeping all the other parameters constant. For each value of the selected parameter, the antenna geometry has been realized and simulated using IE3D. The number of bands is noted from the s(1,1) simulated results, and for each band of a particular antenna, the lower and upper cutoff frequency, return loss, and resonant frequency have been noted. The bandwidth percentage has been calculated for each band of each antenna.

Once the results are obtained for every antenna of each selected variable parameter, the best results are taken out (parametric value at which maximum bandwidth is obtained) from the set of antennas for the particular parameter.

L_1 is initially adjusted in steps of 1 mm from 1 to 18 mm. The basic antenna's L_1 value was 6 mm, and a total of 18 (1 initial + 17) antennas were developed for L_1. L_1 = 12 mm (band 1) achieves a maximum bandwidth of 30.77% at 1.85 GHz resonant frequency with a return loss of -43.19 dB. Furthermore, band 2 obtained a bandwidth of 16.43% with a return loss of -36.71 dB resonating at 3.79 GHz, and band 3 obtained a bandwidth of 8.51% with a return loss of -15.55 dB resonating at 5.10 GHz.

Similarly, L_2 has been varied from 1.4 to 4 mm with the step of 0.1. The value of L_2 in the initial antenna was 1.6 mm, including the initial antenna the total of 27 (1 initial + 26) antennas were designed for L_2. The maximum bandwidth of 43.23% at 2.32 GHz resonating frequency is obtained for L_2 = 3.9 mm (band 1), providing a return loss of -37.001 dB. Band 2 of this antenna has given 12.01% bandwidth with the achievement of -13.63 dB return loss at 4.11 GHz resonating frequency and band 3 provided the bandwidth of 12.67%, return loss of -18.85 dB at 5.32 GHz.

The parameter W_1 proposed 15 (1 initial + 14) different antennas when it is varied in the range of 2.26 to 16.26 mm with the step size of 1mm. As the outcome, it has generated four bands. Out of these, the antenna with $W_1 = 2.26mm$ (band 2) provided the maximum bandwidth of 32.43% at 1.85 GHz Resonating frequency and -32.22 dB return loss. Band 1, band 3, and band 4 have provided 3.33%, 13.32%, and 8.26% bandwidth percentages respectively with the return loss of -20.48 dB, -35.39 dB, and -41.91 dB respectively. The antenna $(W_1 = 2.26mm)$ is resonating at 1.38 GHz, 1.85 GHz, 3.85 GHz, and 5.06 GHz. The fourth variable parameter W_2 is varied in the range of 3 mm to 9 mm in the step of 0.5. The 13 different (1 initial + 12) antennas are obtained. At W_2=3 mm (band 1,), the maximum bandwidth of 31.24% is achieved with the -24.35 dB return loss at 1.88 GHz resonant frequency. This antenna is resonating at 1.88 GHz, 3.83 GHz, and 5.07 GHz. Band 2 and band 3 have revealed the bandwidth of 12.99% and 9.26% as well the return loss is -19.46 dB and -35.70 dB respectively.

Table 3.6: The selected best antenna's all band information.

Variable parameters (mm)	Band	Lower freq. (GHz)	Higher freq. (GHz)	FBW (%)	Rf (GHz)	RL (dB)
L1 =12 mm	B1	1.75	2.38	30.77	1.85	-43.19
	B2	3.47	4.09	16.43	3.79	-36.71
	B3	4.90	5.34	8.51	5.10	-15.55
L2 = 3.9mm	B1	1.83	2.84	43.23	2.32	-37.00
	B2	3.84	4.33	12.01	4.11	-13.63
	B3	4.97	5.64	12.67	5.32	-18.85
W1 = 2.26mm	B1	1.36	1.41	3.33	1.39	-20.48
	B2	1.75	2.43	32.43	1.85	-32.22
	B3	3.59	4.11	13.32	3.86	-35.39
	B4	4.88	5.3	8.26	5.07	-41.91
W2 = 3mm	B1	1.76	2.41	31.24	1.88	-24.35
	B2	3.58	4.08	12.99	3.84	-19.46
	B3	4.86	5.33	9.26	5.07	-35.7

Table 3.6 reflects the information of all the bands of the best antennas chosen from a total of 70 (1 original + 69) antennas and table 3.7 shows the four best antennas with the best band obtained. The comparative return loss graph between L_1, L_2, W_1 and W_2 is shown in figure 3.8

Table 3.7 and figure 3.8 show that the Antenna with L_2 =3.9 mm keeping other param-

Table 3.7: Comparative analysis of best results from L_1, L_2, W_1, and W_2.

Variable parameters	**Band (mm)**	**Lower freq.**	**Higher freq. (GHz)**	FBW (GHz)	Rf (GHz)	RL (dB)
L1 =12mm	B1	1.75	2.38	30.77	1.85	-43.19
L2 =3.9mm	B1	1.83	2.84	43.23	2.32	-37.00
W1= 2.26mm	B2	1.75	2.43	32.43	1.85	-32.22
W2= 3mm	B1	1.76	2.41	31.24	1.88	-24.35

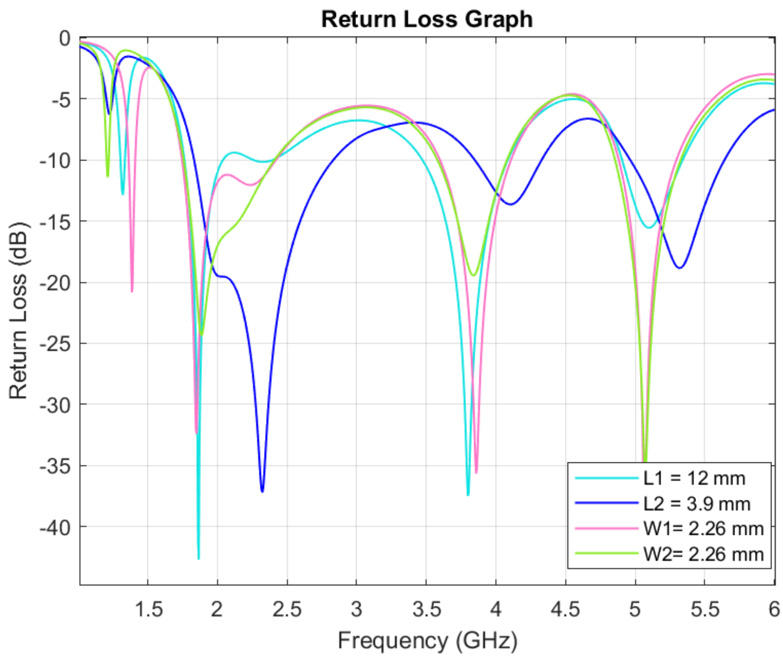

Fig. 3.8: RL versus Freq. graph of comparison for selected dimensional parameters L_1, L_2, W_1 and W_2.

eters at their initial value has provided the best results in terms of bandwidth and return loss by delivering 43.23% bandwidth enhancement with a -37 dB return loss. Also, the antenna with L_2 =3.9 mm is resonating at 2.32 GHz which is closer to the design frequency of 2.45 GHz. Additionally, it is also resonating at 4.11 GHz and 5.32 GHz by providing two more bands hence, it is a triple band antenna. Let's say the antenna obtained from strategy 1 (L_2=3.9 mm) as **Antenna 1**.

3.3.1 Equivalent Model of Antenna 1 for Return Loss and Bandwidth

To represent the antenna's equivalent model for RL and FBW, the equations are generated by establishing a relationship for the bandwidth and return loss concerning each antenna at the different values selected from the range which has been decided while strategic optimization for each selected variable parameters.
The MATLAB curve fitting tool was used to curve fit each variable parameter's connection to the bandwidth (targeting the band with the most bandwidth) and the return loss(RL) independently. Each variable is changed to the desired range, keeping the other parameters the same as the initial antenna, as in strategic optimization 1. The antennas were developed and simulated using IE3D Software for each value of L_1, L_2, W_1, and W_2, and the RL and FBW for each antenna were calculated .f_l, f_u, resonance frequency, FBW, and RL values are recorded for each prominent parameter.

L_1 was first adjusted in 1 mm increments from 1 to 18 mm. To set up the data for the equations, it builds 18 separate antennas (17 + 1 initial). L_2 is varied from 1.4 to 4 mm with 0.1 mm steps for the same purpose, yielding a total of 27 (26 + 1 initial) distinct antennas. With a step size of 1 mm, W_1 can range from 2.26 to 16.26 mm, yielding a total of 15 (14 + 1 initial) distinct antennas. W_2 is also modified in steps of 0.5 mm from 3 to 9 mm, yielding a total of 13(12+1 original) distinct antennas.

As a result, there are a total of 70 distinct antennas accessible for testing. Each antenna's bandwidth percentage has been computed, as well as its return loss is noted. A few of them are shown in Table 3.8. By using the data received from several antennas in

Table 3.8: Some variable parametric antennas out of 73 with the FBW and Return Loss.

Variable Parameters (mm)	Bands	Bandwidth (%)	Resonant freq. (GHz)	Return loss (dB)
L1 = 5 mm	B1	28.11	1.86	-23.12
	B2	11.17	3.78	-18.12
	B3	7.93	5.03	-31.39
L1= 9 mm	B1	30.95	1.85	-24.05
	B2	14.02	3.79	-25.94
	B3	8.17	5.07	-22.17
L2 = 3.7 mm	B1	42.28	2.27	-33.1
	B2	8.93	4.06	-11.54
	B3	11.29	5.28	-15.56
L2 = 3.8 mm	B1	42.12	2.3	-32.56
	B2	8.68	4.09	-11.71
	B3	10.82	5.31	-15.69
W1 = 3.26 mm	B1	3.36	1.37	-18.46
	B2	32.23	1.85	-34.64
	B3	13.19	3.86	-34.52
	B4	8.26	5.07	-49.55
W1 = 4.26 mm	B1	3.09	1.33	-16.81
	B2	31.27	1.85	-45.69
	B3	13.24	3.84	-30.38
	B4	8.15	5.07	-32.45
W2 = 3.5 mm	B1	30.14	1.86	-26
	B2	13.1	3.81	-21.36
	B3	8.8	5.05	-25.85
W2 = 4 mm	B1	29.26	1.85	-27.49
	B2	12.68	3.8	-22.58
	B3	8.26	5.04	-23.05

the MATLAB curve fitting tool, a relationship between one of the four variable parameters and BW and RL has been established. All three other parameters have been treated in the same manner. The equations (3.9 - 3.16) representing the antennas equivalent model for bandwidth and return loss.

The L_1 related to bandwidth (BW):

$$BW_1 = 0.00317L_1^4 - 0.1043L_1^3 + 0.916L_1^2 - 1.37L_1 + 23.71 \quad \text{...........................} \quad (3.9)$$

The L_1 related to Return Loss (RL):

$$RL_1 = 0.00117L_1^4 - 0.0264L_1^3 + 0.1067L_1^2 - 0.1788L_1 - 26.25 \quad \ldots\ldots\ldots\ldots\ldots\ldots\ldots \quad (3.10)$$

The L_2 related to bandwidth (BW):

$$BW_2 = -1.491L_2^4 + 14.78L_2^3 - 53.03L_2^2 + 88L_2 - 26.91 \quad \ldots\ldots\ldots\ldots\ldots\ldots\ldots\ldots \quad (3.11)$$

The L_2 related to Return Loss (RL):

$$RL_2 = 18.11L_2^4 - 178.1L_2^3 + 626.3L_2^2 - 934.1L_2 + 473.8 \quad \ldots\ldots\ldots\ldots\ldots\ldots\ldots\ldots \quad (3.12)$$

The W_1 related to bandwidth (BW):

$$BW_3 = -0.0002414W_1^4 + 0.00849W_1^3 - 0.06644W_1^2 - 0.5421W_1 + 34.12 \quad \ldots\ldots \quad (3.13)$$

The W_1 related to Return Loss (RL):

$$RL_3 = 0.03106W_1^4 - 1.171W_1^3 + 14.82W_1^2 - 68.88W_1 + 62.24 \quad \ldots\ldots\ldots\ldots\ldots\ldots\ldots \quad (3.14)$$

The W_2 related to bandwidth (BW):

$$BW_4 = 0.1157W_2^4 - 2.724W_2^3 + 22.51W_2^2 - 80.01W_2 + 133.3 \quad \ldots\ldots\ldots\ldots\ldots\ldots\ldots \quad (3.15)$$

The W_2 related to Return Loss (RL):

$$RL_4 = -0.07811W_2^4 + 1.335W_2^3 - 5.635W_2^2 - 3.553W_2^+ 8.555 \quad \ldots\ldots\ldots\ldots\ldots\ldots \quad (3.16)$$

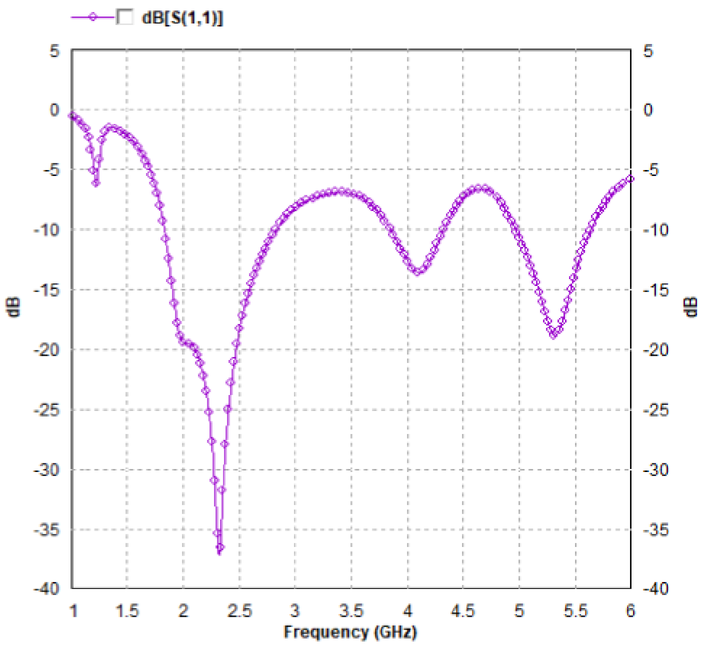

Fig. 3.9: Return loss graph of Antenna 1 (L_2 = 3.9 mm)

3.3.2 Simulation Results:Antenna 1

Return Loss : Antenna 1

Figure 3.9 illustrates the S(1,1) parameter for Antenna 1. We have gained insight knowledge about the upper cutoff frequency and lower cutoff frequency, Return loss, number of bands, and the FBW is noted. The FBW of three of the bands is 43.23%, 12.01% and 12.67% providing the return loss -37 dB, -13.63 dB and -18.85 dB respectively. The antenna is resonating at 2.32 GHz, 4.11 GHz, and 5.32 GHz facilitating work in various applications.

VSWR : Antenna 1

Figure 3.10 describes the VSWR of the Antenna that lies below 2 dB at a resonating frequency of 2.32 GHz which is desirable. The value of VSWR is 1.02865 dB.(VSWR < 2 dB). A lower VSWR value indicates that the optimized antenna is better suited to the transmission line and that the antenna receives more radiating power.

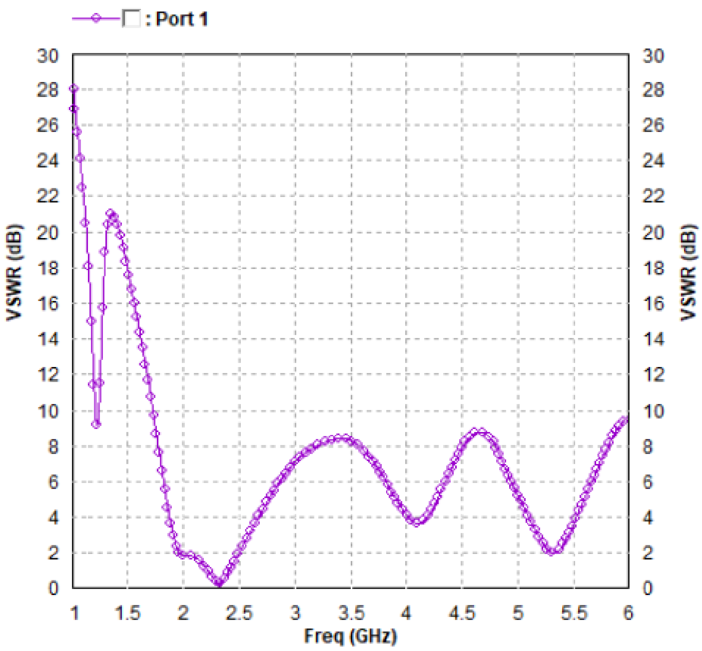

Fig. 3.10: VSWR graph of Antenna 1 (L_2= 3.9 mm)

It can also be determined by RL using :

$$VSWR = \frac{(1+|\Gamma|)}{(1-|\Gamma|)} \tag{3.17}$$

when, Return loss = $20\log|\Gamma|$

Antenna Efficiency

Table 3.9: Information list of Freq. Vs Antenna Efficiency

No.	Freq (GHz)	Efficiency (%)
1.	2.32199	99.5897
2.	4.12173	94.4745
3.	5.32592	96.407

The antenna efficiency of the Antenna 1 is 99.58%, 94.47 %, and 96.704% at the resonating frequency 2.32 GHz, 4.11 GHz, and 5.32 GHz respectively as shown in Figure 3.11.and table 3.9 which is commendable.

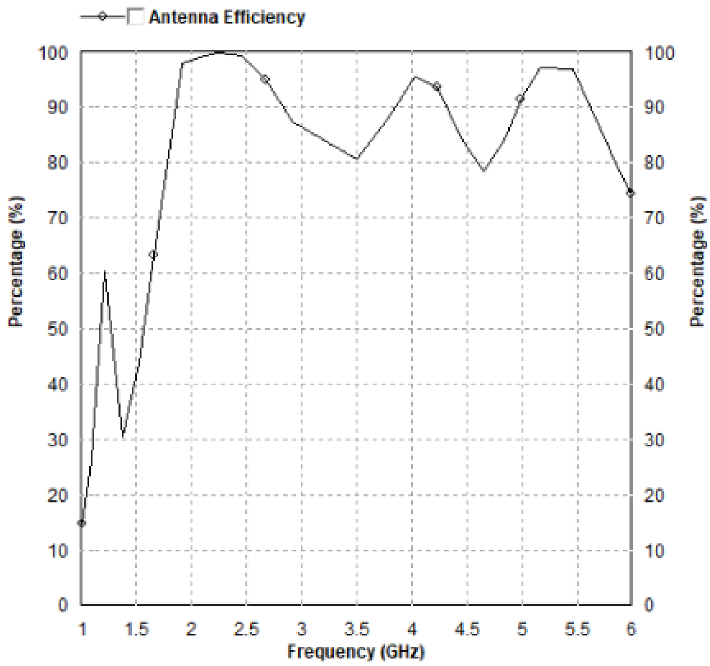

Fig. 3.11: Efficiency versus frequency graph of Antenna 1.

Elevation plain 2-D radiation pattern

Figure 3.12(a) depicts the Main lobe gain of 3.30581dB with Main lobe direction = 0° and Angular Width is 143.5° at frequency = 2.32 GHz Figure 3.12(b) shows the Main lobe gain of 3.8632dB in the Main lobe direction 38.70° with 0.4236° Angular Width at frequency = 4.11 GHz Also,the figure 3.12(c) depicts 1.062 dB Main lobe gain in Main lobe direction of 54.39° with 57.42° angular width at 5.32 GHz frequency.

Azimuth plane Radiation pattern (RP).

The azimuth plane radiation characteristics or pattern of Antenna 1 at Resonant Frequency 2.32GHz is shown in Figure 3.13. In the azimuth plane, The RP has a maximum gain of 3.30 dB at all angles at the resonance frequency of 2.32 GHz and is non-directional. Thus Antenna 1 emits the same amount of energy in all directions in the x-y plane.

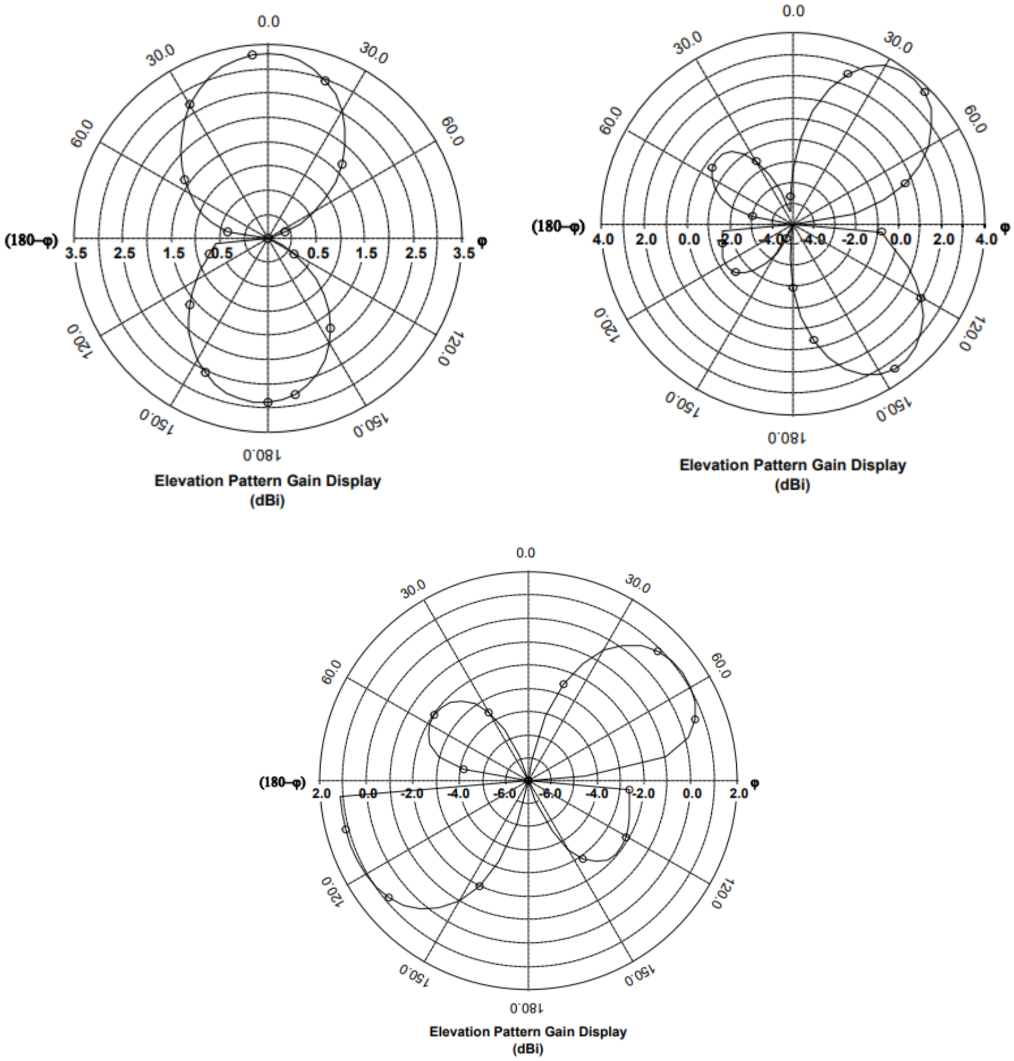

Fig. 3.12: *(a) Elevation plain 2-D radiation pattern of Antenna 1 at 2.32 GHz. (b) Elevation plain 2-D radiation pattern of Antenna 1 at 4.11GHz (c) Elevation plain 2-D radiation pattern of Antenna 1 at 5.32 GHz*

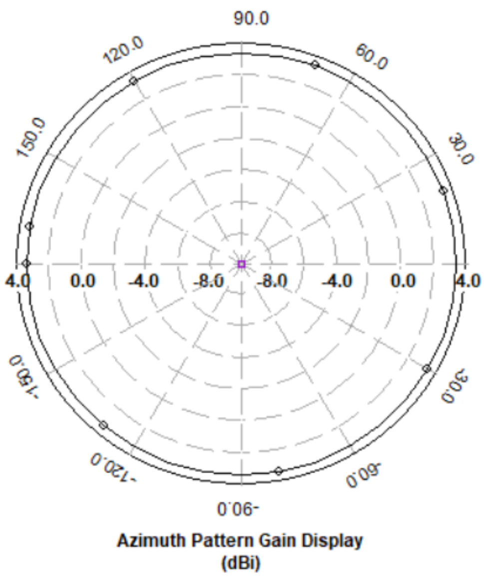

Fig. 3.13: Azimuth plain 2-D radiation pattern of Antenna 1

Gain of Antenna 1.

The Gain versus frequency graph in figure 3.14 shows the gain at the resonating frequencies of Antenna 1 as 3.40 dB at 2.32GHz, 3.45 dB at 4.11 GHz, and 3.76 dB at 5.32 GHz.

3- dimensional Radiation Pattern (RP) of Antenna 1 at all resonating frequencies.

The 3-D radiation pattern in figure 3.15 depicts the gain of 3.36 dB at resonant freq. 2.32 GHz, in the figure 3.16 it is reflected that the gain of 6.410 dB at resonant freq. 4.11 GHz is achieved and in figure 3.17 it is shown that the gain of 5.817 dB at 5.32 GHz (resonant freq.) is obtained.

3.4 Flow Chart

Figure 3.19 shows the complete flow of steps followed to attain the final antenna using strategy 1 of optimization to get an enhancement of FBW of the initial antenna.

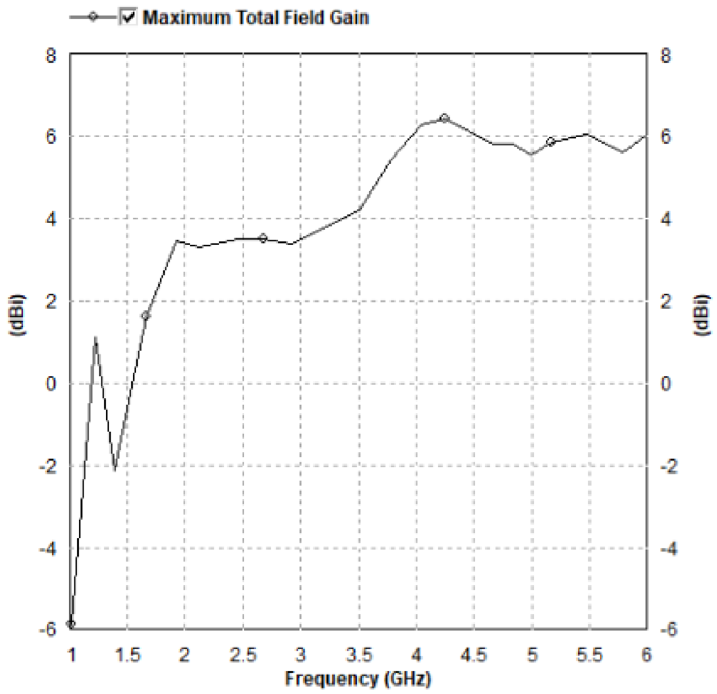

Fig. 3.14: Gain versus Frequency Graph of Antenna 1.

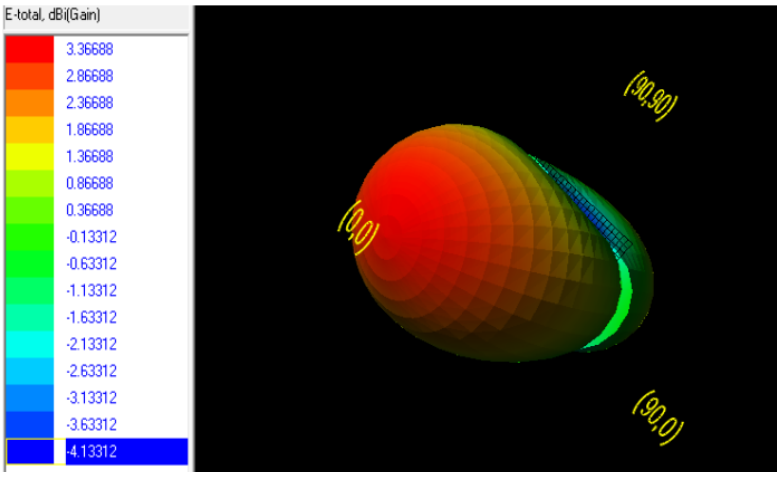

Fig. 3.15: 3-D RP of Antenna 1 at resonating frequency 2.32 GHz.

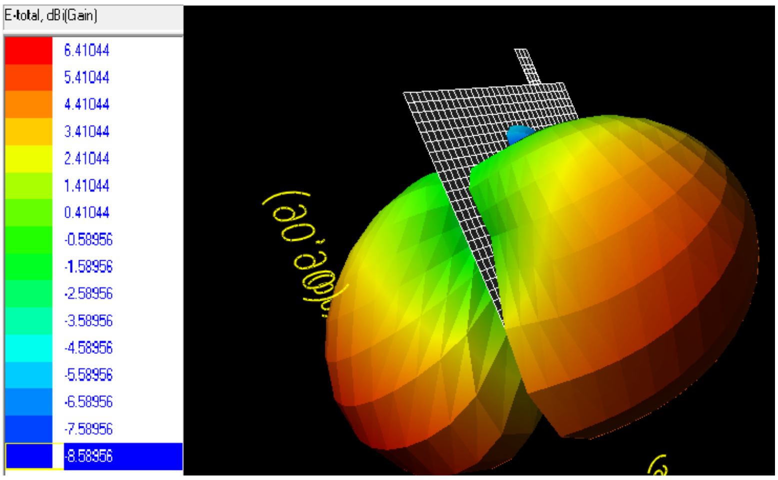

Fig. 3.16: 3-D RP of Antenna 1 at resonating frequency 4.11 GHz.

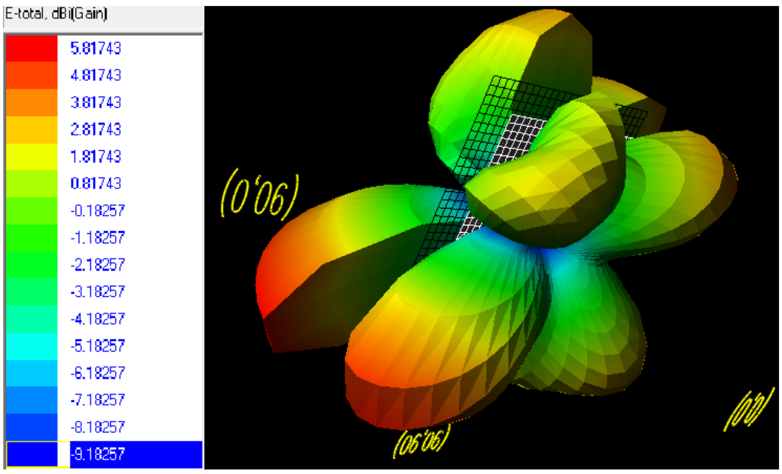

Fig. 3.17: 3-D RP of Antenna 1 at resonating frequency 5.32 GHz .

3.5 Summary

Thus the antenna has been demonstrated to operate effectively in the narrow-band region at a resonant frequency closer to the design frequency owing to the rise in bandwidth. Wireless communications are possible using Antenna 1's resonant frequency of 2.32 GHz, which is in the S-band. Also, the antenna is resonating at 4.11 GHz and 5.32 GHz as well as providing triple-band characteristics due to which areas of application covered are also increased. Hence, this antenna also works in the C band to be used for esp. WiMAX, UMTS (1.9-2.1 GHz), DCSC (1.7-1.8 GHz),ISM bands(2.4GHz-2.48 GHz), PCS (1.85 GHz -1.99 GHz)as well as Wi-Fi. As a result, the Fragmentary bandwidth of the initial antenna has been boosted while maintaining the resonant frequency matched closely to the design frequency. In addition, as compared to the initial inverted T-shaped slotted RMSPA, the Antenna 3 has better RL. In figure 3.18, the comparison graph is illustrated and table 3.10 illustrates the improvement factors of antenna 1 over the initial antenna after optimization.

Table 3.10: Comparison between initial inverted 'T' Shaped slotted antenna and strategically optimized antenna 1.

Improved Parameters	Initial Inverted 'T'-shape slotted antenna	optimized antenna 1
Bandwidth (%)	29.26%	43.23 %
Max. Return loss (dB)	-27.49	-37.00
Efficiency (%)	99.1	99.63
VSWR (dB)	1.088	1.028
Rf (GHz)	1.85, 3.7 , 5.04	2.32, 4.11 , 5.31

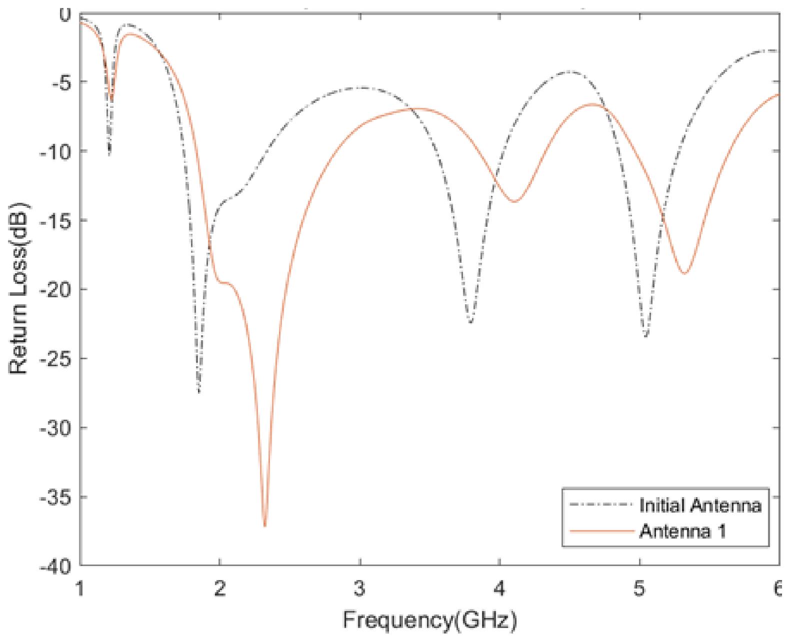

Fig. 3.18: RL versus Freq. comparison graph of the initial Inverted T-shape Slotted RMSPA and Antenna 1.

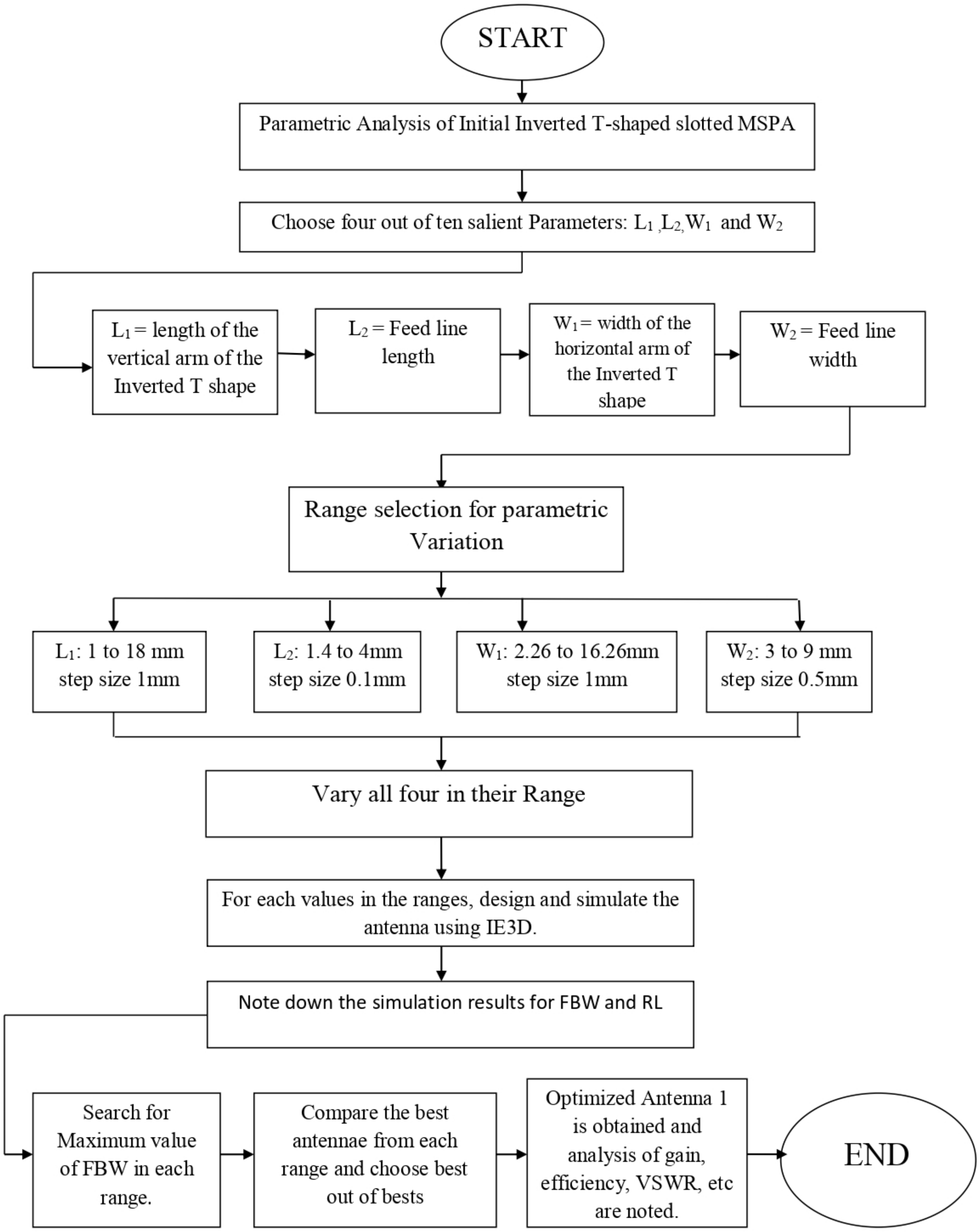

Fig. 3.19: Flow chart for optimization strategy 1.

CHAPTER 4

Antenna Design using Proposed Optimization Technique-II

4.1 Overview

Wideband antenna design is becoming more popular as the number of wireless communication applications grows. As a result, more bandwidth is required to accommodate the desired application, yet microstrip antennas have restricted bandwidth. Therefore, the optimizations are recommended procedures to increase the Fractional Bandwidth of the Microstrip antenna, keeping resonating frequency (fr) fixed close to the design frequency. According to the results, optimization strategy 1 achieved a good bandwidth with a decent return loss. But to increase the impedance bandwidth more has always been the main idea, so it is not stopped there only. As a result, the second strategy of optimization has been implemented to improve the antenna characteristics, mainly fragmentary bandwidth, by maintaining a good return loss. For the increased number of applications, the antenna using approach 2 would be labeled Antenna 2. The antenna 2 provides the application in the PCS band, and with the PCS band, there are many other uses as the spectrum for the Broadband Personal Communications Service (PCS) spans between 1850 and 1990 MHz. Mobile voice and data services, such as cell phones, text messaging, and the Internet, are the most prevalent uses of the Broadband PCS spectrum. Other wireless technologies such as Bluetooth, UMTS, ISM band, WLAN, WiMAX, and Wi-Fi can also utilize the generated antenna.

Antenna 2 is a triple-band Inverted T-shaped slotted RMSPA, which is obtained by optimization strategy 2. Consequently, the antennas that were generated and designed in strategy 1 for each of the variable parameters are taken together to find the best from each batch, and hence the combination of the parametric values obtaining the best antennas is decided, and accordingly, the antennas are designed and simulated again.

Thereafter, the combination providing the best outcomes is selected to be Antenna 2 (optimized by strategy 2 antenna). Using the same substrate FR4 at a dielectric constant of 4.4 and a thickness of 1.6 mm.

This chapter follows the same format as the previous one. The intricacies of the design are covered in subsection 4.2, and the measurements are given in this chapter. The radiation patterns (2-D and 3-D) and gain attributes for each of the antenna's resonant frequencies are also included.

4.2 Basic Design Procedure: Antenna 2

In this, the multiple antennas are designed by taking a rectangular patch that is slotted with the shape of the alphabet T, which is inverted upside down. These antennas are the antennas obtained from optimization strategy 2 and strategy 1 is hereby optimized again to get more improved results in strategy 2. Table 4.1 that follows gives Antenna 2's measurements. The patch is provided with a microstrip line feed technique for the feeding purpose whose details are also provided in the table stated earlier. The geometrical representation of the antenna is shown in figure 4.1.

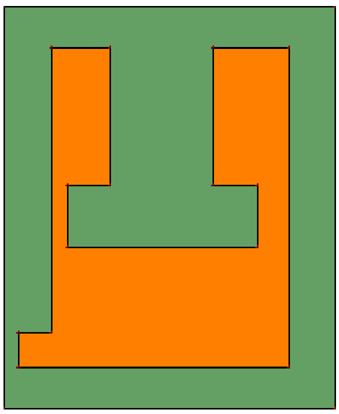

Fig. 4.1: IE3D designed view of Antenna 2

Utilizing the dimensional values of the edges of the T slot related to antenna 2 from the above table 4.1 The antenna and the results are obtained as well as the strategy that is responsible for providing the same antenna is discussed in the upcoming sections.

Table 4.1: Dimensions of the T-shaped slot and the patch.

Substrate (glass proxy)	$\epsilon = 4.4$ h = 1.6 mm
Length of a rectangular shape ground plane	L_g=38.43 mm
Rectangular ground plane width	W_g=46.86 mm
Rectangular patch length	L_p=27.69 mm
Rectangular patch width	W_p=37.26 mm
Vertical slab length of T shape	L_1=12 mm
Horizontal slab length of T shape	L_3=22 mm
Vertical slab width of T shape	W_3=16 mm
Horizontal slab width of T shape	W_1 =7.26 mm
Line feed length	L_2=3.9 mm
Line feed width	W_2=4 mm
Feed location	(-17.545, 16.63)

4.3 Optimization Technique 2

This optimization strategy is followed by strategy 1 for optimization. The values of the variable parameters for which the best results were obtained from the number of antennas that were designed for each value of the parameter in the range provided are utilized. That is the results from tables 3.6 and 3.7 are taken as a base for this procedure. The antennas obtained from table 3.7 are four in total (in terms of the value of parameter selected) at the same time keeping other parameters as same as the initial inverted T shape slotted RMSPA (refer to table 3.3).

Thus the $4c_2$ combinations are obtained for the selected four parameters (Table 3.7), these six combinations,C_1, C_2, C_3, C_4, C_5 and C_6 are reflected in table 4.2. The antenna

Table 4.2: Combinations parameters

Combination parameter	**Selected variable parameters**
$C1$	$L_2 = 3.9mm, L_1 = 12mm$
$C2$	$L_2 = 3.9mm, W_1$ =2.26mm
$C3$	$L_2 = 3.9mm, W_2 = 3mm$
$C4$	$L_1 = 12mm, W_1 = 2.26mm$
$C5$	$L_1 = 12mm, W_2 = 3mm$
$C6$	$W_1 = 2.26mm, W_2 = 3mm$

designed with the combination C_1 is the antenna designed with L_2=3.9 mm,L_1=12 mm, and by keeping other parameters constant. The C_1 combinational parameter antenna has provided the maximum bandwidth of 48.45% (band 1) with the return loss of -39.49 dB at 1.99 GHz resonating frequency. With the combination of L_2 = 3.9 mm ,W_1 = 2.26 mm, the C_2 combination antenna has provided the maximum bandwidth of 46.21% (band 1) at 1.96 GHz resonant frequency. The return loss obtained from C_2 is -35.82 dB. The C_3 antenna with L_2 = 3.9 mm,W_2 = 3 mm keeping other parameters as same as the initial antenna provided the bandwidth 39.55% (band 1) with -35.47 dB return loss at 2.35 GHz resonant frequency. From the C_4 antenna with L_1 = 12 mm ,W_1 = 2.26 mm, we obtained the 14.59% bandwidth and -42.46 dB return loss at a 3.89 GHz resonant frequency. With L_1 = 12 mm, W_2= 3 mm, the C_5 antenna is designed to have the with maximum bandwidth of 32.92% and -20.099 dB return loss at 1.89 GHz resonant frequency. Similarly, for C_6 35.98% bandwidth is obtained with the return loss of -25.19 dB at 1.87 GHz. Thus, from table 4.3, the maximum bandwidth obtained is for C_1, which is 48.45% with a good return loss of -39.49 dB at 1.99 GHz.

Table 4.3 Comparison between C_1, C_2, C_3, C_4, C_5, and C_6.

Combinational parameters(mm)	Band	Lower freq. (GHz)	Higher freq. (GHz)	FBW (%)	Rf (GHz)	RL (dB)
$C1$	B1	1.84	3.01	48.45	1.99	-39.49
$C2$	B1	1.81	2.9	46.21	1.96	-35.82
$C3$	B1	1.86	2.77	39.55	2.35	-35.47
$C4$	B3	3.6	4.17	14.59	3.89	-42.46
$C5$	B1	1.77	2.47	32.92	1.89	-20.09
$C6$	B2	1.76	2.53	35.98	1.87	-25.19

The return loss graph of the combinational antennas exhibited in Fig. 4.2 clearly shows the maximum gain with an enhanced return loss notch provided by the C_1 antenna additionally two other bands are provided due to which antenna is resonating at two more frequencies which are 4.13 GHz and 5.38 GHz. That facilitates the antenna to be multi-band, which provides to work for more and more applications.

From table 4.3, we can see that maximum bandwidth of 48.45% has been obtained when a combination of parameters L_2 = 3.9 mm, L_1 = 12 mm is calculated by maintaining the antenna's other dimensions parameters at their previous value. It is also observed that the resonant frequency of 1.85 GHz of the initial inverted 'T' shaped slot-

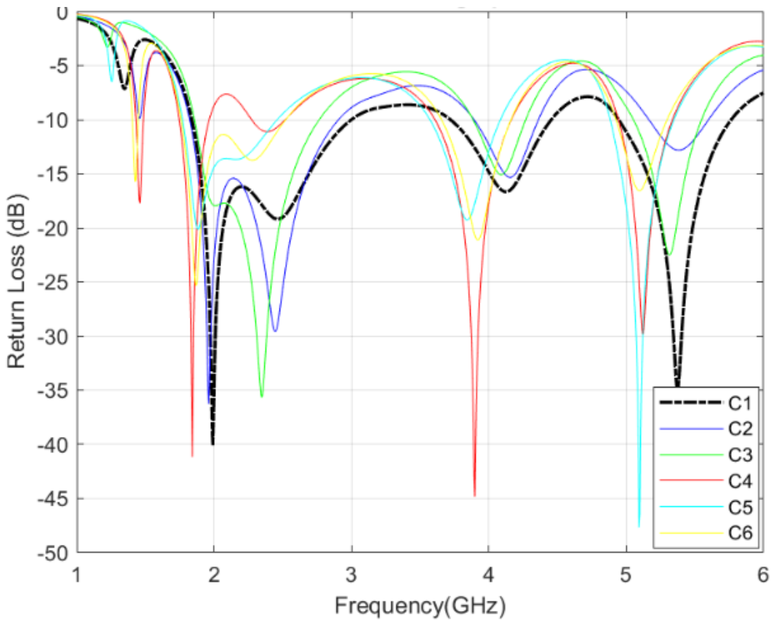

Fig. 4.2: RL versus freq. comparison graph of different combinational parameters: C_1, C_2, C_3, C_4, C_5, and C_6.

ted MSPA is shifted at 1.99 GHz Which is slightly closer to the design frequency.

The antenna's bandwidth has increased, as seen in Table 4.4. The antenna's return loss has also improved. The resonant frequency moved closer to the desired frequency of 2.45 GHz, but not very much. As a result, the Third optimization has been applied to significantly improve the outcomes of an initial inverted 'T'-shape slotted RMSPA in the next chapter. The information of all the bands obtained by the return loss analysis of the Antenna 2 (Obtained by strategy 2) is reflected in table 4.5.

Table 4.4 Comparison between initial inverted 'T' Shaped slotted antenna and strategically optimized antenna 2.

Parameters	**Initial Inverted 'T'-shape slotted antenna**	**optimized antenna 2**
Bandwidth (%)	29.26	48.45
Return loss (dB)	-27.48	-39.49
Fr (GHz)	01.85	01.99

Table 4.5 All bands S (1,1) information of the Antenna 2.

Variable $(L_2 - L_1)$**(mm)**	**Bands**	**Lower freq. (GHz)**	**Higher freq. (GHz)**	**FBW (%)**	**Rf (GHz)**	**RL (dB)**
	B1	1.84	3.01	48.45	1.99	-39.49
(C1)	B2	3.72	4.46	18.18	4.13	-16.67
	B3	4.94	5.76	15.41	5.38	-34.98

4.3.1 Simulation Results: Antenna 2

Return Loss (RL)

The S (1,1) parameter for Antenna 2 is shown in Fig. 4.3. We now have a better understanding of the upper and lower cutoff frequencies, the return loss notch, resonant frequency, and the number of bands. Thus, we can also note the FBW (below -10 dB) of the particular antenna in order to analyze the areas of its application. This graph is obtained after simulating the antenna for 1000 frequency points in the range of 1 GHz to 6 GHz and reflecting the Max. return loss -39.49 dB at 1.99 GHz.

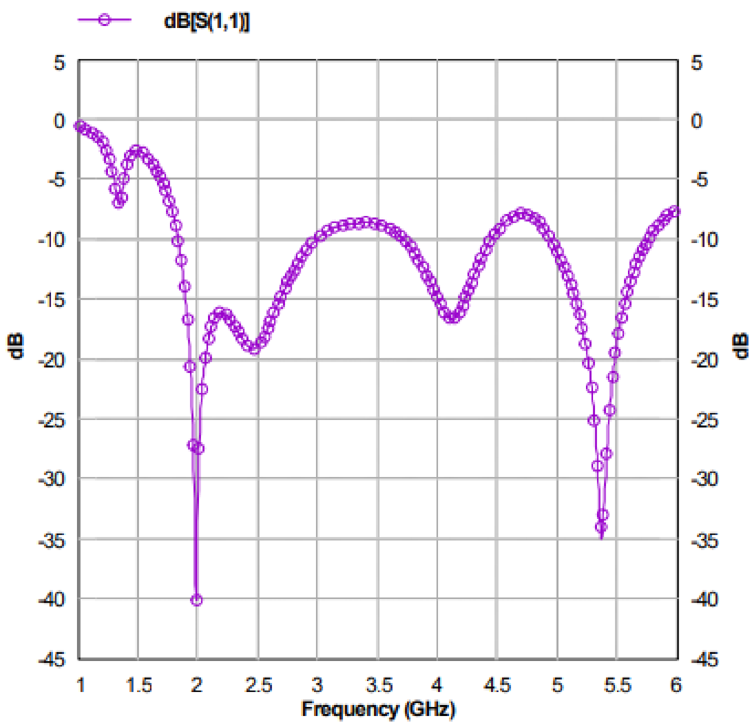

Fig. 4.3: Return loss graph of Antenna 2 (C1).

Voltage standing wave ratio(VSWR)

Figure 4.4 depicts the Antenna's VSWR (Voltage Standing Wave Ratio) of 1.02141 dB, which is less than 2 dB at a resonant frequency of 1.99 GHz, which is excellent. A smaller VSWR value means the optimized antenna is better matched to the transmission line and receives increased radiating power.

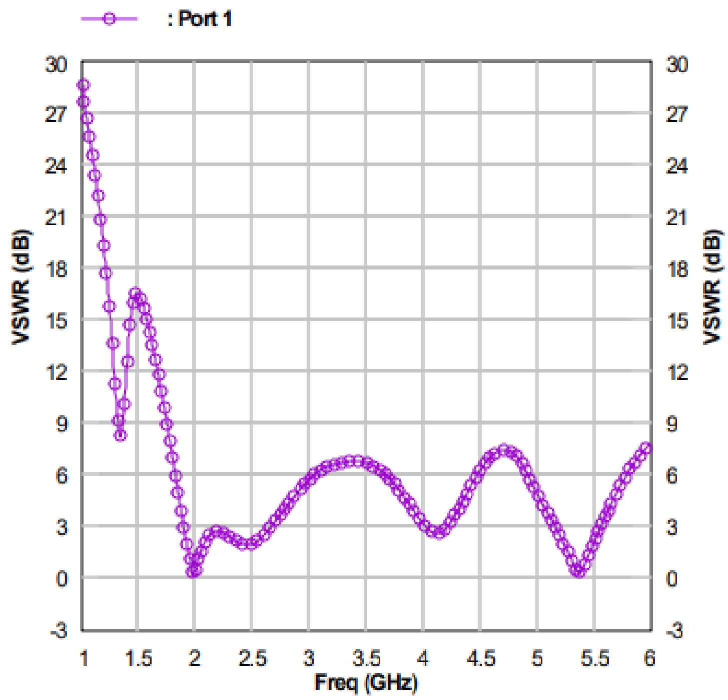

Fig. 4.4: VSWR graph of Antenna 2 (C1).

Gain of the Antenna 2

The Gain versus frequency graph in fig. 4.5 shows the gain of antenna 2 at the resonating frequencies 1.99 GHz, 4.13 GHz, and 5.38 GHz. as 3.6 dB, 6.57 dB, and 5.97 dB which is a good gain. The gain obtained from each band's resonating frequency of antenna 2 is reflected in the upcoming table 4.6

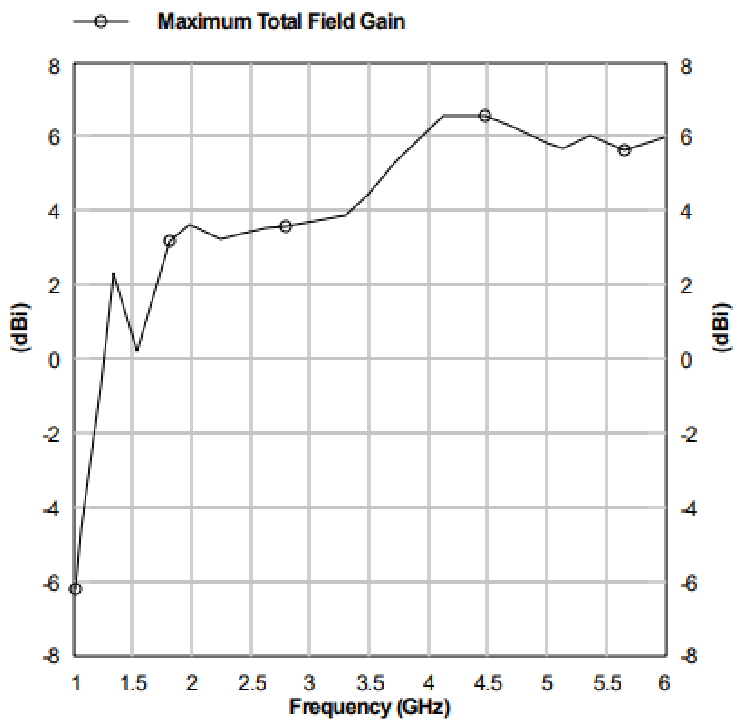

Fig. 4.5: Gain Versus Frequency graph of Antenna 2 (C1).

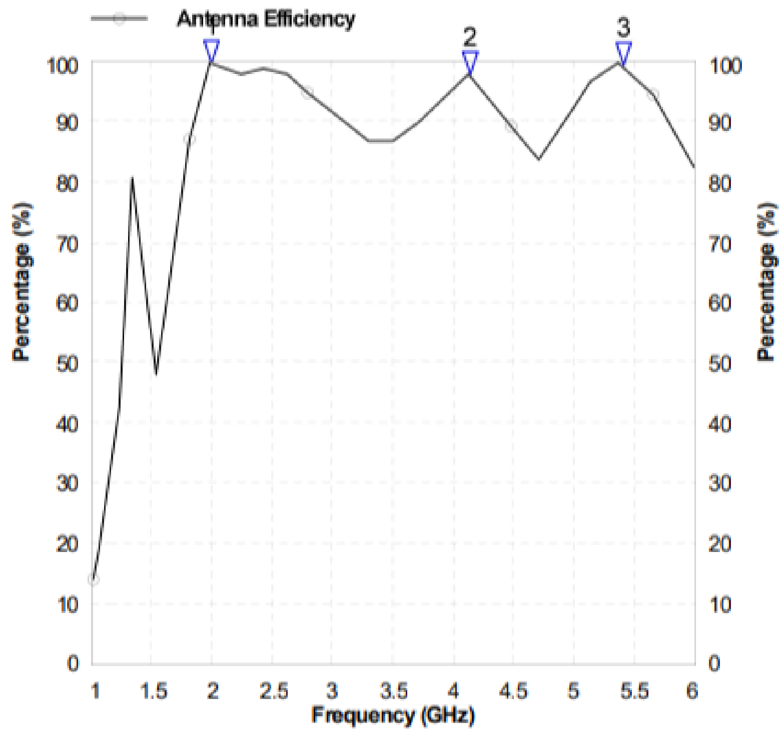

Fig. 4.6: Efficiency Vs. Frequency graph of Antenna 2

Table 4.6 Gain of the Antenna 2 at each resonating frequency.

Band	Resonating frequency(Rf)	Gain(dB)
1.	1.99	3.59
2.	4.13	6.58
3.	5.38	5.97

Efficiency of Antenna 2

At the resonating frequency of 1.99 GHz, the antenna 2 provides the efficiency of 99.96 %, as illustrated in Fig 4.6. This is outstanding. Also, as the antenna is resonating at two more frequencies and the corresponding efficiencies for those are reflected in table 4.7.

Table 4.7 Efficiency vs resonating frequency data.

No.	Freq.(GHz)	Efficiency (%)
1.	1.99388	99.9653
2.	4.13456	97.5664
3.	5.38367	99.1853

Azimuth Plane Radiation Patterns

Antenna 2's azimuth plane (x–y plane) radiation pattern at resonance frequency 1.99 GHz is seen in Figure 4.7. The radiation pattern is non-directional in the azimuth plane, forming a path in a circular manner showing the maximum gain of 3.59 dB at all angles at the resonance frequency of 1.99 GHz at all angles. As a result, Antenna 2 emits the same amount of energy in all azimuth plane directions.

Elevation Plane Radiation Patterns

Fig. 4.8(a) depicts the main lobe gain of 3.59 dB in main lobe direction 0° with angular Width 43.8324° at 1.99 GHz frequency and fig. 4.8(b) shows 4.62 dB main lobe gain in direction 36.82° with angular Width of 40.54° at frequency = 4.13 GHz. The fig. 4.8(c) gives the 3 dB main lobe gain in direction 240.5° with angular Width = 50.42° at

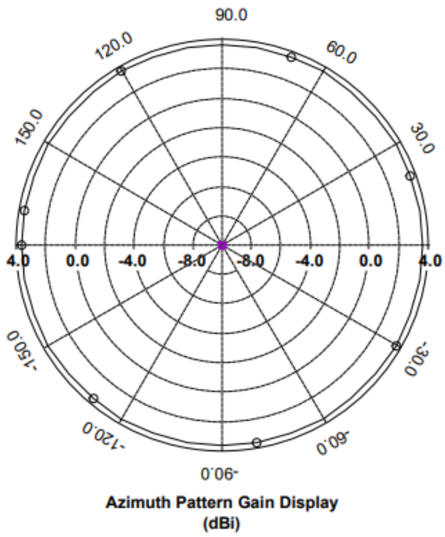

Fig. 4.7: Azimuth Plane Radiation Pattern of Antenna 2.

frequency = 5.38 GHz

3-D Radiation Patterns

The 3-D radiation pattern in Fig. 4.9 depicts the gain of 3.59 dB at resonant freq. 1.99 GHz,in the fig. 4.10 it is reflected that the gain of 6.57 dB at resonant freq.4.13 GHz is achieved and in Fig. 4.11 it is shown that the gain of 6 dB at 5.38 GHz (resonant freq.) is obtained.

4.4 Flow Chart

Figure 4.12 shows the complete flow of steps followed to attain the final antenna using strategy 2 of optimization to get an enhancement of FBW of the initial antenna.

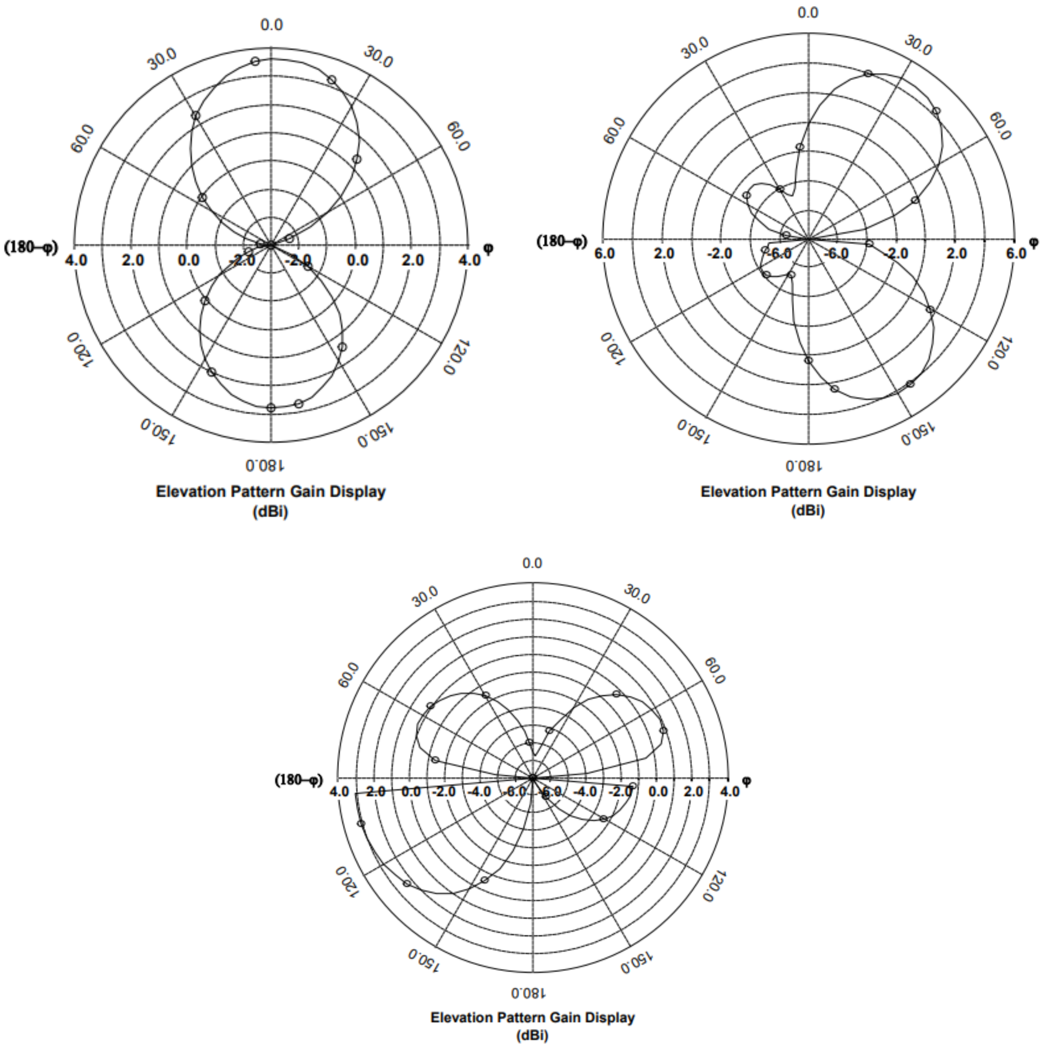

Fig. 4.8: *(a) Elevation Plane Radiation Pattern of Antenna 2 at Rf= 1.99 GHz. (b) Elevation Plane Radiation Pattern of Antenna 2 at Rf= 4.13 GHz. (c) Elevation Plane Radiation Pattern of Antenna 2 at Rf= 5.39 GHz.*

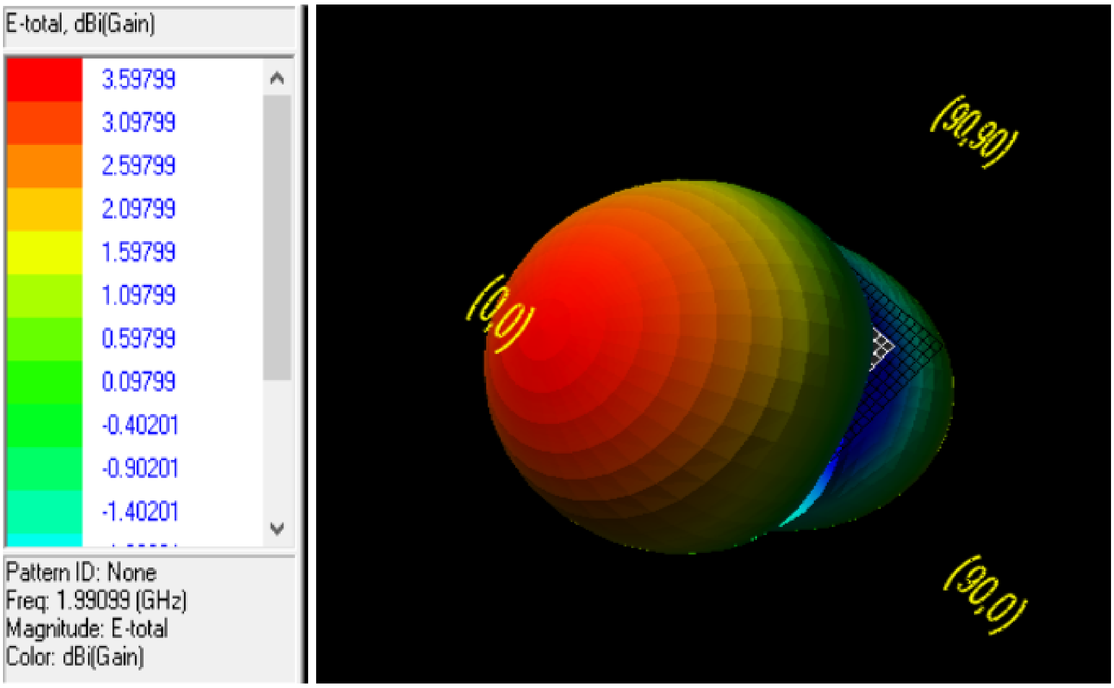

Fig. 4.9: 3-D Radiation Pattern and realized Gain of Antenna 2 at Rf= 1.99 GHz.

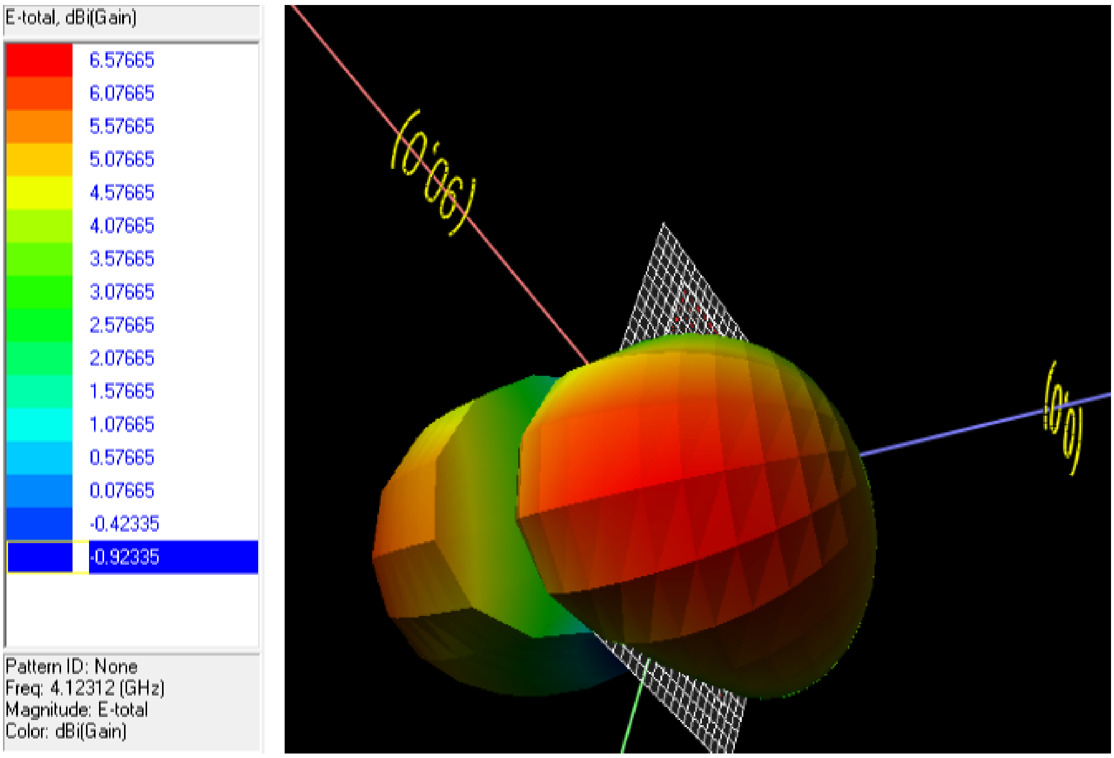

Fig. 4.10: 3-D Radiation Pattern and realized gain of Antenna 2 at Rf = 4.13 GHz

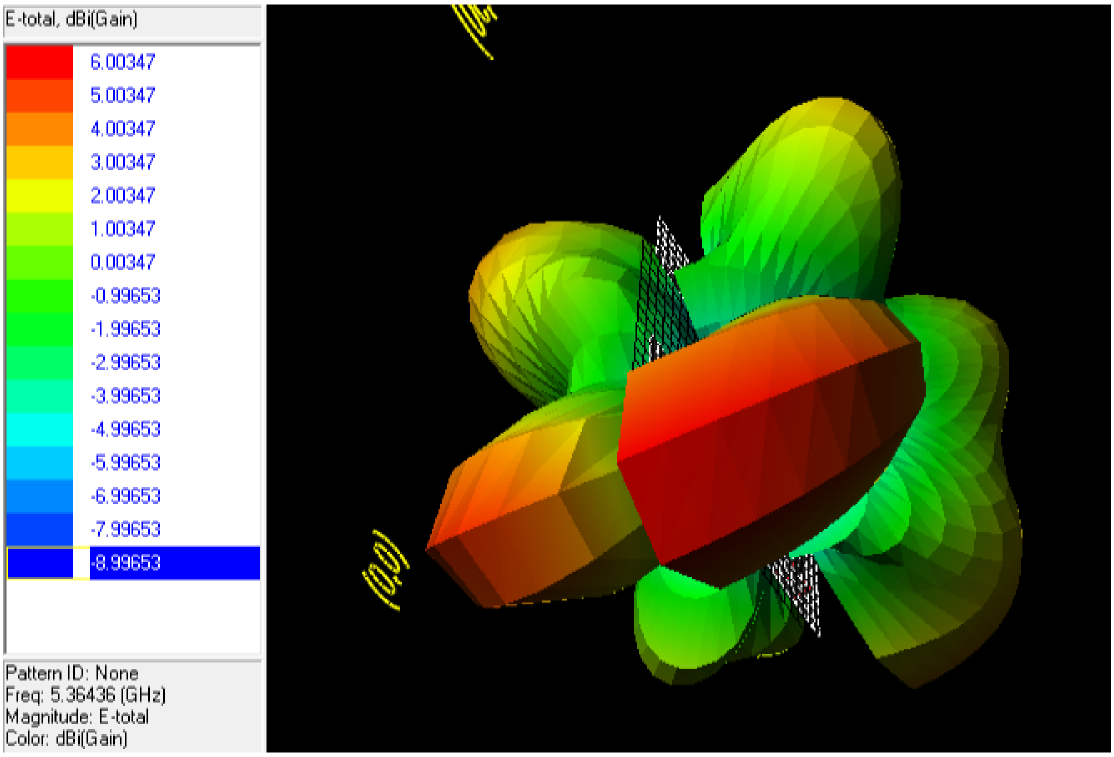

Fig. 4.11: 3-D Radiation Pattern and realized Gain of Antenna 2 at Rf = 5.38 GHz

4.5 Summary

Triple band Antenna that resonates at **1.99 GHz**, **4.13 GHz**, and **5.38 GHz** can be used for a variety of purposes. As previously stated,1.99 GHz is used for WiMAX, PCS, and WCS. The C band includes the next two frequencies and these can be utilized for weather radar systems, surface ship radar, and satellite communications (TV reception). Wi-Fi, 802.11b, and 802.11g wireless LAN equipment.

As a result, the suggested antenna may be used for a variety of purposes.

Also, The Antenna 2 has improved RL and FBW by 19.19% as compared to the Initial inverted T-shaped slotted RMSPA. The RL comparative graph is shown in Fig. 4.13 and VSWR is also improved.

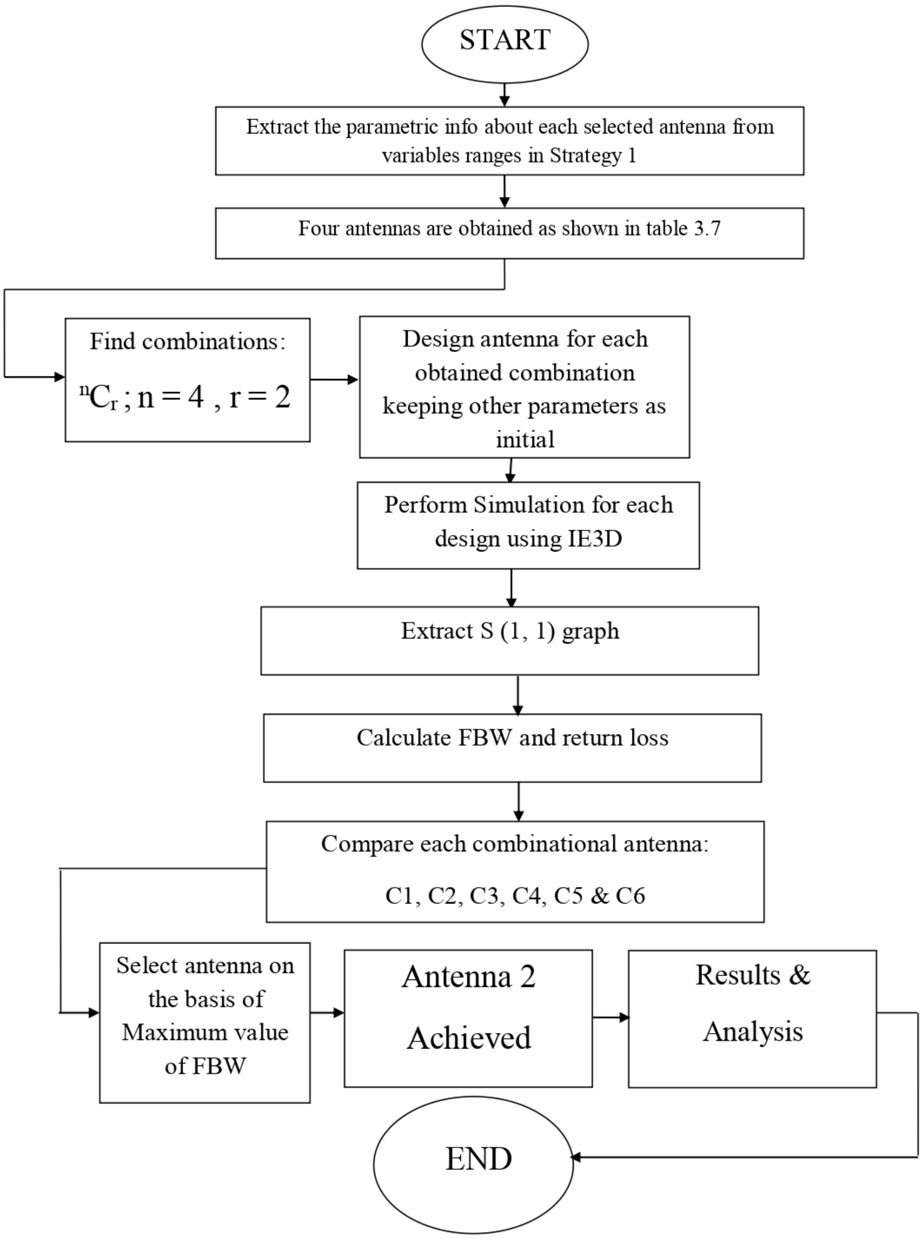

Fig. 4.12: Flow Chart for optimization strategy 2

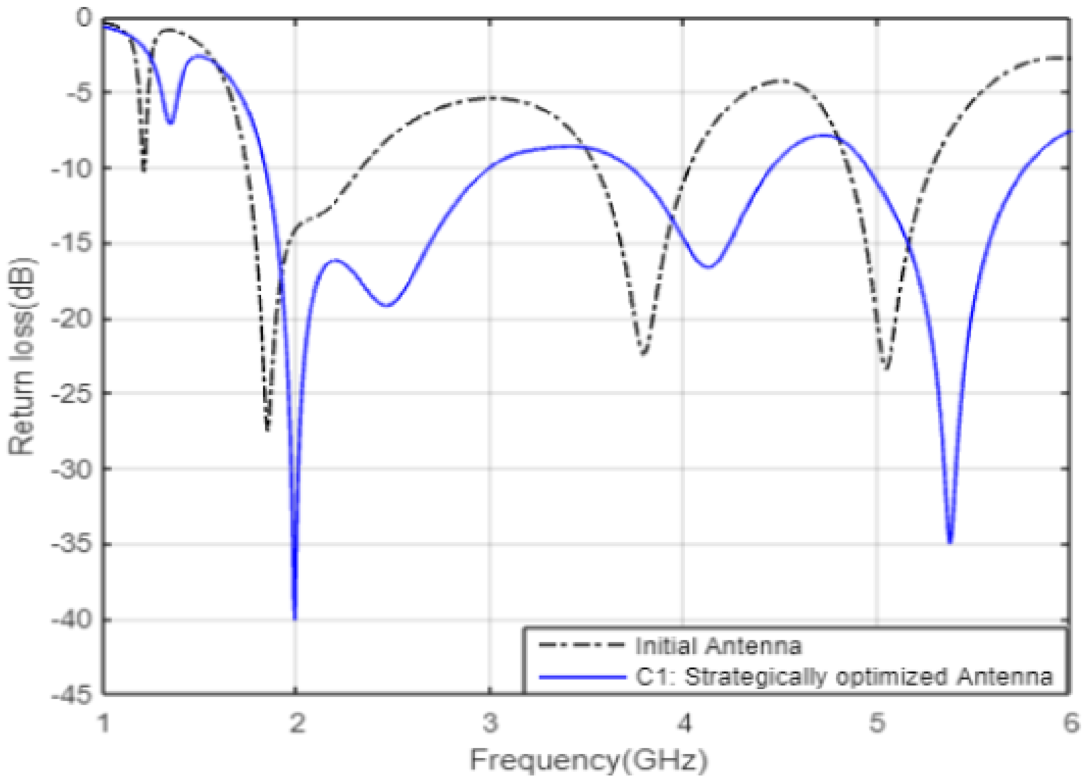

Fig. 4.13: Comparative RL versus freq. graph of the initial Inverted T-shape Slotted RMSPA and Antenna 2.

CHAPTER 5

Antenna Design using Proposed Optimization Technique-III

5.1 Overview

This chapter presents the procedure to obtain the optimized design and fabrication of Antenna 3 (The antenna by optimization strategy 3). Antenna 3 is gained from the initial Inverted T-shape slotted RMSPA by applying strategic optimization. The proposed antenna by this strategy obtained the bandwidth enhancement of 71.59 % The bandwidth enhancement has brought out the antenna to be a UWB antenna. The suggested antenna's operating frequency band is useful in the L, S, and C bands. Which facilitates a wide range of applications such as PCS (1.85–1.99 GHz), DCS (1.9–2.1 GHz), UMTS (1.92–2.17 GHz), ISM band (2.4–2.485 GHz), WLAN (2.4–2.484 GHz), and WiMAX (2.5–2.69 GHz) Also, can be used in Communication satellites (Rx), Weather radar, Surface ship radar and multimedia applications in mobiles TV and Satellite radio, etc. The designing of the antenna is done using IE3D and simulation as well. To obtain the equivalent model of the antenna by the relationship between the varying parameters with the FBW and RL, the curve fitting is employed and the equations are obtained based on the RMSE technique.

This antenna has used FR4 as a substrate having a dielectric constant of 4.4 and a substrate thickness of 1.6 mm. The dimensional parameters like ground plane length and width as well as patch dimensions are obtained utilizing the design equations mentioned in section 3.2 [Basic Design Procedure Antenna]. The dimensional specifications, optimization procedure, and the analysis of the results are explained in this chapter's subsections. It closes with a list of utilities that the suggested design can be utilized.

5.2 Basic Design Procedure Antenna

The antenna design, as well as the method for acquiring the design and the simulation results, are extensively explained in this portion of the chapter.

5.2.1 Design parameters

At 2.45 GHz design frequency, the suggested design is first carried out on a dielectric material glass epoxy (FR4) substrate with a dielectric constant of 4.4 because it is less costly and more easily accessible, the Fr4 was chosen. Also, the rectangular patch is chosen to slot cut with the inverted T shape over it as done in chapter 3. The initial inverted T-shape slotted RMSPA's dimensions are optimized with a different optimization procedure that includes the selection of four-dimensional parameters out of ten and then applying a range to each parameter. Thereafter fix each at its best value to proceed with another parameter. The patch is equipped with a microstrip line feeding technology, the specifications of which may be found in the table beneath. In table 5.1, Antenna 3's dimensions are listed. The antenna is represented geometrically as in figure 5.1.

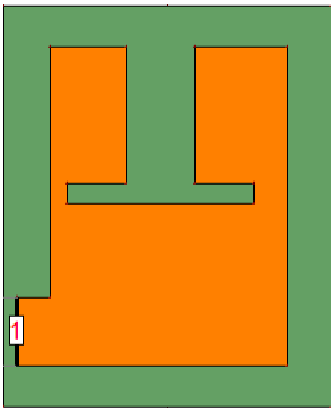

Fig. 5.1: IE3D designed view of Antenna 3

Using the dimensional specifications for T shape related to antenna 3 from table 5.1, The antenna and its results are obtained and analyzed. The parametric specification of the antenna geometry is as same as in fig 3.5. Also, the optimization strategy that brings out the dimensions above is discussed in upcoming sections.

Table 5.1 Dimensions of the T-shaped slot and the patch for Antenna 3.

Substrate (glass proxy)	$\epsilon = 4.4$ h = 1.6 mm
Length of a rectangular shape ground plane	L_g=38.43 mm
Rectangular ground plane width	W_g=46.86 mm
Rectangular patch length	L_p=27.69 mm
Rectangular patch width	W_p=37.26 mm
Vertical slab length of T shape	L_1=8 mm
Horizontal slab length of T shape	L_3=22 mm
Vertical slab width of T shape	W_3=16 mm
Horizontal slab width of T shape	W_1 =2.26 mm
Line feed length	L_2=3.9 mm
Line feed width	W_2=8 mm
Feed location	(-17.545, 14.63)

5.3 Optimization strategy 3

Primarily, The initial inverted T-shape slotted RMSPA is optimized by choosing four parameters L_1, L_2, W_1, and W_2 out of Ten parameters of the antenna patch, Feed line, and T-Slot. The 10 parameters are stated in Table 5.1 as $L_g, W_g, L_p, W_p, L_1, L_2, L_3, W_1, W_2$, and W_3. Two of the parameters L_1 and W_1 are selected from the T-shape and L_2 and W_2 are the feed strip line dimensions. The range is applied to each of the parameters as shown in table 3.5. Starting with L_1, the L_1 parameter is varied in the range of 1 to 18 mm and hence 18 antennas are designed for each value of the L_1 by keeping other parameters as same as the dimensions of the initial inverted T shape slotted RMSPA. The dimensions of all 18 antennas are reflected in table 5.2.

Table 5.2 Dimensional description of antennas obtained from L_1(strategy 3).

Parameter to be varied	**Initial parametric values**		
L_1 = 1 to 18 mm	L_2 (mm)	W_1 (mm)	W_2 (mm)
Step = 1 mm	1.6	7.26	4

As per the table 5.2 above for each value of the parameter L_1, the antennas are designed and simulated using IE3D software. Using the simulation results the return loss, upper bound cutoff frequency, lower cutoff frequency, and the FBW is noted. Also, the information on the number of bands has been grabbed. 18 different antennas are obtained for each value of L_1 starting from 1 mm to 18 mm keeping the other three out of Four selected variable parameters, fixed to their initial value. Also, the other parameters ($L_g, W_g, L_p, W_p, L_3, W_3$) out of ten are also at their initial values. Out of these 18 antennas, The antenna providing maximum Fragmentary Bandwidth is marked. The maximum value of FBW is obtained from the antenna having L_1 = 8 mm, which is 30.77 % with a return loss of -43.19 dB at a resonant frequency of 1.85 GHz. This antenna is also resonating at two other frequencies 3.81 GHz and 5.04 GHz providing the impedance bandwidth of 14.18 % and 8.58 % and return loss of -28.90 dB and -19.91 dB respectively.

Table 5.3 Results of the antenna at L_1 = 8 mm (strategy 3).

Variable L_1 (mm)	Bands	Lower freq. (GHz)	Higher freq. (GHz)	FBW (%)	Rf (GHz)	RL (dB)
	B1	1.75	2.38	30.77	1.85	-43.19
8mm	B2	3.53	4.07	14.18	3.81	-28.9
	B3	4.86	5.3	8.58	5.04	-19.91

Table 5.3 gives a clear understanding of return loss, bandwidth percentage, upper and lower cutoff frequencies, and resonating frequencies with regard to each band obtained from the antenna constructed at L_1 = 8 mm while maintaining other parameters at baseline values.

After getting the value of L_1 = 8 mm that provided maximum FBW, we Fix L_1 at 8 mm for the further optimization procedure. Thereafter we vary the parameter L_2 for the range 1.4 to 4 mm in the step of 0.1 mm. Hence, the 27 distinct antennas can be designed for L_2, when other parameters are kept at their initial value and L_2 is fixed at 8 mm. The dimensional description of all 27 antennas is shown in table 5.4. The

Table 5.4 Dimensional description of antennas obtained from L_2 (strategy 3).

Parameter to be varied	Fixed parametric value	Initial parametric values	
L_2 = 1.4 to 4 mm	L_1 (mm)	W_1 (mm)	W_2 (mm)
Step =0.1 mm	8	7.26	4

antennas are constructed and simulated using IE3D software for each value of the parameter L_2 as shown in table 5.4. The Return loss, upper bound cutoff frequency, lower bound cutoff frequency, and FBW are calculated using the simulation results obtained from IE3D Software. In addition, data on the number of bands is gathered. For each value of L_2, 27 distinct antennas are produced, ranging from 1.4 mm to 4mm in the step of 0.1 mm. Other than L_2 the three selected variable parameters are fixed to certain values as shown in table 5.4. The L_1 is fixed at its best value i.e 8 mm and the other two parameters W_1 and W_2 were set to their initial value. Out of ten parameters, the others $(L_g, W_g, L_p, W_p, L_3, W_3)$ are also at their starting levels. The antenna with the highest fragmentary bandwidth is noted out of the 27 antennas resulting in 44.69 % of maximum FBW at a resonance frequency of 2.37 GHz, the return loss is -32.80 dB. It also possesses resonating frequency much closer to the design frequency of 2.45 GHz. These results are from $L_2 = 3.9mm$. This antenna also resonates at 4.12 GHz and 5.35 GHz, with impedance bandwidths of 11.06 % and 12.10 %, respectively, with return losses of -13.09 dB and -18.08 dB.

Table 5.5 Results of the antenna at L_2 =3.9 mm (strategy 3).

Variable L2 (mm)	**Bands**	**Lower freq. (GHz)**	**Higher freq. (GHz)**	**FBW (%)**	**Rf (GHz)**	**RL (dB)**
	B1	1.838	2.896	44.689	2.374	-32.804
3.9	B2	3.871	4.324	11.063	4.118	-13.091
	B3	5.011	5.657	12.104	5.354	-18.079

The information on return loss, FBW, UB and LB frequencies, and resonating frequencies with respect to each band acquired from the antenna designed at L_2 = 3.9 mm while keeping L_1 fixed at 8mm and other parameters at starting levels are described by the table 5.5.

Thus, to proceed further into another parameter's range the L_2 is fixed at 3.9 mm also L_1 is fixed at 8 mm (the L_1's best). The W_1 is therefore varied in the range of 2.26 to 16.26 mm with the step of 1 mm which implies the 15 different antennas. Every antenna designed for W_1 has dimensional characteristics as shown in table 5.6. All the 15 antennas are designed and their results are carried out by utilizing IE3D software. For

Table 5.6 Dimensional description of antennas obtained from W_1 (strategy 3).

Parameter to be varied	**Fixed parametric value**		**Initial parametric values**
W_1 = 2.26 to 16.26 mm	L_1 (mm)	L_2(mm)	W_2 (mm)
Step =1 mm	8	3.9	4

every value of the W_1 parameter the return loss, upper cutoff frequency, lower cutoff frequency, Fragmentary bandwidth, central frequency, The VSWR, 2-D radiation pattern in both planes, and 3-D radiation pattern, and Gain, efficiency, and the number of bands are noted. Also, its relevance with respect to the applications these are possessing are also acquired. Initially, after simulation with the help of the S (1,1) graph the FBW is noted, analyzed, and compared within the range provided antennas. This one is in order to bring out maximum FBW in the picture. Each antenna is constructed by keeping the previous two variable parameters $(L_1\&L_2)$ fixed at their best values and the next parameter W_2 at its initial value as shown in table 5.6. The other parameters which are not variable are at their initial values $(L_g, W_g, L_p, W_p, L_3, W_3)$. The antenna at W_1 = 2.26 mm has provided the Maximum Bandwidth percentage of 48.92%(Band 2) with the upper bound frequency 3.005GHz and lower bound frequency of 1.824 GHz with the return loss of -26.27 GHz at the resonating frequency of 1.96 GHz. This antenna is possessing Four bands hence, this antenna is Quad- Band antenna with other three bands resonating at 1.49 GHz(Band 1), 4.19 GHz(Band 3), and 5.44 GHz(Band 4) Providing 2.74 %, 14.22 %, and 9.87 % of bandwidth percentage respectively. The return loss from band 1 is -11.73 dB, band 3 is -18.41 dB, and Band 4 is -14.38 dB as shown in table 5.7. Table 5.7 summarizes the data on return loss, FBW, upper and lower

Table 5.7 Results of the antenna at W_1 = 2.26 mm (strategy 3).

Variable W_1 (mm)	**Bands**	**Lower freq. (GHz)**	**Higher freq. (GHz)**	**FBW (%)**	**Rf (GHz)**	**RL (dB)**
2.26 mm	B1	1.48	1.52	2.74	1.49	-11.73
	B2	1.82	3.01	48.92	1.96	-26.27
	B3	3.86	4.45	14.22	4.19	-18.41
	B4	5.16	5.7	9.87	5.44	-14.38

cutoff frequencies, and resonating frequencies for each band obtained from an antenna constructed with W_1=2.26 mm while leaving L_1 constant at 8 mm, L_2 Fixed at 3.9 mm and other parameters at beginning values.

To go further into the scope of another parameter W_2, the L_1 is fixed at 8 mm (the L_1's best), and the L_2 is fixed at 3.9 mm(the L_2's best), while the W_1 is fixed at 2.26 mm (the W_1's best). The W_2 is therefore tuned in a range of 3 to 9 mm with a 0.5 mm step, resulting in 13 identical antennas. Table 5.8 shows the dimensional specifications of each antenna developed for W_2. For each value of the parameter W_2, the antennas are

Table 5.8 Dimensional description of antennas obtained from W2 (strategy 3).

Parameter to be varied	Fixed parametric value		
W_2 = 3 to 9 mm	L_1 (mm)	L_2 (mm)	W_1 (mm)
Step =0.5 mm	8	3.9	2.26

built and simulated using the IE3D application as shown in table 5.8. Using the simulation results generated from the IE3D Software, the upper bound cutoff frequency, lower bound cutoff frequency, FBW, and Return loss are computed. Furthermore, information on the number of bands is gathered. There are 13 different antennas for each value of W_2, ranging in size from 3 mm to 9 mm in 0.5 mm increments meanwhile, the other variable parameters are fixed to their best values. The L_1, L_2, and W_1 are fixed at 8 mm, 3.9 mm and 2.26 mm respectively. Also, the other non-variable parameters are at their primary values. The antenna with the highest Fragmentary Bandwidth is highlighted out of these 13 antennas. At a resonance frequency of 2.456 GHz, the antenna with W_2 = 8 mm has the highest value of FBW, which is 100.85% with a return loss(RL) of -63.73 dB. This Antenna turned out to be a single band antenna with boosted bandwidth and resonating frequency is closest to the design frequency which is desirable for a microstrip patch antenna.

Thus, in total, the four best Antennas are obtained from this strategy of optimization. These four antennas come from each selected variable parameter's Range. The best bands of four selected antennas are aforementioned in table 5.9 with the intention of comparison.

Table 5.9 Comparison between L_1, L_2, W_1, and W_2 (strategy 3).

Variable at best (mm)	Bands	Lower freq. (GHz)	Higher freq. (GHz)	FBW (%)	Rf (GHz)	RL (dB)
L_1 = 8	B1	1.75	2.38	30.77	1.85	-43.19
L_2 = 3.9	B1	1.84	2.9	44.69	2.37	-32.8
W_1 = 2.26	B2	1.82	3.01	48.92	1.96	-26.27
W_2 = 8	B1	1.76	5.33	100.85	2.45	–63.73

Table 5.9 shows the comparative analysis of the bands obtaining maximum bandwidth percentage from each of the antennas that were selected as bests from the set of

the antennas which were defined by the range provided as mentioned in prior sections. Hence, it is clear that the antenna obtained with W_2 = 8 mm, when $L_1, L_2, and W_1$ are

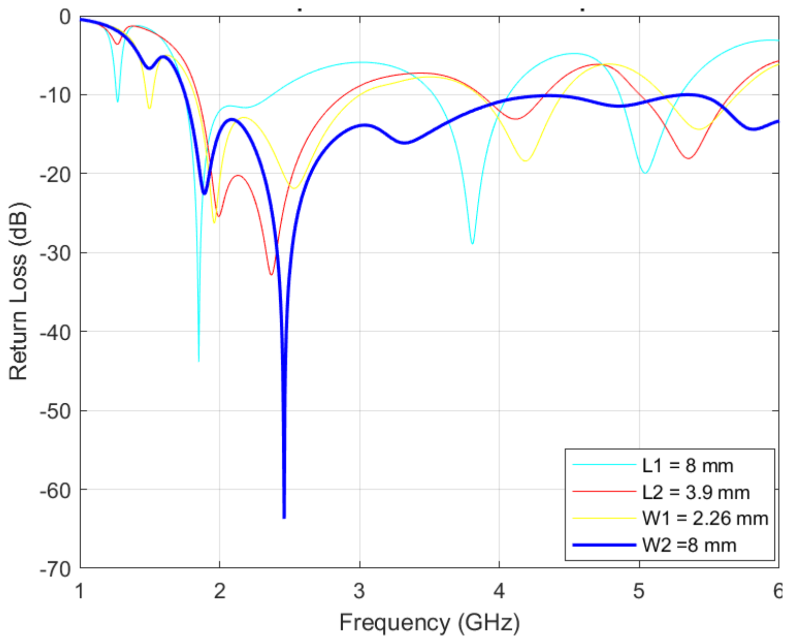

Fig. 5.2: Comparative return loss versus frequency graph of selected antennas at L_1, L_2, W_1, and W_2.

fixed at 8 mm, 3.9 mm, and 2.26 mm respectively, has provided the boosted fragmentary bandwidth keeping the antenna resonant at its design frequency as in fig 5.2. The Optimized antenna with strategy 3 is stated as Antenna 3.

5.3.1 Equivalent Model of Antenna for Return Loss and Band Width

To express the antenna's salient dimensional characteristics, equations are created by creating a connection between the bandwidth and return loss for each antenna at various values chosen from a range determined by strategic optimization for each variable parameter. Each variable parameter's link to the bandwidth (seeking the band with the maximum bandwidth) and the return loss (RL) were curve fitted separately using the MATLAB curve fitting tool. Each variable is modified to the desired range while the other parameters remain the same as the original antenna, and they are also fixed at their optimal value before moving on to the modification of other variables as in strategic optimization 3. For each value of L_1, L_2, W_1, and W_2, the antennas were cre-

ated and simulated using IE3D Software, and each antenna's RL and BW values were established. The lower cutoff frequency, higher cutoff frequency, resonant frequency, bandwidth, and RL values are presented for each significant parameter.
L_1 was originally changed from 1 to 18 mm in 1 mm increments. It constructs 18 different antennas to set up the data for the equations. For the same reason, L_2 is adjusted from 1.4 to 4mm in 0.1 mm increments, providing a total of 27 different antennas. W_1 may vary from 2.26 to 16.26 mm with a 1 mm step size, providing a total of 15 different antennas. W_2 is likewise changed in 0.5 mm increments from 3 to 9 mm, resulting in a total of 13 antennas.
As an outcome, a total of 73 different antennas are available for testing. The bandwidth % of each antenna has been calculated, as well as its return loss. Table 5.10 depicts a handful of them.

A link between each of the four variable parameters and BW and RL has been created using data from multiple antennas in the MATLAB curve fitting tool. The antenna variables relating to bandwidth and return loss are represented by the equations (5.1-5.24).

Curve fit : Polynomial-degree 6

The L_1 related to bandwidth (BW):

$$\begin{aligned} BW_1 = &-0.0001265\, L_1^6 + 0.007017\, L_1^5 - 0.1457\, L_1^4 + 1.408\, L_1^3 - 6.631\, L_1^2 \\ &+ 15.28\, L_1 + 12.14 \end{aligned} \tag{5.1}$$

The L_1 related to Return Loss (RL):

$$\begin{aligned} RL_1 = &\ 0.0002015\, L_1^6 - 0.01231\, L_1^5 + 0.2918\, L_1^4 - 3.345\, L_1^3 + 18.73\, L_1^2 \\ &- 45.85\, L_1 + 6.766 \end{aligned} \tag{5.2}$$

The L_2related to bandwidth (BW):

$$BW_2 = -0.2249 L_2^6 + 4.19 L_2^5 - 32.16 L_2^4 + 128.3 L_2^3 - 278.6 L_2^2 + 318.3 L_2 - 120.8 \tag{5.3}$$

Table 5.10 Insides of Some antennas out of 73 antennas.

Variable parameters (mm)	Bands	Lower freq. (GHz)	Higher freq. (GHz)	FBW (%)	Rf (GHz)	RL (dB)
L1 = 10 mm	B1	1.75	2.39	30.69	1.85	-32.93
	B2	3.5	4.07	15.03	3.8	-41.71
	B3	4.89	5.32	8.54	-17.2	-5.08
L1 = 11 mm	B1	1.76	2.03	14.37	1.86	-26.08
	B2	3.49	4.06	15.12	3.8	-32.52
	B3	4.9	5.34	8.54	5.09	-18.34
L2 = 1.4 mm	B1	1.75	2.33	28.25	1.85	-24.88
	B2	3.54	4.02	12.78	3.79	-27.81
	B3	4.88	5.28	7.9	5.06	-20.18
L2 = 1.5 mm	B1	1.75	2.35	29.12	1.85	-24.32
	B2	3.54	4.03	13.05	3.79	-26.02
	B3	4.88	5.28	8	5.06	-21.19
W1 = 2.26 mm	B1	1.48	1.52	2.74	1.49	-11.73
	B2	1.82	3.01	48.92	1.96	-26.27
	B3	3.86	4.45	14.22	4.19	-18.41
	B4	5.16	5.7	9.87	5.44	-14.38
W1 = 3.26 mm	B1	1.82	2.98	48.05	1.96	-37
	B2	3.84	4.42	13.96	4.17	-16.9
	B3	5.15	5.71	10.37	5.42	-15.42
W2 = 3 mm	B1	1.47	1.52	3.68	1.49	-14.57
	B2	1.84	2.91	45.14	1.98	-38.31
	B3	3.88	4.41	12.59	4.17	-28.37
	B4	5.16	5.62	8.41	5.4	-18.58
W2 = 3.5 mm	B1	1.82	2.95	47.18	1.96	-28.35
	B2	3.87	4.43	13.56	4.19	-21.18
	B3	5.16	5.66	9.14	5.41	-15.82

The L_2 related to Return Loss (RL):

$$RL_2 = -0.4506\,L_2^6 + 9.058\,L_2^5 - 68.63\,L_2^4 + 256.7\,L_2^3 - 511.2\,L_2^2 + 526.4\,L_2 - 246 \quad (5.4)$$

The W_1 related to bandwidth (BW):

$$BW_3 = -4.355e^{-5}W_1^6 + 0.00238\,W_1^5 - 0.05073\,W_1^4 + 0.5273\,W_1^3 - 2.708\,W_1^2 + 5.373\,W_1 + 45.7 \quad (5.5)$$

The W_1 related to Return Loss (RL):

$$RL_3 = 0.0005223 * W_1^6 - 0.03147 * W_1^5 + 0.7506 * W_1^4 - 8.94 * W_1^3 + 55.02 * W_1^2 - 163.2 * W_1 + 146.7 \tag{5.6}$$

The W_2 related to bandwidth (BW):

$$BW_4 = 0.02244\, W_2^6 - 0.6452\, W_2^5 + 6.907\, W_2^4 - 33.77\, W_2^3 + 72.66\, W_2^2 - 36.1\, W_2 - 7.55 \tag{5.7}$$

The W_2 related to Return Loss (RL):

$$RL_4 = 0.02414\, W_2^6 - 0.7346\, W_2^5 + 8.8\, W_2^4 - 51.71\, W_2^3 + 146.1\, W_2^2 - 144.4\, W_2 - 75.96 \tag{5.8}$$

Curve fit : Exponential

The L_1 related to bandwidth (BW):

$$BW_1 = 29.65\, exp(-0.02246\, x) \tag{5.9}$$

The L_1 related to Return Loss (RL):

$$RL_1 = -28.01\, exp(0.009794\, x) \tag{5.10}$$

The L_2related to bandwidth (BW):

$$BW_2 = 23.63\, exp(0.1724\, x) \tag{5.11}$$

The L_2 related to Return Loss (RL):

$$RL_2 = -13.89\, exp(0.2275\, x) \tag{5.12}$$

The W_1 related to bandwidth (BW):

$$BW_3 = 49.59\, exp(-0.01355\, x) \tag{5.13}$$

TheW_1 related to Return Loss (RL):

$$RL_3 = -30.95\, exp(0.01643\, x) \tag{5.14}$$

TheW_2 related to bandwidth (BW):

$$BW_4 = 35.91\, exp(0.113\, x) \tag{5.15}$$

The W_2 related to Return Loss (RL):

$$RL_4 = -18.49\, exp(0.1067\, x) \tag{5.16}$$

Curve fit : Fourier

The L_1 related to bandwidth (BW):

$$BW_1 = 24.08 - 4.39\, cos(x\, 0.3471) + 4.693\, sin(x\, 0.3471) \tag{5.17}$$

The L_1 related to Return Loss (RL):

$$RL_1 = -30.97 - 0.9338\, cos(x\, 0.3943) + 4.328\, sin(x\, 0.3943) \tag{5.18}$$

The L_2related to bandwidth (BW):

$$BW_2 = 35.5 - 7.686\, cos(x\, 0.9246) - 4.814\, sin(x\, 0.9246) \tag{5.19}$$

The L_2 related to Return Loss (RL):

$$RL_2 = -27.01 - 3.134\, cos(x\, 1.923) - 6.775\, sin(x\, 1.923) \tag{5.20}$$

The W_1 related to bandwidth (BW):

$$BW_3 = 2144000000 - 2144000000 cos(x - 0.000004239) + 223400 sin(x - 0.000004239) \tag{5.21}$$

TheW_1 related to Return Loss (RL):

$$RL_3 = -36.09 - 1.194\, cos(x\, 0.4149) + 5.256\, sin(x\, 0.4149) \tag{5.22}$$

TheW_2 related to bandwidth (BW):

$$BW_4 = 70.55 + 25.53\, cos(x\, 0.8223) - 3.806\, sin(x\, 0.8223) \tag{5.23}$$

The W_2 related to Return Loss (RL):

$$RL_4 = -36.27 - 5.655\, cos(x\, 0.8888) - 10.23\, sin(x\, 0.8888) \tag{5.24}$$

5.3.2 Simulation Results: Antenna 3

Return loss graph

Figure 5.3 depicts the S(1,1) parameter for Antenna 3. Which, provides a detailed understanding of the upper and lower cutoff frequencies, the return loss notch, the fractional bandwidth, the resonant frequency, and the number of bands. As a result, take note of the antenna's FBW (below -10 dB) in order to examine the areas in which it can be used. After modeling the antenna for 1000 frequency points in the range of 1 GHz to 6 GHz, this graph was produced and shows the return loss of -63.73 dB providing the FBW of 100.8533%.

VSWR graph

At a resonance frequency of 2.45 GHz, the Antenna's VSWR (Voltage Standing Wave Ratio) is 1.00130 dB, which is less than 2 dB, which is outstanding as shown in figure

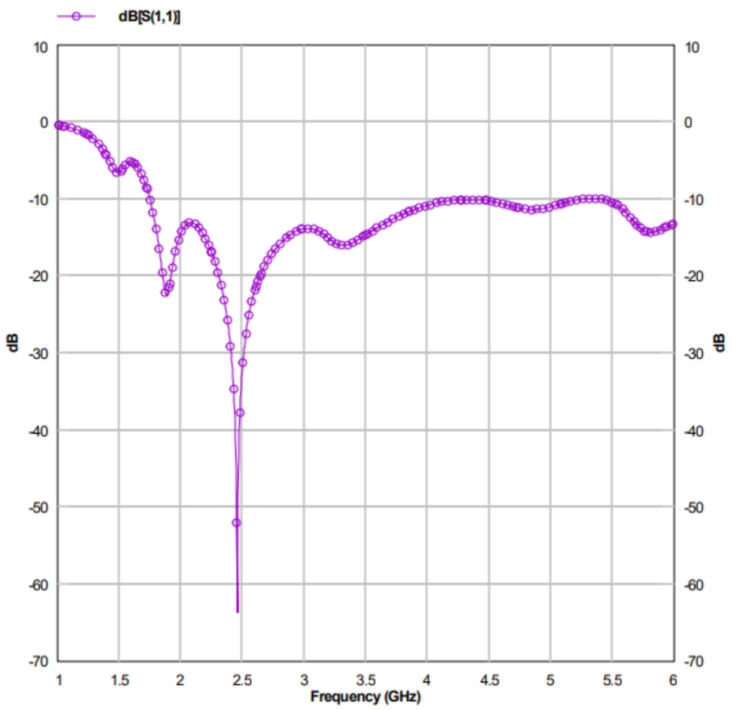

Fig. 5.3: Return loss graph of Antenna 3.

5.4. The improved antenna is better suited to the transmission line and receives more radiating power with a lower VSWR value.

It can also be calculated by:

$$VSWR = \frac{(1 + |\Gamma|)}{(1 - |\Gamma|)} \tag{5.25}$$

when, Return loss = $20log|\Gamma|$

Efficiency graph

According to Fig. 5.5, Antenna 3 has a 99.9 % antenna efficiency at its resonance frequency of 2.45 GHz. This is really good.

Gain graph

The gain of antenna 3 at the resonating frequencies of 2.45GHz is 3.407 dB, according to the Gain versus Frequency graph in figure 5.6

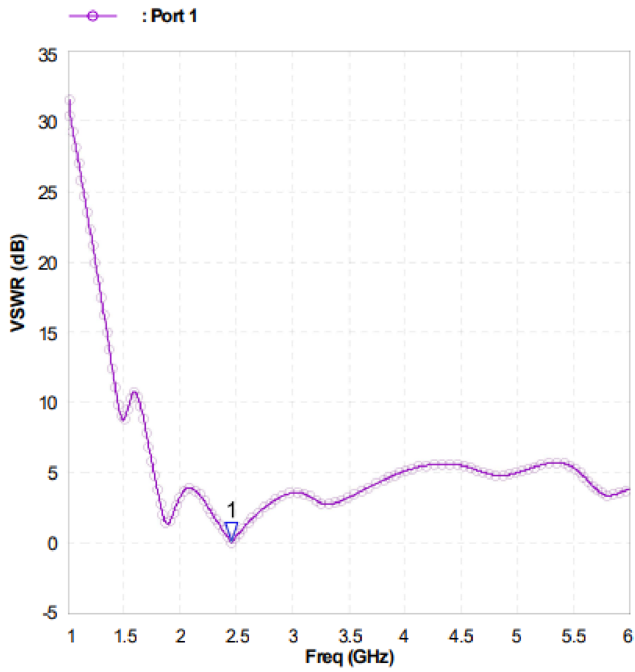

Fig. 5.4: VSWR graph of Antenna 3.

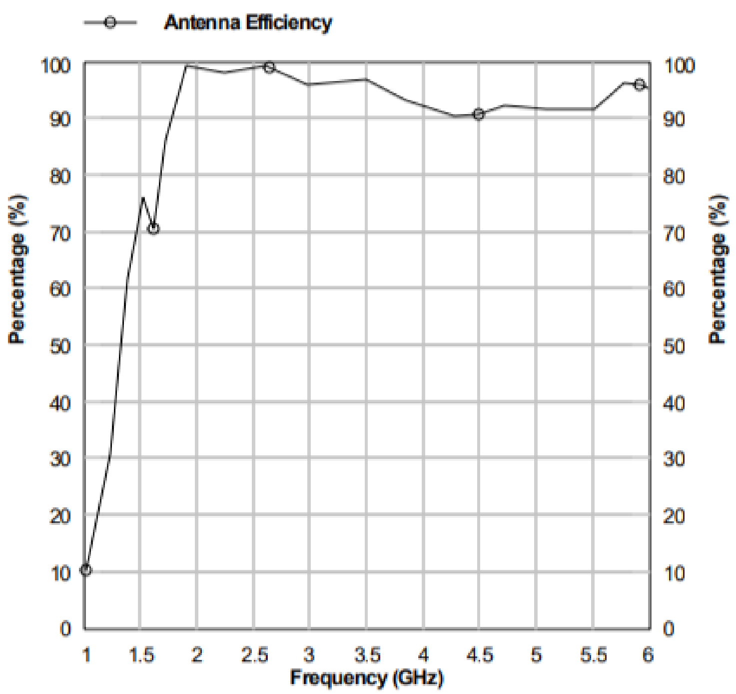

Fig. 5.5: Efficiency Versus Frequency graph of Antenna 3.

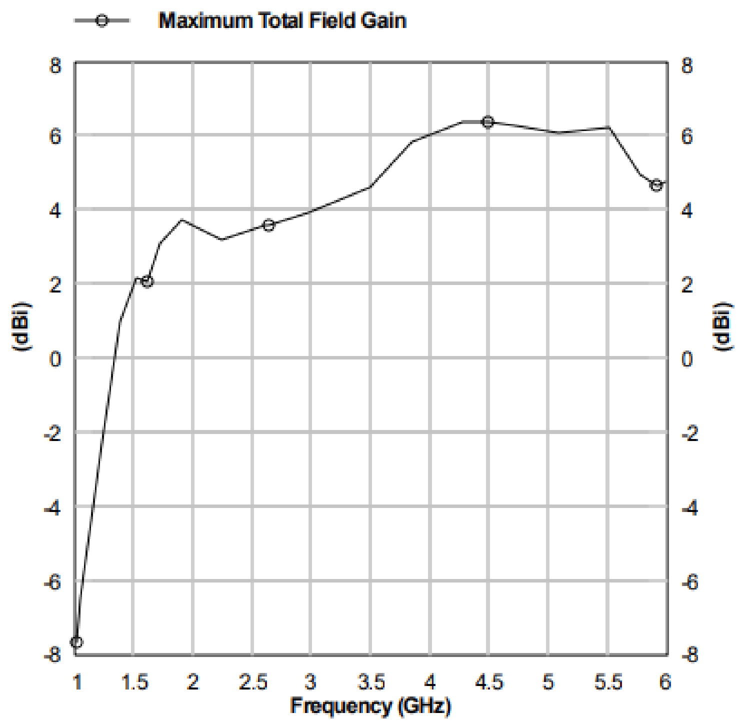

Fig. 5.6: Gain versus Frequency graph of Antenna 3.

Azimuth Plane Radiation Pattern

Figure 5.7 shows the (x–y plane) RP of Antenna 3 at resonance frequency 2.45 GHz. The radiation pattern is non-directional in the azimuth plane, forming a path in a circular manner showing the maximum gain of 3.266 dB at all angles at the resonance frequency of 2.45 GHz. As an outcome, in all azimuth plane directions, the Antenna 3 emits the same amount of energy.

Elevation Plane Radiation Pattern

Fig 5.8 depicts the following:

- Main lobe gain = 3.327dB
- Main lobe direction = 10.01°
- Angular Width (-3dB) =37.408°

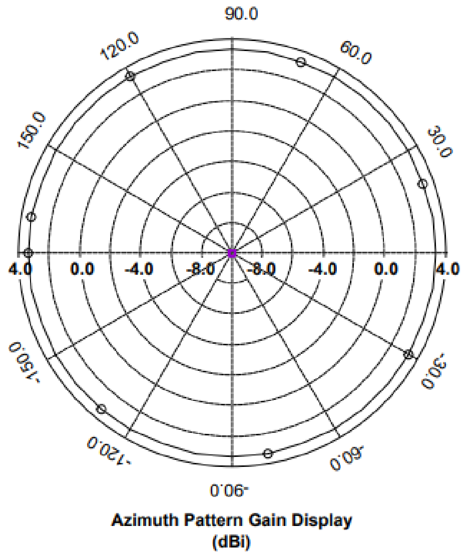

Fig. 5.7: Azimuth Plane Radiation Pattern of Antenna 3.

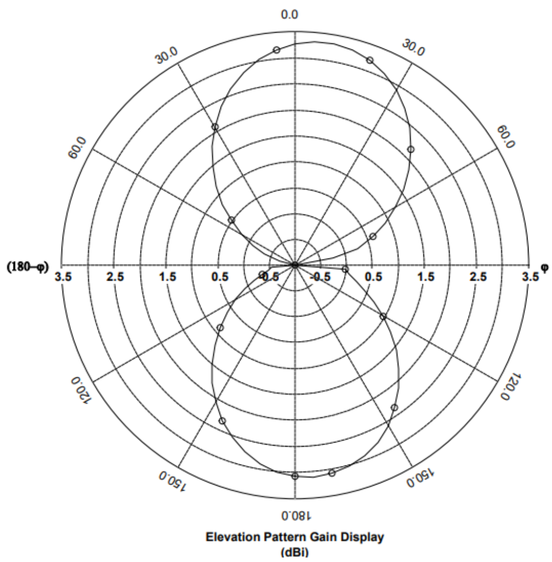

Fig. 5.8: Elevation Plane Radiation Pattern of Antenna 3 at Rf= 2.45 GHz.

- Frequency = 2.45 GHz

3-D Radiation Pattern

The 3-Dimensional radiation pattern in Fig 5.9 also shows the gain of 3.54 dB at 2.45 GHz (resonant freq.)

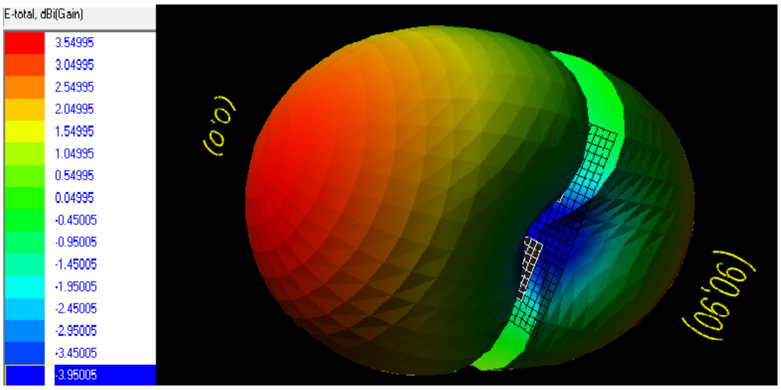

Fig. 5.9: 3-D RP of Antenna 3 at Rf= 2.45 GHz.

5.4 Flow Chart

Figure 5.10 shows the complete flow of steps followed to attain the final antenna using strategy 3 of optimization to get an enhancement of FBW of the initial antenna.

5.5 Summary

A wide band Antenna with a 2.45 GHz resonance can be employed for a range of applications. WiMAX, PCS, wireless communication systems, satellite communications (TV reception), weather radar systems, and surface ship radar are all possible applications. 802.11b and 802.11g wireless LAN, as well as Wi-Fi devices As a result, the antenna described can be utilized for a wide range of applications. In addition, as compared to the initial inverted T-shaped slotted RMSPA, The Antenna 3 has better RL and FBW. In figure 5.11, you can see a comparison graph.

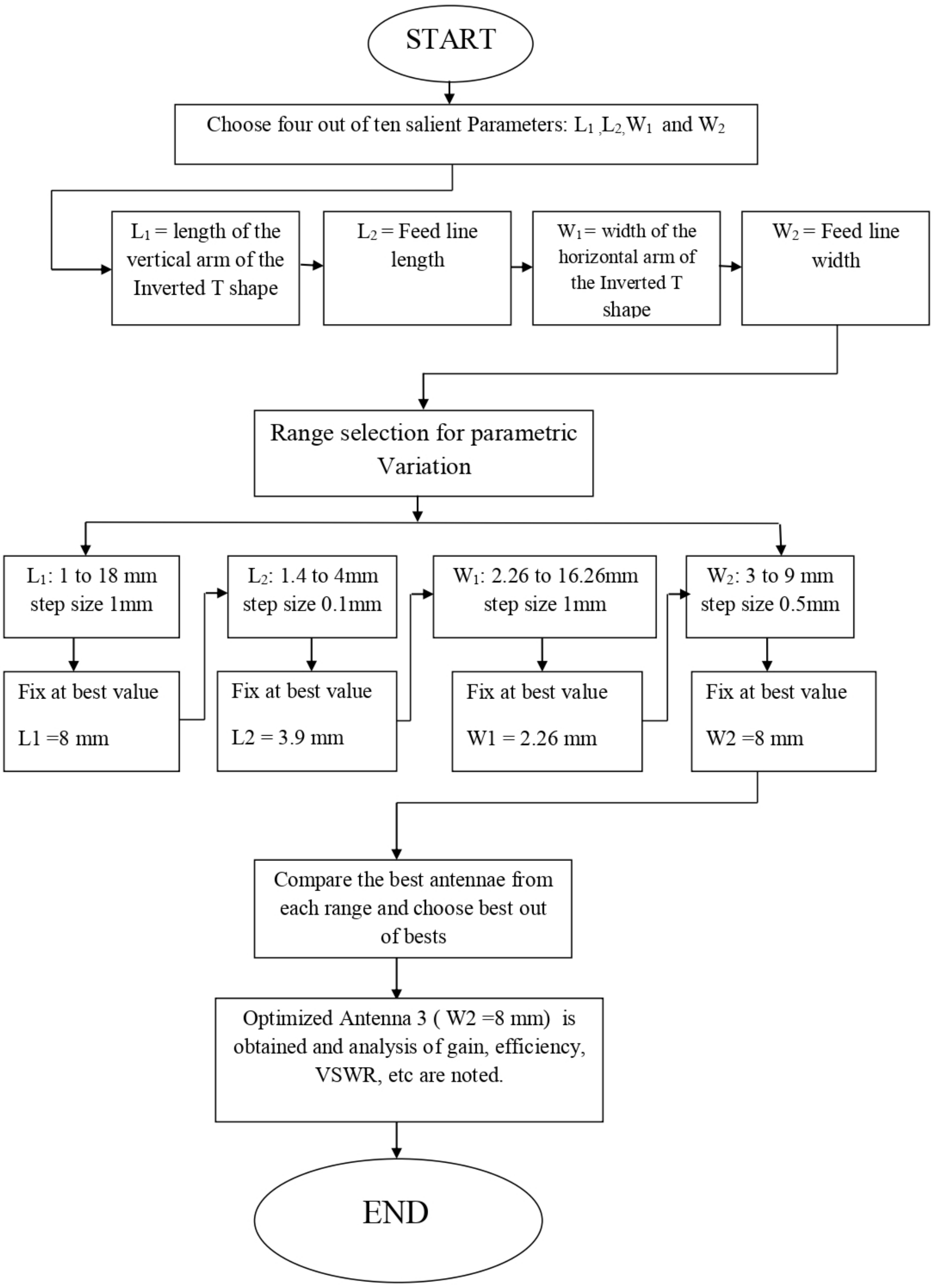

Fig. 5.10: Flow Chart for optimization strategy 3.

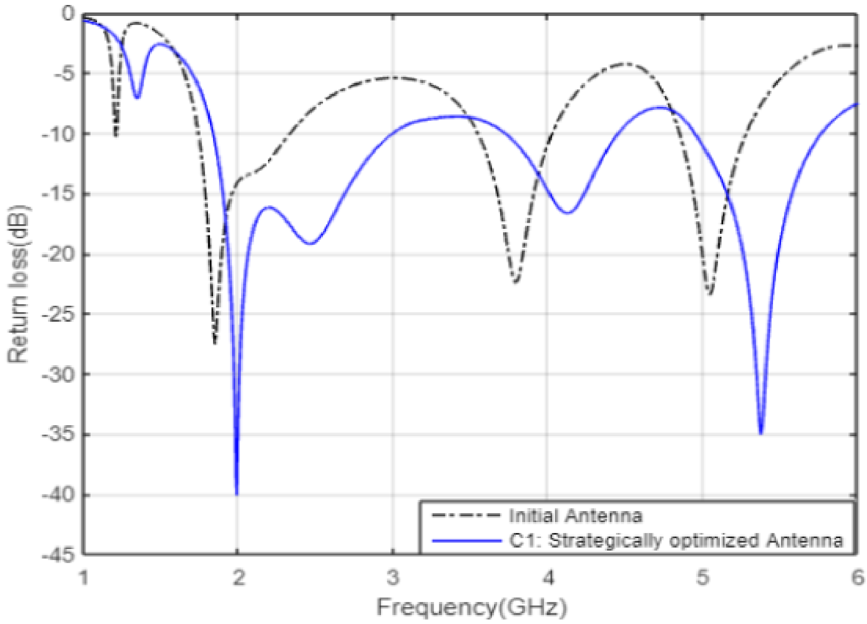

Fig. 5.11: RL versus Freq. graph of the initial Inverted T-shape Slotted RMSPA and Antenna 3.

CHAPTER 6

Particle swarm optimization

6.1 Overview

A stochastic evolutionary-based technique called particle swarm optimization (PSO) was first reported in 1995 by Kennedy and Eberhart.[11][57] In order to find optima, this technique uses a swarm of particles that travel over a multidimensional search space. [58] The social psychology principles and inherent characteristics of swarms are the foundations of PSO, this provides insight into information about social behavior. Also, the electromagnetic community now employs this method. This approach occasionally works better than other optimization methods, such as genetic algorithms (GA) [59] Understanding with an analogy on which the algorithm is designed as the nature of birds, they move in a swarm over the fields or area in search of the worms and food from one location to another and try to find the exact location providing maximum food availability as well as other conditions to be best fulfilled at the same time like water availability and safety from other animals. They randomly start their search with random velocity keeping remembering the best locations in their own search to outstretch the perfect location, they continuously change their position and wander here and there certainly between two points until they found the best location of food. Also, they consider the locations found by other members of the swarms called particles. The entire swarm would then be lured there in addition to making their own individual discovery. The birds fly over areas that best meet their needs, they are drawn back toward them as they continue to investigate the region. They constantly cross-reference the area they are flying over with known places in an effort to determine the precise position of food, water, and safety. The birds eventually arrive at the location in the area that best meets their needs thereafter all of the birds quickly congregate around this area. Every bird (particle) contains a possible remedy and is influenced by its own experiences as well as those of its neighbors (other particles of the swarm).

Considering the same actions Computer models of various interpretations of how creatures move in a fish school or a flock of birds have been created by a number of scientists.

Phraseology for PSO from above analogy.

- **Particles:** A particle is an individual bird or member of the swarm (Birds flock).
- **Swarm:** Flock of birds.
- Position: The field-based N-dimensional coordinate of a bird was referred to as its position. Each coordinate has a single parameter.
- **Cost function:** A single number indicating the value of that point is returned by the cost function for a particular position in the solution space.
- p_{best}**:** The place where a bird individually encountered the best position is what each bird recalls. The personal best, or p_{best}, is the place that a bird personally found to have the highest cost value that is the location that best meets their needs.
- g_{best} **:** The area that best meets the needs found by the entire swarm is known as the global best (g_{best}). There is a single g_{best} that the entire swarm is drawn to.

$$p_{best_{it}} = X_i^* | f(X_i^*) = min(f(X_i^k)), \tag{6.1}$$

where $i \in 1, 2, \ldots, N, k \in 1, 2 \ldots$,and

$$g_{best_t^*} = X_*^t | f(X_*^t) = min(f(X_i^k)), \tag{6.2}$$

where, $i \in 1, 2, \ldots, N, k \in 1, 2, \ldots, t$

here, The objective function to be optimised is f , 'i' is the index of the particle ,t is present iteration and N shows the total number of particles. The adjustment of particle velocity is the essential component for a successful PSO outcome. Therefore, equation given will be used to mathematically form the particle's position manipulation to give velocity v , position x of the particles at each iteration t+1[60].

$$v_i(t+1) = \omega v_i(t) + c_1 r_1 (p_{best_i}(t) - x_i(t)) + c_2 r_2 (g_{best}(t) - x_i(t)), \tag{6.3}$$

$$x_i(t+1) = x_i(t) + v_i(t+1) \tag{6.4}$$

where, **v** is velocity vector and the inertia weight known as ω is used to counteract local exploitation. Also,the global exploration, where D is the dimension of the search space or the magnitude of the task at hand, r1 and r2 are uniformly distributed random vectors, and c1 and c2, also known as "acceleration coefficients," which are positive constants.It is customary to provide an upper bound for the velocity vector[61].ω is given by

$$\omega = \omega_{max} - \frac{(\omega_{max} - \omega_{min}) * Iteration}{Max_{iteration}} \tag{6.5}$$

where, ω_{max} is the initial weight and ω_{min} is the final weight, $Max_{iteration}$ is maximum number of iteration.

In the realm of antenna design, it is always desirable to find the antenna properties and shape that will deliver the required antenna performance. Depending on the application, the performance could be a return loss, feed location, gain, FBW, or any other feature.

This has the effect of mapping each point's coordinates in the solution space onto a particular antenna design for antenna optimization purposes. This requires the definition of a minimum and maximum value for each dimension in an N-dimensional optimization. Other scenarios that could be considered when choosing an objective function include the ideal feed placement by tuning and the lowering of the Rf error of a patch antenna. Also, maximizing FBW is the goal function for the proposed PSO optimized antenna. Optimizing RMSPA's FBW is the work's main goal. The following criteria were chosen for optimization:

1. Location (Edge) of the microstrip feed.

2. Four selected parametric values.

A 3-D solution space is created using the five optimization parameters L1, L2, W1 & W2, and position of the microstrip feed and the particles, each of which corresponds to a potential solution, are free to move around in the solution space at random positions and speeds.

A cost value is determined for each particle and is determined to be the local best for the particle. This value is contrasted with the global best, and if any local best value is higher, it takes the place of the global best value. The process is considered to be complete once it has gone through 100 iterations. The cost function is given as :

$$J_{fr}, f_{RL}, J_{BW} = f(x_1, x_2 \ldots x_N, f_1, f_2) \tag{6.6}$$

where,$x_1, x_2, \ldots x_N$ are dimension of rectangles used for making "T" shape slot and f_1, f_2 denotes feed location.

$$J_{fr} = |(f_r - f_{rd})| \tag{6.7}$$

$$J_{RL} = \frac{1}{1 + (Max.RL)} \tag{6.8}$$

$$J_{BW} = \frac{1}{1 + BW} \tag{6.9}$$

$$J = \alpha_1 J_{fr} + \alpha_2 J_{RL} + \alpha_3 J_{BW} \tag{6.10}$$

α_1, α_2, α_3 are weight factor to normalize the individual objective function and α_1 =10^-9, α_2=1 and α_3 =1.

CHAPTER 7

Results and Discussion

The proposed PSO optimized Inverted T-shaped slotted rectangular patch antenna has been obtained with specific parametric results which provide the enhanced FBW, improved RL, VSWR, gain, and efficiency using MATLAB. Also, as mentioned in Chapter 3,4,5, strategically optimized results were obtained, which also showed better specifications as compared to the initial design. The initial antenna's Amplified results at each type of optimization technique using different strategies and the PSO algorithm are reflected in table 7.1.

Table 7.1 Results comparison of Initial and all optimized Antennas.

Parameters	Initial antenna	Optimized antenna 1	Optimized antenna 2	Optimized antenna 3	PSO Optimized antenna
Bandwidth (%)	29.26	43.23	48.45	100.86	101.36
Max. Return loss (dB)	-27.49	-37.00	-39.49	-63.73	-56.028
Efficiency (%)	99.1	99.63	99.96	99.9	99.99
VSWR (dB)	1.088	1.028	1.021	1.001	1.003
Rf (GHz)	1.85, 3.7 , 5.04	2.32, 4.11 , 5.31	1.99, 4.13 , 5.38	2.46	1.8,2.42, 3.83,4.8

The final strategically optimized antenna (Antenna 3)has been implemented using IE3D, and MATLAB, and also fabricated using institutional laboratories and tools.

A relationship of parametric ranges for each selected parameter to the bandwidth percentage and return loss is also obtained in the form of equations, which are the outcomes of the curve fitting. Curve fitting is carried out using different fitness functions (like exponential, polynomial of degree 4 and 6, Fourier, etc.) as shown in equations (3.9 - 3.16)(5.1- 5.24). This is done by utilizing the curve fitting tool in MATLAB to develop a relationship of parametric ranges for each selected parameter to the bandwidth percentage and return loss.

The comparison of RL (dB), VSWR, efficiency, and gain of all the antennas was analyzed at resonating frequencies. These comparative results are shown in figs 6.1(a), 6.1(b), 6.2(a), and 6.2(b), and each graph is plotted against the frequency band of 1GHz to 6GHz. The comparison of the return loss results of the initial, antenna 1, antenna 2, and antenna-3 is shown in fig 7.1(a).

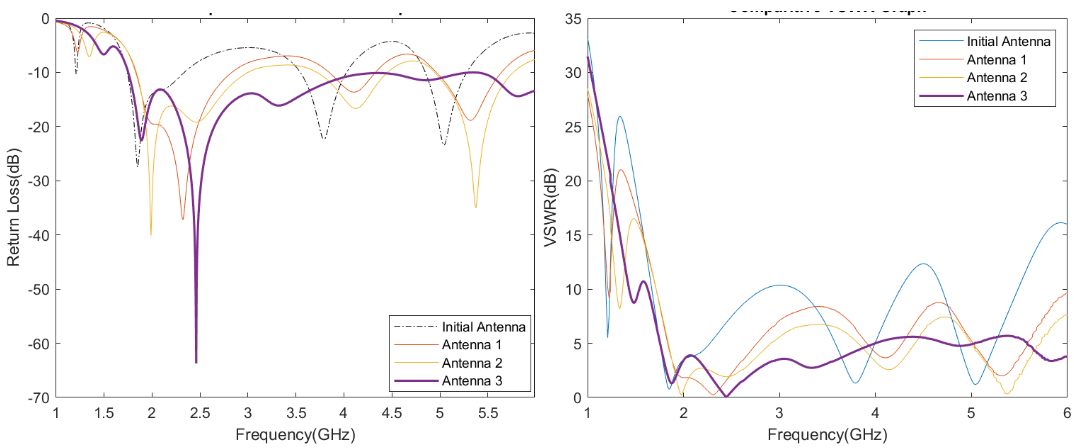

Fig. 7.1: *(a) The comparisons of RL (dB) Vs. Freq. (GHz) Graph of optimized antennas. (b) The comparative VSWR (dB) Vs. Freq. (GHz) Graph of optimized antennas.*

Figure 7.1(b) compares the VSWR plots of the initial inverted "T"-slotted RMSPA with those of strategically optimized antennas 1, 2, and 3.
The initial antenna, Strategic antenna 1, Strategic antenna 2, and Strategic antenna 3 antennas are arranged throughout the entire working frequency range between 1 and 2. It is intriguing that the optimized antenna's VSWR values are 1.0286, 1.02141, and 1.00130 at resonance frequencies of 2.32 GHz, 1.99 GHz, and 2.46 GHz, respectively, whereas the initial antenna's VSWR is 1.08816 at its resonant frequency.

The antenna gains vs frequency plots for the initial antenna, strategically upgraded antennas 1, 2, and 3, and antenna 3 are shown in Figure 7.2(a). The initial antenna's maximum antenna gains are 3.56 dB and 6 dB at 1.8 GHz and 3.8 GHz, respectively. While the gain of Strategy 3 optimal antenna is 3.30 dB and 6.12 dB at 2.32 GHz and 4.11 GHz, respectively and PSO-optimized antenna gain is 3.432 dB at resonance frequency 2.46 GHz. For all the other strategies, the gain and parameters are discussed in sections 3.3.2, 4.3.1, and 5.3.2.

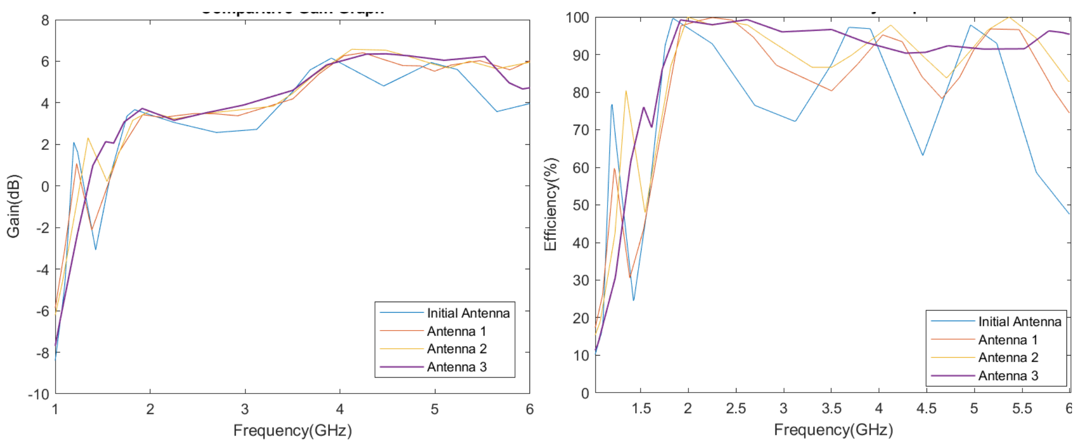

Fig. 7.2: *(a) The comparative Gain (dB) Vs. Freq. (GHz) Graph of optimized antennas. (b) The comparative Efficiency Graph of optimized antennas.*

The ratio of the antenna's output power(P_{rad}) to its input power (P_s) is known as the antenna's efficiency. It depends on the frequency and is represented as a percentage.

At resonance frequencies of 1.85 GHz, 3.80 GHz, and 5.04 GHz, respectively, the antenna efficiency of the initial antenna is 99.45%,97.03 % and 96.46%, as shown in Fig.7.2(b). At 2.46 GHz, the antenna efficiency of optimized antenna 3 is 99.99 %. Also, the antenna efficiency of a PSO-optimized antenna is 99.99 % at the resonant frequency. As compared to the initial efficiency, the antenna efficiency is extremely good at antennas that are optimized with strategies and algorithms.

The initial antenna limited bandwidth % and RL problem has been solved using different strategical optimization techniques and the Particle swarm optimization (PSO) algorithm. The parametric values of the slot variable dimensions and feed line dimensions, obtained post optimization, are listed in and have been outlined in Table 7.2.

Table 7.2 Slot and feed line Variable dimensions of all antennas.

Variable parameters (mm)	Initial Antenna (mm)	Optimized Antenna 1 (mm)	Optimized Antenna 2 (mm)	Optimized Antenna 3 (mm)	PSO Optimized Antenna (mm)
L1	6.00	6.00	12.0	8.00	12.00
L2	1.60	3.90	3.90	3.90	3.899
W1	7.26	7.26	7.26	2.260	2.26
W2	4.00	4.00	4.00	8.00	8.012

The PSO antenna is found to be resonating at four different frequencies which are 1.81

GHz, 2.42 GHz, 3.83 GHz, and 4.8 GHz while keeping resonating itself near to design frequency as well. The bandwidth percentage (FBW) of the PSO-optimized antenna is obtained as 101.36% and the PSO-optimized antenna's maximum obtained gain is 6.60 dB, Also, the antenna efficiency of a PSO-optimized antenna is 99.99 % at one of the resonant frequencies. The VSWR of the PSO optimized antenna is also improved to 0.081 Thus, as compared to the initial antenna in every aspect the PSO optimized antenna shows excellent results.

Simulation and Compared Results of PSO optimized antenna with initial antenna are established in figures 7.3(a) to 7.3 (d).

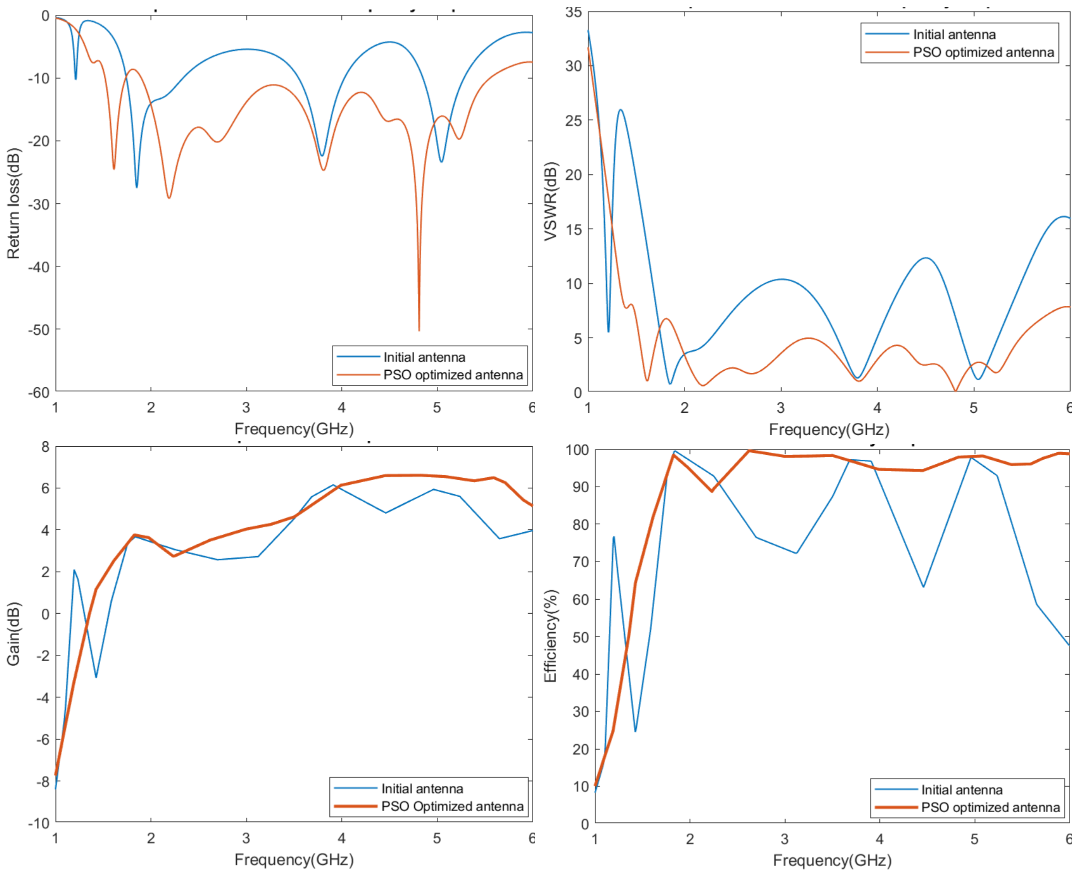

Fig. 7.3: *(a) Initial Vs. PSO optimized the antenna's Return loss graph. (b) Initial Vs. PSO optimized the antenna's VSWR graph. (c) Initial Vs. PSO optimized the antenna's Gain graph. (d) Initial Vs. PSO optimized antenna Efficiency graph.*

Experimental validation

To test the effectiveness of the proposed methods the experimental setup is established and the physical design of the proposed antennas has been fabricated and tested using the VNA (Vector Network Analyzer).

The test results obtained are quite good and valid for the simulated results. The experimental results obtained are in terms of RL Vs. Freq. graph obtained from VNA as shown in figure 7.6. The experimental impedance bandwidth of the maximum optimized antenna 3 has obtained 70.17% FBW in the range of frequency 2.10–4.37 GHz at 2.43 GHz resonant frequency with a return loss -39.55 dB. The data of each point has been extracted in CSV. The file from VNA and hence analyzed and the above-mentioned results were obtained.
Antenna measurements have been performed and are shown to be in good agreement with the simulations as shown in figure 7.7

The fabricated antenna is reflected in fig. 7.4(a),(b) with front and back views, as well as the setup is also shown in fig. 7.5.

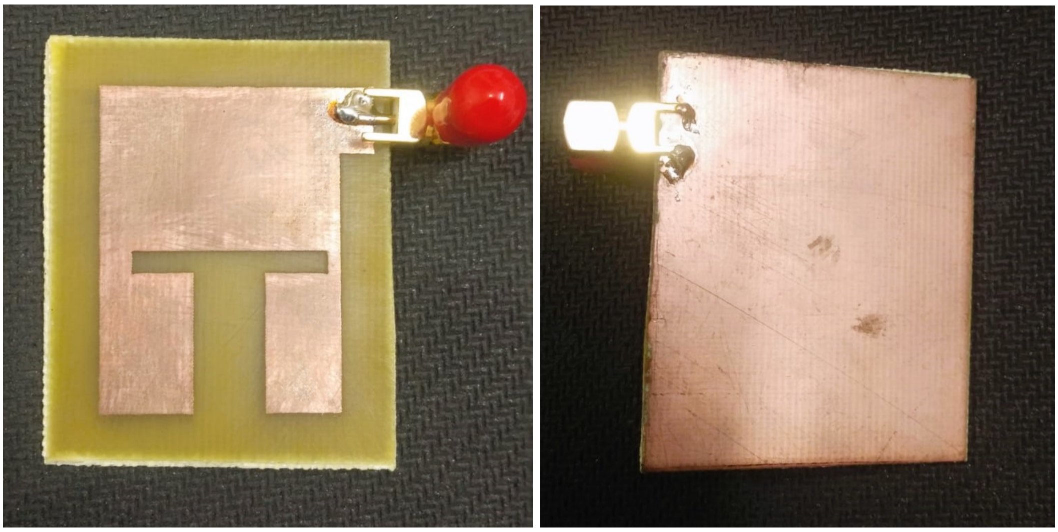

Fig. 7.4: *(a) Fabricated antenna's front patch view. (b) Fabricated antenna's backside ground view.*

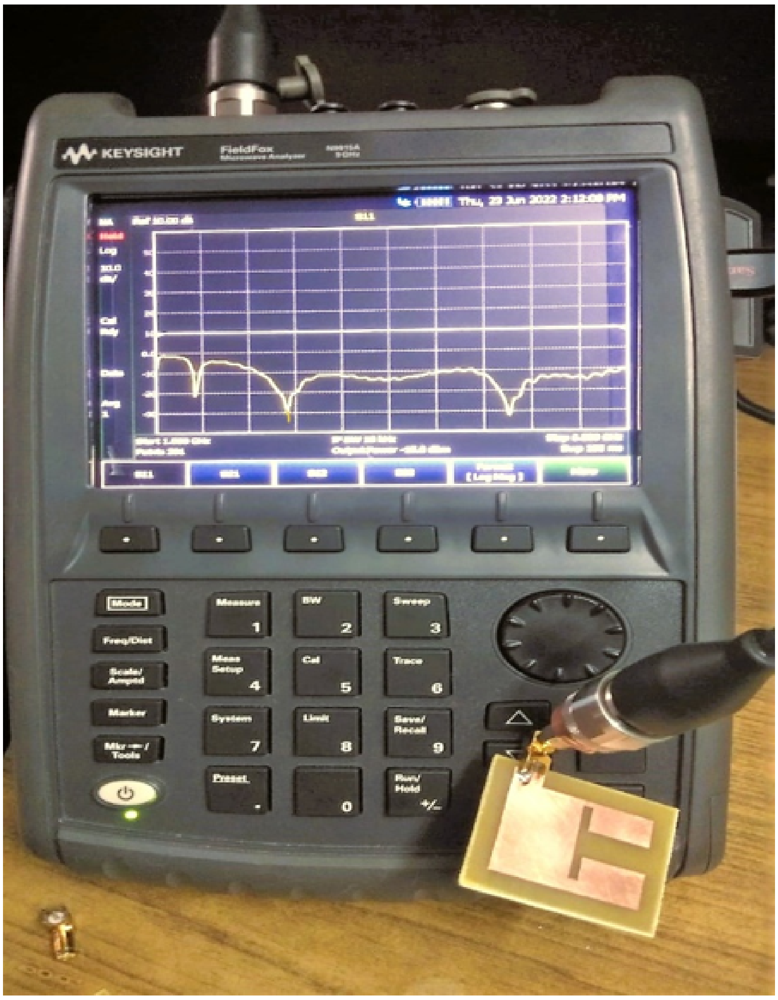

Fig. 7.5: Experimental setup

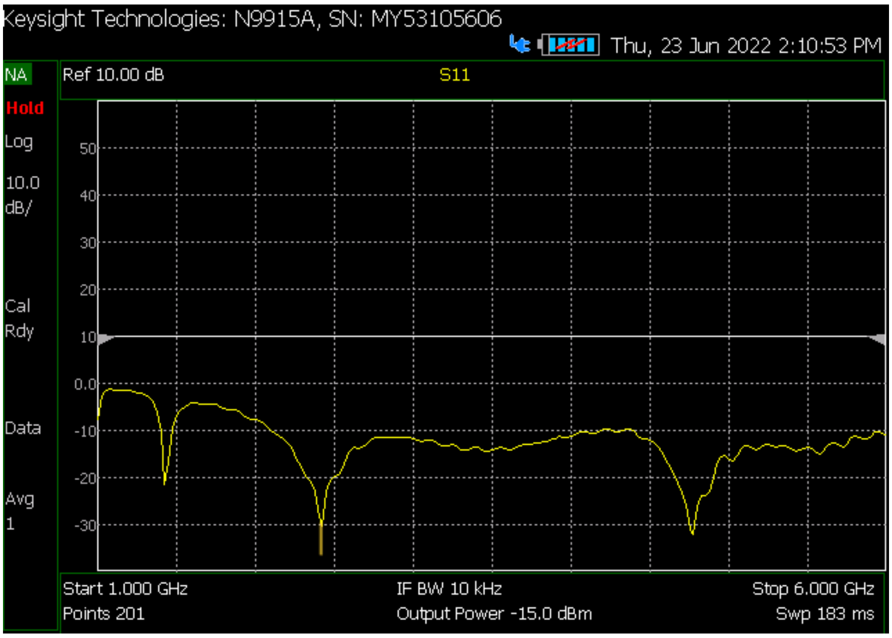

Fig. 7.6: RL Vs Frequency graph from VNA (Antenna 3)

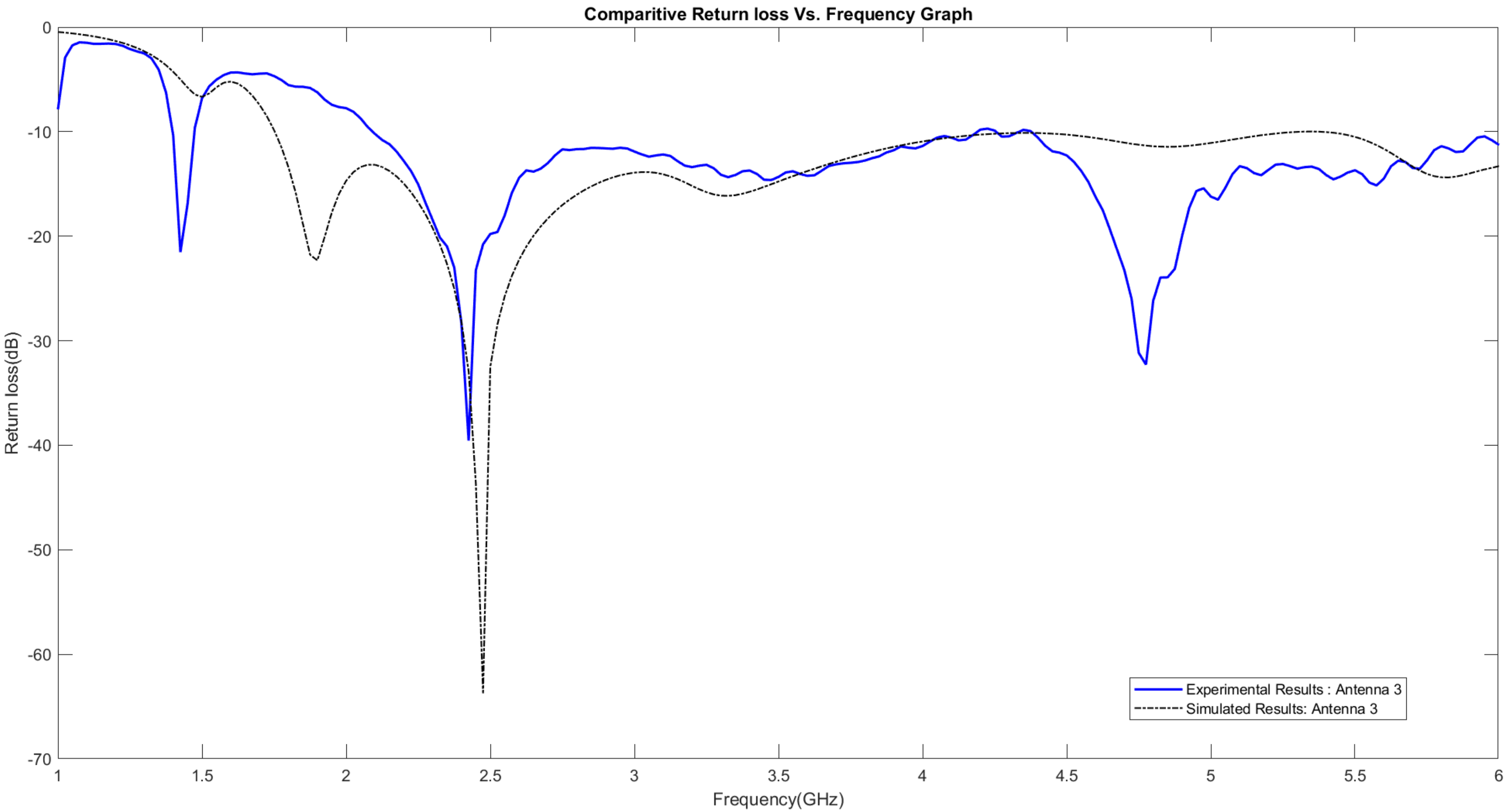

Fig. 7.7: simulated Vs. experimental S(1,1) comparative graph plot.

CHAPTER 8

Conclusion

In this project, new strategic methods of optimization have been developed for the inverted "T"-shaped slotted rectangular microstrip patch antenna. Also, the approach of three strategic optimization schemes has been proposed, which has brought a wider bandwidth with an increment of 71.6 % as compared to the initial design. In addition, bandwidth enhancement has been carried out using the particle swarm optimization technique as well which has attained the 72.1% bandwidth increment. Also, the return loss and VSWR are improved. A comparative analysis has been done of the designed, initial antenna, and other reported techniques. The equations to represent the equivalent model of antenna for return loss and FBW were also been obtained.

APPENDIX A

Plagiarism Report

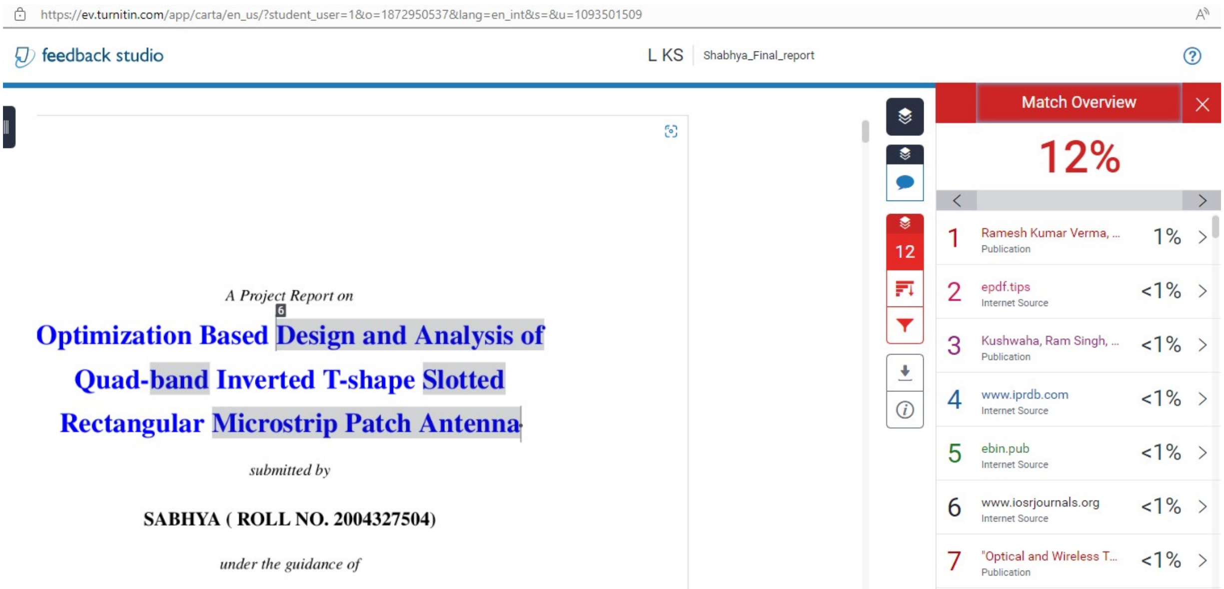

APPENDIX B

Important data and Programs

NOTE : Green highlighted cells in the tables indicate that for highlighted parametric value the antenna provides the best FBW in the bounded range.

Table B.1 Variation results of the parameter L1 in the range 1 to 18 mm.(Strategy 1)

Variable L1 (mm)	Bands	Lower Freq. (GHz)	Higher Freq. (GHz)	FBW (%)	R_f (GHz)	RL (dB)
1	B1	1.751	2.188	22.199	1.895	-20.560
	B2	3.623	3.901	7.383	3.767	-12.840
	B3	4.848	5.239	7.752	5.023	-46.172
2	B1	1.756	2.260	25.102	1.900	-42.177
	B2	3.598	4.030	11.330	3.803	-17.333
	B3	4.796	5.239	8.817	4.966	-17.994
3	B1	1.746	2.260	25.681	1.869	-23.961
	B2	3.587	3.948	9.558	3.767	-15.392
	B3	4.843	5.244	7.956	5.023	-41.554
4	B1	1.164	1.149	-1.330	1.159	-11.980
	B2	1.738	2.292	27.481	1.856	-28.637
	B3	3.559	4.000	11.669	3.779	-19.867
	B4	4.841	5.256	8.228	5.031	-24.261
5	B1	1.746	2.317	28.108	1.859	-23.122
	B2	3.567	3.989	11.166	3.778	-18.124
	B3	4.858	5.259	7.932	5.033	-31.392
6	B1	1.207	1.216	0.743	1.212	-10.430
	B2	1.742	2.338	29.261	1.852	-27.489
	B3	3.545	4.025	12.683	3.797	-22.582
	B4	4.855	5.274	8.262	5.040	-23.053
7	B1	1.751	2.358	29.544	1.849	-23.118
	B2	3.546	4.020	12.510	3.793	-21.712
	B3	4.868	5.285	8.208	5.053	-25.230

continued.....

Variable L1 (mm)	Bands	Lower freq. (GHz)	Higher freq. (GHz)	FBW (%)	R_f (GHz)	RL (dB)
8	B1	1.749	2.385	30.769	1.851	-43.186
	B2	3.528	4.067	14.180	3.805	-28.904
	B3	4.862	5.297	8.582	5.036	-19.915
9	B1	1.756	2.399	30.948	1.854	-24.049
	B2	3.515	4.045	14.016	3.793	-25.944
	B3	4.894	5.311	8.166	5.074	-22.167
10	B1	1.754	2.390	30.693	1.851	-32.931
	B2	3.503	4.072	15.030	3.800	-41.710
	B3	4.887	5.323	8.538	-17.201	-5.082
11	B1	1.761	2.034	14.367	1.859	-26.076
	B2	3.490	4.061	15.125	3.798	-32.517
	B3	4.899	5.336	8.544	5.090	-18.342
12	B1	1.748	2.384	30.769	1.851	-43.185
	B2	3.467	4.087	16.429	3.795	-36.714
	B3	4.903	5.338	8.513	5.097	-15.553
13	B1	1.319	1.350	2.313	1.334	-13.041
	B2	1.772	2.029	13.535	1.869	-40.372
	B3	3.459	4.092	16.760	3.798	-33.635
	B4	4.920	5.347	8.317	5.110	-14.732
14	B1	1.344	1.379	2.637	1.364	-12.173
	B2	1.779	2.010	12.179	1.877	-24.841
	B3	3.446	4.103	17.391	3.800	-32.167
	B4	4.923	5.349	8.288	5.103	-15.103
15	B1	1.787	2.013	11.911	1.880	-40.808
	B2	3.418	4.081	17.698	3.788	-38.107
	B3	4.940	5.378	8.475	5.115	-14.782
16	B1	1.349	1.395	3.364	1.369	-13.418
	B2	1.790	2.026	12.366	1.887	-27.174
	B3	3.410	4.097	18.306	3.785	-27.988
	B4	4.954	5.379	8.238	5.133	-13.150
17	B1	1.802	2.019	11.309	1.895	-32.167
	B2	3.382	4.076	18.623	3.778	-32.617
	B3	4.961	5.408	8.632	5.146	-13.866
18	B1	1.374	1.426	3.663	1.395	-13.805
	B2	1.810	2.031	11.482	1.903	-22.543
	B3	3.369	4.092	19.381	3.779	-26.417
	B4	4.995	5.400	7.795	5.169	-12.225

Table B.2 Variation results of the parameter L2 in the range 1.4 to 4 mm (Strategy 1).

Variable L2 (mm)	Bands	Lower freq. (GHz)	Higher freq. (GHz)	FBW (%)	Rf (GHz)	RL (dB)
1.4	B1	1.738	2.292	27.481	1.841	-31.850
	B2	3.549	4.021	12.466	3.790	-27.552
	B3	4.862	5.262	7.903	5.041	-19.444
1.5	B1	1.748	2.311	27.764	1.845	-23.871
	B2	3.556	3.997	11.666	3.787	-21.073
	B3	4.863	5.257	7.796	5.032	-25.071 7
1.6	B1	1.742	2.338	29.261	1.852	-27.489
	B2	3.545	4.025	12.683	3.797	-22.582
	B3	4.855	5.274	8.262	5.040	-23.053
1.7	B1	1.753	2.347	28.986	1.856	-22.854
	B2	3.551	4.007	12.065	3.792	-18.896
	B3	4.858	5.273	8.193	5.042	-31.462
1.8	B1	1.744	2.364	30.212	1.856	-27.608
	B2	3.538	4.036	13.135	3.790	-21.339
	B3	4.841	5.287	8.810	5.046	-24.983
1.9	B1	1.748	2.388	30.964	1.866	-26.903
	B2	3.531	4.038	13.402	3.791	-20.359
	B3	4.842	5.298	8.993	5.044	-27.041
2	B1	1.749	2.405	31.605	1.862	-26.180
	B2	3.533	4.046	13.532	3.795	-19.235
	B3	4.836	5.308	9.302	5.046	-31.575
2.1	B1	1.753	2.423	32.064	1.868	-21.731
	B2	3.552	4.023	12.428	3.803	-16.034
	B3	4.849	5.299	8.864	5.048	-30.808
2.2	B1	1.754	2.441	32.763	1.877	-25.829
	B2	3.533	4.056	13.784	3.805	-17.732
	B3	4.831	5.328	9.793	5.051	-48.882
2.3	B1	1.762	2.460	33.048	1.891	-21.970
	B2	3.558	4.023	12.270	3.804	-14.916
	B3	4.850	5.315	9.151	5.057	-25.515

Continued.......

Variable L2 (mm)	Bands	Lower freq. (GHz)	Higher freq. (GHz)	FBW (%)	Rf (GHz)	RL (dB)
2.4	B1	1.759	2.477	33.898	1.892	-25.904
	B2	3.544	4.077	13.997	3.815	-16.448
	B3	4.821	5.349	10.388	5.062	-32.098
2.5	B1	1.775	2.499	33.857	1.904	-22.514
	B2	3.571	4.036	12.228	3.804	-13.917
	B3	4.850	5.328	9.393	5.057	-22.070
2.6	B1	1.764	2.523	35.407	1.908	-26.716
	B2	3.554	4.092	14.085	3.836	-15.322
	B3	4.826	5.369	10.664	5.077	-26.523
2.7	B1	1.775	2.550	35.842	1.930	-23.879
	B2	3.597	4.049	11.828	3.842	-13.091
	B3	4.863	5.354	9.611	5.083	-19.847
2.8	B1	1.774	2.574	36.792	1.996	-24.170
	B2	3.574	4.113	14.009	3.856	-14.388
	B3	4.831	5.400	11.128	5.099	-22.990
2.9	B1	1.788	2.602	37.081	1.956	-26.608
	B2	3.636	4.075	11.394	3.868	-12.370
	B3	4.863	5.380	10.091	5.109	-18.086
3	B1	1.779	2.636	38.792	1.959	-33.800
	B2	3.605	4.138	13.775	3.892	-13.645
	B3	4.846	5.436	11.471	5.133	-20.319
3.1	B1	1.801	2.654	38.283	1.982	-33.380
	B2	3.687	4.101	10.617	3.894	-11.798
	B3	4.902	5.419	10.015	5.147	-16.551
3.2	B1	1.790	2.687	40.092	1.979	-46.728
	B2	3.662	4.179	13.211	3.933	-13.134
	B3	4.856	5.482	12.103	5.149	-19.201
3.3	B1	1.801	2.718	40.595	1.995	-42.823
	B2	3.726	4.127	10.201	3.959	-11.465
	B3	4.902	5.470	10.962	5.186	-15.914

Continued.......

Variable L2 (mm)	Bands	Lower freq. (GHz)	Higher freq. (GHz)	FBW (%)	Rf (GHz)	RL (dB)
3.4	B1	1.805	2.749	41.441	2.179	-47.878
	B2	3.718	4.226	12.782	3.974	-12.893
	B3	4.877	5.528	12.518	5.179	-18.202
3.5	B1	1.814	2.757	41.266	2.214	-38.401
	B2	3.817	4.178	9.050	3.997	-11.363
	B3	4.941	5.509	10.880	5.225	-15.512
3.6	B1	1.815	2.779	41.964	2.236	-40.195
	B2	3.774	4.267	12.245	4.010	-12.926
	B3	4.908	5.579	12.812	5.231	-18.088
3.7	B1	1.825	2.803	42.285	2.266	-33.103
	B2	3.868	4.230	8.934	4.062	-11.536
	B3	4.966	5.561	11.291	5.276	-15.563
3.8	B1	1.836	2.815	42.117	2.303	-32.565
	B2	3.897	4.251	8.685	4.092	-11.709
	B3	5.021	5.595	10.821	5.313	-15.686
3.9	B1	1.830	2.839	43.230	2.318	-37.001
	B2	3.842	4.333	12.010	4.114	-13.632
	B3	4.966	5.638	12.671	5.315	-18.852
4	B1	1.841	2.790	40.975	2.349	-2.349
	B2	3.872	4.349	11.603	4.118	-14.009
	B3	4.990	5.656	12.524	5.338	-19.469

Table B.3 Variation results of the parameter W1 in the range 2.26 to 16.26 mm (Strategy 1).

Variable W1 (mm)	Bands	Lower freq. (GHz)	Higher freq. (GHz)	FBW (%)	Rf (GHz)	RL (dB)
2.26	B1	1.364	1.410	3.327	1.390	-20.483
	B2	1.749	2.426	32.430	1.850	-32.220
	B3	3.595	4.108	13.316	3.856	-35.399
	B4	4.882	5.303	8.258	5.067	-41.911
3.26	B1	1.349	1.395	3.364	1.369	-18.464
	B2	1.749	2.421	32.226	1.851	-34.639
	B3	3.595	4.103	13.191	3.856	-34.523
	B4	4.882	5.303	8.258	5.067	-49.553
4.26	B1	1.308	1.349	3.089	1.328	-16.813
	B2	1.744	2.390	31.266	1.851	-45.688
	B3	3.579	4.087	13.244	3.841	-30.380
	B4	4.887	5.303	8.153	5.067	-32.453
5.26	B1	1.272	1.303	2.390	1.287	-14.627
	B2	1.744	2.369	30.424	1.851	-40.399
	B3	3.569	4.067	13.029	3.821	-27.590
	B4	4.872	5.297	8.371	5.062	-26.755
6.26	B1	1.236	1.256	1.646	1.246	-12.995
	B2	1.744	2.349	29.574	1.851	-33.043
	B3	3.554	4.046	12.955	3.805	-25.377
	B4	4.862	5.287	8.388	5.056	-24.021
7.26	B1	1.207	1.216	0.743	1.212	-10.430
	B2	1.742	2.338	29.261	1.852	-27.489
	B3	3.545	4.025	12.683	3.797	-22.582
	B4	4.855	5.274	8.262	5.040	-23.053
8.26	B2	1.744	2.328	28.715	1.851	-26.559
	B3	3.528	4.010	12.789	3.774	-22.003
	B4	4.831	5.262	8.537	5.021	-21.766

continued.....

Variable W1 (mm)	Bands	Lower freq. (GHz)	Higher freq. (GHz)	FBW (%)	Rf (GHz)	RL (dB)
9.26	B2	1.738	2.318	28.571	1.851	-24.695
	B3	3.513	3.990	12.714	3.749	-20.501
	B4	4.821	5.241	8.359	5.005	-20.953
10.26	B2	1.738	2.308	28.137	1.846	23.225
	B3	3.497	3.964	12.509	3.738	-19.324
	B4	4.805	5.226	8.384	4.985	-21.015
11.26	B2	1.738	2.297	27.700	1.851	-22.053
	B3	3.487	3.938	12.155	3.718	-18.064
	B4	4.795	5.205	8.205	4.974	-21.824
12.26	B2	1.738	2.297	27.700	1.851	-21.070
	B3	3.467	3.908	11.961	3.718	-16.711
	B4	4.779	5.195	8.329	4.964	-23.194
13.26	B2	1.738	2.297	27.700	1.851	-20.412
	B3	3.446	3.872	11.633	3.672	-15.742
	B4	4.785	5.179	7.926	4.949	-29.272
14.26	B2	1.738	2.292	27.481	1.851	-20.608
	B3	3.431	3.831	11.017	3.651	-14.774
	B4	4.759	5.164	8.165	4.938	-28.798
15.26	B2	1.738	2.287	27.261	1.856	19.254
	B3	3.405	3.769	10.150	3.590	-13.502
	B4	4.754	5.149	7.975	4.928	35.371
16.26	B2	1.738	2.292	27.481	1.851	-18.953
	B3	3.385	3.703	8.973	3.554	-12.447
	B4	4.749	5.133	7.784	4.918	-48.222

Table B.4 Variation results of the parameter W2 in the range 3 to 9 mm (Strategy 1).

Variable W2 (mm)	Bands	Lower freq. (GHz)	Higher freq. (GHz)	FBW (%)	Rf (GHz)	RL (dB)
3	B1	1.759	2.410	31.242	1.887	-24.347
	B2	3.579	4.077	12.994	3.836	-19.463
	B3	4.856	5.328	9.265	5.072	-35.700
3.5	B1	1.749	2.369	30.137	1.862	-25.997
	B2	3.549	4.046	13.099	3.805	-21.361
	B3	4.846	5.292	8.801	5.046	-25.847
4	B1	1.207	1.216	0.743	1.212	-10.430
	B2	1.742	2.338	29.261	1.852	-27.489
	B3	3.545	4.025	12.683	3.797	-22.582
	B4	4.855	5.274	8.262	5.040	-23.053
4.5	B1	1.738	2.313	28.354	1.841	-35.674
	B2	3.533	4.015	12.772	3.779	-3.779
	B3	4.856	5.256	7.911	5.041	-5.041
5	B1	1.738	2.287	27.261	1.836	-47.164
	B2	3.538	4.000	12.245	3.774	-32.472
	B3	4.867	5.241	7.407	5.031	-17.094
5.5	B1	1.738	2.251	25.707	1.831	-32.821
	B2	3.538	3.995	12.117	3.769	-44.763
	B3	4.882	5.231	6.897	5.041	-15.518
6	B1	1.738	2.236	25.032	1.826	-27.172
	B2	3.544	3.985	11.717	3.769	-36.290
	B3	4.897	5.215	6.288	5.026	-14.518
6.5	B1	1.738	2.205	23.667	1.826	-23.880
	B2	3.549	3.979	11.444	3.769	-29.342
	B3	4.918	5.205	5.674	5.051	-13.475
7	B1	1.744	2.164	21.522	1.826	-21.447
	B2	3.554	3.974	11.172	3.764	-25.873
	B3	4.938	5.190	4.962	5.056	-12.587
7.5	B1	1.744	2.036	15.468	1.821	-19.623
	B2	3.559	3.974	11.028	3.769	-23.288
	B3	4.964	5.174	4.148	5.067	-11.515

continued.....

Variable W2 (mm)	Bands	Lower freq. (GHz)	Higher freq. (GHz)	FBW (%)	Rf (GHz)	RL (dB)
8	B1	1.749	1.974	12.121	1.821	-18.131
	B2	3.569	3.969	10.612	3.769	-21.400
	B3	4.995	5.159	3.232	5.072	-10.831
8.5	B1	1.754	1.954	10.788	1.826	-16.821
	B2	3.574	3.964	10.340	3.774	-19.966
	B3	5.031	5.128	1.918	5.082	-10.373
9	B1	1.759	1.944	9.972	1.826	-15.754
	B2	3.585	3.964	10.054	3.774	-18.786

Table B.5 Simulation results of the combinational parametric antennas.

Variables (mm)	Bands	Lower freq. (GHz)	Higher freq. (GHz)	FBW (%)	Rf (GHz)	RL (dB)
L2 = 3.9	B1	1.835	3.008	48.445	1.989	-39.499
& L1 =12 mm	B2	3.715	4.458	18.177	4.125	-16.668
(C1)	B3	4.940	5.764	15.411	5.375	-34.984
L2=3.9	B1	1.814	2.904	46.211	1.959	-35.822
& W1=2.26 mm	B2	3.892	4.372	11.607	4.154	-15.341
(C2)	B3	5.172	5.608	8.091	5.390	-12.811
L2=3.9	B1	1.858	2.773	39.548	2.352	-35.467
& W2=3 mm	B2	3.878	4.270	9.633	4.081	-15.063
(C3)	B3	5.055	5.549	9.320	5.302	-22.267
L1=12	B2	1.741	1.959	11.783	1.843	-38.288
& W1=2.26 mm	B3	3.602	4.169	14.590	3.892	-42.458
(C4)	B4	4.939	5.331	7.642	5.128	-29.377
L1=12	B1	1.770	2.468	32.922	1.887	-20.099
& W2=3 mm	B2	3.573	4.081	13.293	3.849	-19.243
(C5)	B3	4.881	5.346	9.096	5.009	-46.583
W1=2.26	B1	1.405	1.445	2.807	1.425	-15.740
&	B2	1.756	2.526	35.981	1.872	-25.186
W2=3 mm	B3	3.645	4.169	13.393	3.922	-21.116
(C6)	B4	4.924	5.302	7.391	5.099	-16.570

Table B.6 Variation of L1 for fixing best parametric value (Strategy 3).

Variable L1 (mm)	Bands	Lower freq. (GHz)	Higher freq. (GHz)	FBW (%)	Rf (GHz)	RL (dB)
1	B1	1.751	2.188	22.199	1.895	-20.560
	B2	3.623	3.901	7.383	3.767	-12.840
	B3	4.848	5.239	7.752	5.023	-46.172
2	B1	1.756	2.260	25.102	1.900	-42.177
	B2	3.598	4.030	11.330	3.803	-17.333
	B1	4.796	5.239	8.817	4.966	-17.994
3	B1	1.746	2.260	25.681	1.869	-23.961
	B2	3.587	3.948	9.558	3.767	-15.392
	B3	4.843	5.244	7.956	5.023	-41.554
4	B1	1.164	1.149	-1.330	1.159	-11.980
	B2	1.738	2.292	27.481	1.856	-28.637
	B3	3.559	4.000	11.669	3.779	-19.867
	B4	4.841	5.256	8.228	5.031	-24.261
5	B1	1.746	2.317	28.108	1.859	-23.122
	B2	3.567	3.989	11.166	3.778	-18.124
	B3	4.858	5.259	7.932	5.033	-31.392
6	B1	1.207	1.216	0.743	1.212	-10.430
	B2	1.742	2.338	29.261	1.852	-27.489
	B3	3.545	4.025	12.683	3.797	-22.582
	B4	4.855	5.274	8.262	5.040	-23.053
7	B1	1.751	2.358	29.544	1.849	-23.118
	B2	3.546	4.020	12.510	3.793	-21.712
	B3	4.868	5.285	8.208	5.053	-25.230
8 (Fix)	B1	1.749	2.385	30.769	1.851	-43.186
	B2	3.528	4.067	14.180	3.805	-28.904
	B3	4.862	5.297	8.582	5.036	-19.915
9	B1	1.756	2.399	30.948	1.854	-24.049
	B2	3.515	4.045	14.016	3.793	-25.944
	B3	4.894	5.311	8.166	5.074	-22.167
10	B1	1.754	2.390	30.693	1.851	-32.931
	B2	3.503	4.072	15.030	3.800	-41.710
	B3	4.887	5.323	8.538	-17.201	-5.082

continued....

Variable L1 (mm)	Bands	Lower freq. (GHz)	Higher freq. (GHz)	FBW (%)	Rf (GHz)	RL (dB)
11	B1	1.761	2.034	14.367	1.859	-26.076
	B2	3.490	4.061	15.125	3.798	-32.517
	B3	4.899	5.336	8.544	5.090	-18.342
12	B1	1.764	2.405	30.750	1.862	-41.370
	B2	3.467	4.087	16.429	3.795	-36.714
	B3	4.903	5.338	8.513	5.097	-15.553
13	B1	1.319	1.350	2.313	1.334	-13.041
	B2	1.772	2.029	13.535	1.869	-40.372
	B3	3.459	4.092	16.760	3.798	-33.635
	B4	4.920	5.347	8.317	5.110	-14.732
14	B1	1.344	1.379	2.637	1.364	-12.173
	B2	1.779	2.010	12.179	1.877	-24.841
	B3	3.446	4.103	17.391	3.800	-32.167
	B4	4.923	5.349	8.288	5.103	5.103
15	B1	1.787	2.013	11.911	1.880	-40.808
	B2	3.418	4.081	17.698	3.788	-38.107
	B3	4.940	5.378	8.475	5.115	-14.782
16	B1	1.349	1.395	3.364	1.369	-13.418
	B2	1.790	2.026	12.366	1.887	-27.174
	B3	3.410	4.097	18.306	3.785	-27.988
	B4	4.954	5.379	8.238	5.133	-13.150
17	B1	1.802	2.019	11.309	1.895	-32.167
	B2	3.382	4.076	18.623	3.778	-32.617
	B3	4.961	5.408	8.632	5.146	-13.866
18	B1	1.374	1.426	3.663	1.395	-13.805
	B2	1.810	2.031	11.482	1.903	-22.543
	B3	3.369	4.092	19.381	3.779	-26.417
	B4	4.995	5.400	7.795	5.169	-12.225

Table B.7 Variation results of L2 for fixing best parametric value (Strategy 3).

Variable L2 (mm)	Bands	Lower freq. (GHz)	Higher freq. (GHz)	FBW (%)	Rf (GHz)	RL (dB)
1.4	B1	1.751	2.327	28.254	1.849	-24.883
	B2	3.541	4.025	12.782	3.793	-27.813
	B3	4.879	5.280	7.900	5.059	-20.182
1.5	B1	1.751	2.348	29.116	1.849	-24.318
	B2	3.536	4.030	13.054	3.793	-26.018
	B3	4.879	5.285	7.997	5.059	-21.193
1.6	B1	1.753	2.383	30.448	1.852	-23.505
	B2	3.531	4.037	13.377	3.790	-23.678
	B3	4.889	5.296	8.000	5.074	-27.146
1.7	B1	1.753	2.395	30.952	1.852	-22.905
	B2	3.531	4.037	13.377	3.790	-22.552
	B3	4.877	5.309	8.485	5.062	-24.621
1.8	B1	1.756	2.420	31.781	1.859	-22.460
	B2	3.526	4.040	13.598	3.793	-21.382
	B3	4.868	5.311	8.692	5.064	-26.596
1.9	B1	1.753	2.432	32.448	1.864	-22.044
	B2	3.519	4.049	14.029	3.790	-20.343
	B3	4.864	5.321	8.970	5.062	-29.013
2	B1	1.753	2.457	33.431	1.864	-21.550
	B2	3.519	4.049	14.029	3.802	-19.197
	B3	4.864	5.333	9.201	5.074	-35.960
2.1mm	B1	1.761	2.471	33.544	1.869	-21.300
	B2	3.521	4.056	14.123	3.798	-18.362
	B3	4.863	5.336	9.280	5.074	-49.085
2.2	B1	1.765	2.506	34.682	1.877	-21.089
	B2	3.519	4.062	14.332	3.802	-17.627
	B3	4.864	5.346	9.432	5.074	-40.018
2.3	B1	1.765	2.519	35.159	1.889	-20.818
	B2	3.519	4.074	14.634	3.815	-16.943
	B3	4.864	5.346	9.432	5.086	-33.010

Continued......

Variable L2 (mm)	Bands	Lower freq. (GHz)	Higher freq. (GHz)	FBW (%)	Rf (GHz)	RL (dB)
2.4	B1	1.765	2.543	36.103	1.889	-20.890
	B2	3.519	4.074	14.634	3.827	-16.277
	B3	4.864	5.358	9.662	5.099	-28.645
2.5	B1	1.765	2.568	37.037	1.889	-20.870
	B2	3.519	4.074	14.634	3.827	-15.698
	B3	4.864	5.370	9.891	5.086	-26.583
2.6	B1	1.778	2.580	36.827	1.901	-21.106
	B2	3.531	4.086	14.587	3.827	-15.142
	B3	4.864	5.395	10.349	5.099	-24.627
2.7	B1	1.778	2.630	38.655	1.914	-21.371
	B2	3.531	4.099	14.887	3.840	-14.631
	B3	4.864	5.407	10.577	5.111	-22.964
2.8	B1	1.790	2.704	40.659	1.951	-23.251
	B2	3.580	4.136	14.400	3.877	-13.369
	B3	4.877	5.444	11.005	5.148	-19.596
2.9	B1	1.790	2.679	39.779	1.926	-22.465
	B2	3.568	4.123	14.446	3.864	-13.748
	B3	4.877	5.432	10.778	5.123	-20.523
3	B1	1.790	2.716	41.096	1.938	-23.408
	B2	3.580	4.136	14.400	3.914	-13.292
	B3	4.877	5.444	11.005	5.136	-19.596
3.1	B1	1.802	2.741	41.304	1.951	-24.974
	B2	3.605	4.148	14.013	3.914	-13.035
	B3	4.889	5.469	11.204	5.160	-18.821
3.2	B1	1.797	2.772	42.694	1.962	-26.822
	B2	3.637	4.173	13.718	3.953	-12.754
	B3	4.901	5.492	11.367	5.176	-18.210
3.3	B1	1.810	2.786	42.439	1.962	-29.202
	B2	3.679	4.187	12.924	3.953	-12.601
	B3	4.901	5.519	11.864	5.190	-17.720
3.4	B1	1.810	2.827	43.839	1.975	-33.752
	B2	3.706	4.214	12.834	3.995	-12.486
	B3	4.915	5.533	11.833	5.217	-17.421

Continued......

Variable L2 (mm)	Bands	Lower freq. (GHz)	Higher freq. (GHz)	FBW (%)	Rf (GHz)	RL (dB)
3.5	B1	1.824	2.841	43.581	1.975	-40.309
	B2	3.747	4.242	12.380	3.995	-12.436
	B3	4.929	5.560	12.048	5.217	-17.044
3.6	B1	1.824	2.841	43.581	1.989	-41.456
	B2	3.775	4.255	11.974	4.049	-12.508
	B3	4.942	5.588	12.262	5.272	-17.217
3.7	B1	1.824	2.868	44.496	1.989	-32.655
	B2	3.816	4.283	11.533	4.077	-12.623
	B3	4.970	5.615	12.198	5.299	-17.365
3.8	B1	1.824	2.868	44.496	1.989	-32.655
	B2	3.816	4.283	11.533	4.077	-12.623
	B3	4.970	5.615	12.198	5.299	-17.365
3.9 (Fix)	B1	1.838	2.896	44.689	2.374	-32.804
	B2	3.871	4.324	11.063	4.118	-13.091
	B3	5.011	5.657	12.104	5.354	-18.079
4	B1	1.852	2.901	44.156	2.395	-31.858
	B2	3.889	4.346	11.094	4.123	-13.430
	B3	5.025	5.667	12.009	5.370	-18.695

Table B.8 Variation results of W1 for fixing best parametric value (Strategy 3).

Variable W1 (mm)	Bands	Lower freq. (GHz)	Higher freq. (GHz)	FBW (%)	Rf (GHz)	RL (dB)
2.26 (Fix)	B1	1.824	3.005	48.919	1.962	-26.273
	B2	3.857	4.448	14.224	4.187	-18.409
	B3	5.162	5.698	9.866	5.437	-14.377
3.26	B1	1.824	2.978	48.055	1.962	-37.000
	B2	3.843	4.420	13.963	4.173	-16.902
	B3	5.148	5.712	10.372	5.423	-15.419
4.26	B1	1.838	2.951	46.472	1.975	-35.589
	B2	3.843	4.393	13.342	4.146	-15.703
	B3	5.107	5.712	11.173	5.409	-16.391
5.26	B1	1.838	2.923	45.586	1.975	-29.136
	B2	3.857	4.365	12.362	4.146	-14.706
	B3	5.080	5.698	11.471	5.396	-17.203
6.26	B1	1.838	2.909	45.139	2.387	-30.364
	B2	3.857	4.352	12.048	4.146	-13.827
	B3	5.038	5.670	11.801	5.382	-17.802
7.26mm	B1	1.838	2.896	44.689	2.374	-32.804
	B2	3.871	4.324	11.063	4.118	-13.091
	B3	5.011	5.657	12.104	5.354	-18.079
8.26	B1	1.838	2.882	44.237	2.346	-36.227
	B2	3.871	4.297	10.427	4.091	-12.266
	B3	4.970	5.629	12.442	5.327	-17.915
9.26	B1	1.852	2.868	43.073	2.332	-38.909
	B2	3.898	4.255	8.760	4.077	-11.606
	B3	4.942	5.602	12.507	5.299	-17.522
10.26	B1	1.838	2.854	43.326	2.319	-40.449
	B2	3.926	4.214	7.087	4.091	-10.965
	B3	4.915	5.574	12.572	5.258	-16.919
11.26	B1	1.852	2.854	42.615	2.305	-42.116
	B2	4.901	5.547	12.359	5.258	-16.207

Continued.....

Variable W1 (mm)	Bands	Lower freq. (GHz)	Higher freq. (GHz)	FBW (%)	Rf (GHz)	RL (dB)
12.26	B1	1.852	2.841	42.155	2.291	-42.522
	B2	4.901	5.533	12.112	5.231	-15.408
13.26	B1	1.852	2.813	41.225	2.277	-40.444
	B2	4.887	5.519	12.144	5.231	-14.708
14.26	B1	1.852	2.813	41.225	2.277	-39.132
	B2	4.901	5.505	11.616	5.231	-14.004
15.26	B1	1.852	2.799	40.756	2.264	-37.121
	B2	4.929	5.492	10.809	5.231	-13.379
16.26	B1	1.852	2.772	39.810	2.250	-33.654
	B2	4.956	5.478	10.005	5.217	-12.955

Table B.9 Variation results of W2 for fixing best parametric value (Strategy 3).

Variable W2 (mm)	Bands	Lower freq. (GHz)	Higher freq. (GHz)	FBW (%)	Rf (GHz)	RL (dB)
3	B1	1.467	1.522	3.676	1.495	-14.574
	B2	1.838	2.909	45.139	1.975	-38.313
	B3	3.885	4.407	12.591	4.173	-28.369
	B4	5.162	5.615	8.412	5.396	-18.580
3.5	B1	1.824	2.951	47.181	1.962	-28.350
	B2	3.871	4.434	13.563	4.187	-21.178
	B3	5.162	5.657	9.142	5.409	-15.824
4	B1	1.824	3.005	48.919	1.962	-26.273
	B2	3.843	4.448	14.579	4.187	-18.409
	B3	5.162	5.698	9.866	5.423	-14.393
4.5	B1	1.810	3.074	51.744	1.962	-24.538
	B2	3.816	4.462	15.599	4.187	-16.524
	B3	5.176	5.753	10.558	5.451	-13.420

Continued.....

Variable W2 (mm)	Bands	Lower freq. (GHz)	Higher freq. (GHz)	FBW (%)	Rf (GHz)	RL (dB)
5	B1	1.797	3.266	58.058	2.525	-26.155
	B2	3.788	4.489	16.927	4.214	-14.756
	B3	5.176	5.821	11.741	5.478	-12.569
5.5	B1	1.797	3.431	62.533	2.511	-28.687
	B2	3.720	4.503	19.044	4.173	-13.675
	B3	5.162	5.794	11.535	5.451	-11.695
6	B1	1.783	4.530	87.032	2.511	-31.563
	B2	5.176	5.986	14.521	5.725	-12.482
6.5mm	B1	1.769	4.558	88.146	2.497	-34.947
7mm	B1	1.769	4.571	88.388	2.484	-39.574
7.5mm	B1	1.755	5.272	100.078	2.470	-44.521
8mm (Fix)	B1	1.755	5.327	100.853	2.461	-63.730
8.5	B1	1.755	4.132	80.728	2.442	-46.104
	B2	4.475	5.258	16.088	4.846	-12.253
9mm	B1	1.755	4.049	79.035	2.442	-45.245
	B2	4.516	5.231	14.656	4.860	-13.114

REFERENCES

[1] C. A. Balanis, *Antenna theory: analysis and design*. John Wiley & sons, 2015.

[2] K. Mahendran, R. Gayathri, and H. Sudarsan, "Design of multi band triangular microstrip patch antenna with triangular split ring resonator for s band, c band and x band applications," *Microprocessors and Microsystems*, vol. 80, p. 103400, 2021.

[3] J. R. James *et al.*, *Handbook of microstrip antennas*. IET, 1989, vol. 1.

[4] A. Abdelaziz, "Bandwidth enhancement of microstrip antenna," *Progress In Electromagnetics Research*, vol. 63, pp. 311–317, 2006.

[5] L. C. Paul and N. Sultan, "Design, simulation and performance analysis of a line feed rectangular micro-strip patch antenna," *International Journal of Engineering Sciences and Emerging Technologies*, vol. 4, no. 2, pp. 117–126, 2013.

[6] T. Eibert, "Iterative-solver convergence for loop-star and loop-tree decompositions in method-of-moments solutions of the electric-field integral equation," *IEEE Antennas and Propagation Magazine*, vol. 46, no. 3, pp. 80–85, 2004.

[7] K. S. Sultan, H. H. Abdullah, and E. A. Abdallah, "Method of moments analysis for antenna arrays with optimum memory and time consumption," *Progress In Electromagnetics Research*, vol. 1353, 2012.

[8] J. R. Mosig and F. E. Gardiol, "Analytical and numerical techniques in the green's function treatment of microstrip antennas and scatterers," in *IEE Proceedings H (Microwaves, Optics and Antennas)*, vol. 130, no. 2. IET, 1983, pp. 175–182.

[9] D. M. Pozar, "Microstrip antenna aperture-coupled to a microstripline," *Electronics letters*, vol. 21, p. 49, 1985.

[10] S. Chourasia, S. Changlani, and M. P. Gupta, "Comparative study and designing of different radiating patch in microstrip patch antenna," *IEEE Communications Magazine*, vol. 42, no. 6, pp. S29–S32, 2004.

[11] J. Kennedy and R. Eberhart, "Particle swarm optimization," in *Proceedings of ICNN'95-international conference on neural networks*, vol. 4. IEEE, 1995, pp. 1942–1948.

[12] Y. Del Valle, G. K. Venayagamoorthy, S. Mohagheghi, J.-C. Hernandez, and R. G. Harley, "Particle swarm optimization: basic concepts, variants and applications in power systems," *IEEE Transactions on evolutionary computation*, vol. 12, no. 2, pp. 171–195, 2008.

[13] A. Patnaik, S. Sinha *et al.*, "Design of custom-made fractal multi-band antennas using ann-pso [antenna designer's notebook]," *IEEE Antennas and Propagation Magazine*, vol. 53, no. 4, pp. 94–101, 2011.

[14] C.-F. Juang, "A hybrid of genetic algorithm and particle swarm optimization for recurrent network design," *IEEE Transactions on Systems, Man, and Cybernetics, Part B (Cybernetics)*, vol. 34, no. 2, pp. 997–1006, 2004.

[15] A. D. Boursianis, S. K. Goudos, T. V. Yioultsis, K. Siakavara, and P. Rocca, "Mimo antenna design for 5g communication systems using salp swarm algorithm," in *2020 International Workshop on Antenna Technology (iWAT)*. IEEE, 2020, pp. 1–3.

[16] A. K. Mondal and P. Saxena, "Thinning of concentric circular antenna array using binary salp swarm algorithm," in *2019 IEEE Conference on Information and Communication Technology*. IEEE, 2019, pp. 1–4.

[17] U. Singh and M. Rattan, "Design of linear and circular antenna arrays using cuckoo optimization algorithm," *Progress in Electromagnetics research C*, vol. 46, pp. 1–11, 2014.

[18] S. K. Goudos, K. Siakavara, and J. N. Sahalos, "Novel spiral antenna design using artificial bee colony optimization for uhf rfid applications," *IEEE Antennas and Wireless Propagation Letters*, vol. 13, pp. 528–531, 2014.

[19] S. K. Goudos, D. E. Anagnostou, C. Kalialakis, P. Vasant, and S. Nikolaou, "Evolutionary algorithms applied to antennas and propagation: emerging trends and applications," *International Journal of Antennas and Propagation*, vol. 2016, 2016.

[20] G. Singh and U. Singh, "Triple band-notched uwb antenna design using a novel hybrid optimization technique based on de and nmr algorithms," *Expert Systems with Applications*, vol. 184, p. 115299, 2021.

[21] M. Kaur and J. S. Sivia, "Minkowski, giuseppe peano and koch curves based design of compact hybrid fractal antenna for biomedical applications using ann and pso," *AEU-International Journal of Electronics and Communications*, vol. 99, pp. 14–24, 2019.

[22] N. Jin and Y. Rahmat-Samii, "Parallel particle swarm optimization and finite-difference time-domain (pso/fdtd) algorithm for multiband and wide-band patch antenna designs," *IEEE Transactions on Antennas and Propagation*, vol. 53, no. 11, pp. 3459–3468, 2005.

[23] M. T. Islam, N. Misran, T. C. Take, and M. Moniruzzaman, "Optimization of microstrip patch antenna using particle swarm optimization with curve fitting," in *2009 International Conference on Electrical Engineering and Informatics*, vol. 2. IEEE, 2009, pp. 711–714.

[24] K. Sharma and G. P. Pandey, "Efficient modelling of compact microstrip antenna using machine learning," *AEU-International Journal of Electronics and Communications*, vol. 135, p. 153739, 2021.

[25] R. Jiao, X. Huang, H. Ouyang, G. Li, Q. Zheng, and Z. Jiang, "Optimal electric business centre location by centre–decentre quantum particle swarm optimization," *Systems Science & Control Engineering*, vol. 7, no. 1, pp. 222–233, 2019.

[26] X. Zhang, X. Zhang, and L. Wang, "Antenna design by an adaptive variable differential artificial bee colony algorithm," *IEEE Transactions on Magnetics*, vol. 54, no. 3, pp. 1–4, 2017.

[27] D. Ustun and A. Akdagli, "Design of band–notched uwb antenna using a hybrid optimization based on abc and de algorithms," *AEU-International Journal of Electronics and Communications*, vol. 87, pp. 10–21, 2018.

[28] Z. Bayraktar, M. Komurcu, J. A. Bossard, and D. H. Werner, "The wind driven optimization technique and its application in electromagnetics," *IEEE transactions on antennas and propagation*, vol. 61, no. 5, pp. 2745–2757, 2013.

[29] V. Rajpoot, D. Srivastava, and A. K. Saurabh, "Optimization of i-shape microstrip patch antenna using pso and curve fitting," *Journal of Computational Electronics*, vol. 13, no. 4, pp. 1010–1013, 2014.

[30] R. K. Verma and D. Srivastava, "Design, optimization and comparative analysis of t-shape slot loaded microstrip patch antenna using pso," *Photonic Network Communications*, vol. 38, no. 3, pp. 343–355, 2019.

[31] M. Singh and S. Singh, "Design and performance investigation of miniaturized multi-wideband patch antenna for multiple terahertz applications," *Photonics and Nanostructures-Fundamentals and Applications*, vol. 44, p. 100900, 2021.

[32] K. Y. Yazdandoost and R. Kohno, "Ultra wideband antenna," *IEEE Communications Magazine*, vol. 42, no. 6, pp. S29–S32, 2004.

[33] J. D. Kraus, R. J. Marhefka, and A. S. Khan, *Antennas and wave propagation*. Tata McGraw-Hill Education, 2006.

[34] H. F. Pues and A. R. Van De Capelle, "An impedance-matching technique for increasing the bandwidth of microstrip antennas," *IEEE transactions on antennas and propagation*, vol. 37, no. 11, pp. 1345–1354, 1989.

[35] A. Thatere, P. Zade, and D. Arya, "Bandwidth enhancement of microstrip patch antenna using 'u'slot with modified ground plane," in *2015 International Conference on Microwave, Optical and Communication Engineering (ICMOCE)*. IEEE, 2015, pp. 408–411.

[36] S. M. Wentworth, *Fundamentals of electromagnetics with engineering applications*. John Wiley & Sons, 2006.

[37] R. Garg, P. Bhartia, I. J. Bahl, and A. Ittipiboon, *Microstrip antenna design handbook*. Artech house, 2001.

[38] A. Kumar, J. Kaur, and R. Singh, “Performance analysis of different feeding techniques,” *International journal of emerging technology and advanced engineering*, vol. 3, no. 3, pp. 884–890, 2013.

[39] A. Yahia, N. Shaalan, and N. Gad, “B13. cpw-fed square-spiral slot antenna design for wideband applications,” in *2012 29th National Radio Science Conference (NRSC)*. IEEE, 2012, pp. 103–110.

[40] S.-C. Gao, L.-W. Li, M.-S. Leong, and T.-S. Yeo, “Wide-band microstrip antenna with an h-shaped coupling aperture,” *IEEE Transactions on vehicular technology*, vol. 51, no. 1, pp. 17–27, 2002.

[41] N. Jin and Y. Rahmat-Samii, “Particle swarm optimization for antenna designs in engineering electromagnetics,” *Journal of Artificial evolution and applications*, vol. 2008, 2008.

[42] R. S. Kushwaha, D. Srivastava, J. Saini, and S. Dhupkariya, “Bandwidth enhancement for microstrip patch antenna with microstrip line feed,” in *2012 Third International Conference on Computer and Communication Technology*. IEEE, 2012, pp. 183–185.

[43] M. D. Sharma, A. Katariya, and R. Meena, “E shaped patch microstrip antenna for wlan application using probe feed and aperture feed,” in *2012 International Conference on Communication Systems and Network Technologies*. IEEE, 2012, pp. 66–70.

[44] U. Raithatha and S. S. Kashyap, “Microstrip patch antenna parameters, feeding techniques & shapes of the patch–a survey,” *International Journal of Scientific & Engineering Research*, vol. 6, no. 4, pp. 981–984, 2015.

[45] A. K. Sidhu and J. S. Sivia, “Microstrip rectangular patch antenna for s and x band applications,” in *2016 International Conference on Wireless Communications, Signal Processing and Networking (WiSPNET)*. IEEE, 2016, pp. 248–251.

[46] K. Anum, M. S. Singh, R. Mishra, and G. Tripathi, “Bandwidth enhancement of a microstrip patch antenna for ultra-wideband applications,” in *AIP Conference Proceedings*, vol. 1952, no. 1. AIP Publishing LLC, 2018, p. 020053.

[47] A. Kumar and M. K. Singh, “Band-notched planar uwb microstrip antenna with t-shaped slot,” *Radioelectronics and Communications Systems*, vol. 61, no. 8, pp. 371–376, 2018.

[48] E. M. F. Fernandes, M. W. B. da Silva, L. da Silva Briggs, A. L. P. de Siqueira Campos, H. X. de Araújo, I. R. S. Casella, C. E. Capovilla, V. P. R. M. Souza, and L. J. de Matos, “2.4–5.8 ghz dual-band patch antenna with fss reflector for radiation parameters enhancement,” *AEU-International Journal of Electronics and Communications*, vol. 108, pp. 235–241, 2019.

[49] D. S. P. Rajan, “Design of microstrip patch antenna for wireless application using high performance fr4 substrate,” *Advances and Applications in Mathematical Sciences, ISSN*, no. 0974-6803, pp. 819–837, 2019.

[50] R. K. Verma and D. Srivastava, "Bandwidth enhancement of a slot loaded t-shape patch antenna," *Journal of Computational Electronics*, vol. 18, no. 1, pp. 205–210, 2019.

[51] M. Sabir and G. Ratnu, "A design of compact t-shaped fractal patch antenna for x-band applications," *Materials Today: Proceedings*, vol. 29, pp. 295–299, 2020.

[52] R. K. Maurya, B. K. Kanaujia, A. Gautam, S. Chatterji, and A. K. Singh, "Circularly polarized hexagonal ring microstrip patch antenna with asymmetrical feed and dgs," *Microwave and Optical Technology Letters*, vol. 62, no. 4, pp. 1702–1708, 2020.

[53] K. Mazen, A. Emran, A. S. Shalaby, and A. Yahya, "Design of multi-band microstrip patch antennas for mid-band 5g wireless communication," *International Journal of Advanced Computer Science and Applications*, vol. 12, no. 5, 2021.

[54] J. P. Dunsmore, *Handbook of microwave component measurements: with advanced VNA techniques*. John Wiley & Sons, 2020.

[55] S. Kumar and H. Gupta, "Design and study of compact and wideband microstrip u-slot patch antenna for wi-max application," *IOSR Journal of Electronics and Communication Engineering (IOSR-JECE) e-ISSN*, pp. 2278–2834, 2013.

[56] Z. Dafalla, W. Kuan, A. A. Rahman, and S. Shudakar, "Design of a rectangular microstrip patch antenna at 1 ghz," in *2004 RF and Microwave Conference (IEEE Cat. No. 04EX924)*. IEEE, 2004, pp. 145–149.

[57] J. Robinson and Y. Rahmat-Samii, "Particle swarm optimization in electromagnetics," *IEEE transactions on antennas and propagation*, vol. 52, no. 2, pp. 397–407, 2004.

[58] S. Sengupta, S. Basak, and R. A. Peters, "Particle swarm optimization: A survey of historical and recent developments with hybridization perspectives," *Machine Learning and Knowledge Extraction*, vol. 1, no. 1, pp. 157–191, 2018.

[59] J. Kennedy and W. M. Spears, "Matching algorithms to problems: an experimental test of the particle swarm and some genetic algorithms on the multimodal problem generator," in *1998 IEEE International Conference on Evolutionary Computation Proceedings*. IEEE, 1998, pp. 78–83.

[60] A. G. Gad, "Particle swarm optimization algorithm and its applications: A systematic review," *Archives of Computational Methods in Engineering*, pp. 1–31, 2022.

[61] F. Shahzad, S. Masood, and N. K. Khan, "Probabilistic opposition-based particle swarm optimization with velocity clamping," *Knowledge and information systems*, vol. 39, no. 3, pp. 703–737, 2014.